Non-Synonymous Variants in the Premelanosome Protein (PMEL) Gene are Associated with Pigment Dispersion Syndrome/Pigmentary Glaucoma and Cause Biochemical Defects

by
Adrian Alexander Lahola-Chomiak

A thesis submitted in partial fulfillment for the degree of

Master of Science
Medical Sciences-Medical Genetics
University of Alberta

Abstract

Pigmentary Glaucoma (PG) is a common glaucoma subtype that results from release of pigment from the iris (Pigment Dispersion Syndrome) and its deposition throughout the anterior chamber of the eye. Although PG has a substantial heritable component, no causative gene variants have yet been identified in humans. Whole Exome Sequencing (WES) of two independent pedigrees identified the first candidate gene for heritable PDS/PG - premelanosome protein (*PMEL*), which encodes a key component of the organelle (melanosome) essential for melanin synthesis, storage and transport. Targeted screening of *PMEL* in three independent replication cohorts (n= 394) identified nine additional PDS/PG-associated variants. These variants exhibited either defective post-translational processing of the PMEL (5/9), altered amyloid fibril formation (5/9), or both (3/9). Suppresion of the homologous *pmela* in zebrafish caused profound pigmentation and ocular defects further supporting PMEL's role in PDS/PG. Taken together, these data support a model in which protein altering PMEL variants represent dominant negative mutations that impair PMEL's normal ability to form functional amyloid fibrils. While *PMEL* mutations have previously been shown to cause pigmentation and ocular defects in animals, this research is the first report of mutations in *PMEL* that cause human eye disease.

Preface

This thesis contains an original work completed by Adrian Lahola-Chomiak in partial fulfillment towards a Master of Science degree.

Some of the research for this thesis is a part of a research collaboration at the University of Alberta led by Dr. Michael Walter in the Department of Medical Genetics, and with Dr. Ordan J. Lehmann from the Department of Medical Genetics, and Dr. Ted Allison from the Department of Medical Genetics. Additionally, collaborators outside the University of Alberta include Dr. Janey Wiggs from the Massachusetts Eye and Ear Institute at Harvard Medical School and Dr. Jamie Craig from the Department Ophthalmology at the University of Flinders. Clinical assessment of patients and DNA collection was done by Dr. Ordan J. Lehmann for Family 1 and 2 as well as the CA singleton panel, Dr. Janey Wiggs for Family 3 and the US singleton panel, and Dr. Jamie Craig for the AU singleton panel; Tim Footz completed WES for Family 1 and 2, designed the high-throughput sanger sequencing method, and completed DNA quantification, some primary PCRs and all subsequent steps. He also provided significant support with experimental design, data analysis, and figure/table preparation for Table 1, 2, 3 and Figure 5, 6, 7. Dr. Janey Wiggs and Dr. Bao-Jian Fan together completed the genetic analysis of Family 3 and the US singleton panel. The lab of Dr. Jamie Craig completed the genetic analysis of Family 3 and the AU singleton panel. I assisted with the high throughput sanger sequencing by completing a majority of the primary PCRs. I cloned all PDS/PG variant PMEL constructs. I performed the transfections and western blotting experiments for figures 9 and 10. I developed and performed the transfection, immunofluoresence, and imaging for figures 12 and 13. I transfected and prepared cells for TEM imaging and imaged cells with the assistance of Woo Jung Cho of the Cell Imaging Center for figure 14. I performed the statistical analysis for figures 9 and 15.

To my mother, who showed me I could do anything I put my mind to.

To Calli-Ann who supported me through every obstacle.

To Mike who trusted me.

To my friends for keeping me happy through all of it.

To my Oswald, Minou, and Tully for making our house a home.

To Alli who shared my burdens and accomplishments, I could not have done it alone
I love you.

It's a dangerous business, Frodo, going out your door.
You step onto the road, and if you don't keep your feet,
there's no knowing where you might be swept off to.
J.R.R. Tolkien

Acknowledgements
It would be impossible to express in words the appreciation I feel for those who gave me their guidance and support during the journey of my master's thesis. Although I will do my best I know this section will fall short of reconciling the debt of gratitude I owe my colleagues, peers, friends, and family. I hope to impress upon everyone I mention that you made the late-nights running gels, deadline straining dashes for signatures, endless paper draft generation, and fights to stay awake during long boring seminars a pleasure to experience.

Mike, you took me into your lab and gave me your full and total trust. Although many students have productive relationships with their supervisor I think that very few are fortunate enough to feel like colleagues. You let me take risks which sporadically payed off, included me in every project discussion, listened to my ideas and concerns, and gave me a level of freedom that I hope you feel payed off. When I think about what I will take from this project, it is not the details of PMEL and glaucoma but the scholarly principles I hope to one day bring to a lab of my own. Ordan, your mentorship throughout my degree constantly inspired me to push myself to think more skeptically about my data and more creatively about my problems. Nobody else challenged my assumptions in as constructive and fun way as you did. I hope to live up to your idea of a scholar who uses knowledge as a laser instead of a battering ram. I am grateful to the mentorship my other committee members (Alan, Yves, and Rachel) provided me which made both my masters and my defense a challenging but enjoyable experience.

There is one person who perhaps more than any other had a direct hand in my successes. He is a wizard at the bench, a sorcerer at the computer, and a dad in every other circumstance. Though I could call him many things there are some who call him…Tim. My man, I know that I would have accomplished nothing without you. Everyone who knows you understands that you're a dad first and a scientist second. It's not because you are lacking when it comes to proficiency in the lab (nobody comes close) but instead because you are overflowing with compassion and an infectious excitement for research. If you're reading this you're probably bored (and sleepy) but I owe so much of my success to you I hope one day you understand the massive contribution you made to my growth not just as a scholar, but as a person (and board game addict). The same could be sent for you Lance. When I first joined the lab, Tim made me feel welcome, but you made me feel at home. From the moment I correctly identified AGDQ I think both of us knew we would grow close. You trusted me enough to bring me into a tight circle of friends and over my years in medgen you have been a colleague I can trust for intelligent critique, a lab mate I could depend on for help in tough spots, and a friend I could trust for anything I needed. You're my best man for a reason.

Jamie, you and Marino have both become close friends of both Alli and myself for good reason. Seeing you and Alli together I am not surprised that you became so close. I could never predict however how positive an influence the two of you would have on both of us. You brought us into the medgen family and demonstrated time and again professional and personal qualities we still strive to emulate. Nicole, more so than any of my other peers you challenged me academically. Nobody else pushed me to think harder about our shared intellectual passion for the eye than

you. Taking directed reading with you reignited my passion for science and taking powerlifting together made me excited to exercise again. I am excited to see your meteoric rise through both medicine and academia, but I am ecstatic to call you a friend through all of it. Of course, I would be mistaken to mention you without Kim. Kim you and I met in what I consider the worst class I have ever taken but out of that grew a friendship and collaboration that grew to define my masters. You and I have bonded over PMEL, board games, camping, Hawaii, DnD, and of course Asian food (well food in general). Hunter, I have known you since I was a dweeby undergrad and I'm glad our paths intertwined later in life as they did. You helped me feel welcome in the department and have been a close friend to both myself and Alli. I hope to stay in touch, and not just because your cat Chester is adorable. Vanessa, you took care of Alli more times then I can count and your friendship with us both during work hours and wine night hours will be a cherished memory. Josh, the world just isn't ready for universal sandwich theory, but I hope one day we can unleash it if only for the dreams, memes, and dreams of memes.

My mother though more than anyone listed here deserves credit for making me who I am today. Science can be challenging but my mom always taught me that persevering through those challenges is what defines success. For every challenge I have faced in my life you have faced at least two. Defying the odds, you raised both me and my sister while achieving personal success. You have taught me to always shoot for the stars, trust my instincts, and be generous to everyone around me. Everything I have become is thanks to you. Of course, the other member of family who has given me all the support I need to get here is Calli-Ann. You provided me unconditional support through every challenge I have faced. As much as everything I am is thanks to my mom none of what she has done would have been possible without you. Both you and my mom have inspired me to dream big because you have demonstrated it is possible.

Alli. If I could all the credit to anybody it would be you. Our relationship has been the foundation for everything I have accomplished since we met. I couldn't have predicted where we are today, but it would have been easy for me to believe in our successes thanks to your drive and vision. If I came home frustrated, you were there to help me find an answer. When I came home happy, you were there to celebrate. Most of those days ended up happy in no small part thanks to you. Your partnership makes me feel like nothing is impossible, and that in fact doing the impossible can even be fun. I love you.

Table of Contents

List of Tables

List of Figures

Chapter One:

Pigment Dispersion Syndrome, Pigmentary Glaucoma, and Premelanosome Protein Biology (PMEL)

Portions of this section were previously published in
"*Molecular Genetics of Pigment Dispersion Syndrome and Pigmentary Glaucoma: New Insights into Mechanisms*"
by Adrian A. Lahola-Chomiak and Michael A. Walter
in the *Journal of Ophthalmology* Volume 2018 March 26 2018

1.1 The Eye and Glaucoma

The human eye is a highly specialized sensory organ which, in combination with the visual cortex of the brain, is responsible for vision. It develops as a fusion of several distinct embryonic cell populations to form a complex structure which senses not only light vs dark but also a variety of other factors involved in high definition vision such as color and motion. At its most basic the human eye is a pairing between a neural sensory component (retina) and an advanced structural housing which not only protects the retina but participates in vision through aperture control, light focusing, and eye movement. Substructures of the eye are commonly subdivided into either the anterior or posterior segment (Figure1). The posterior segment encompasses the retina as well as its support structures, the vasculature, choroid, and vitreous humor. In the posterior segment the optic nerve, responsible for transmission of information to the brain for processing, meets the retina at a point called the optic disc.

In contrast the anterior segment contains several structures such as the cornea, lens, ciliary body, trabecular meshwork, and importantly for this investigation the complex biological aperture known as the iris. The cornea helps focus light and provides a robust barrier between the eye and external environment. It is largely comprised of a mostly acellular stroma (excluding some resident keratinocytes and macrophages), but this structure is importantly maintained by the corneal epi- and endothelium. Suspensory ligaments attached to the ciliary body hold the lens in place and complete the focusing apparatus of the eye. Aqueous humor is produced by the ciliary body and fills the intervening space between the cornea and the iris nourishing the structures of the anterior segment and clearing waste products from the eye.

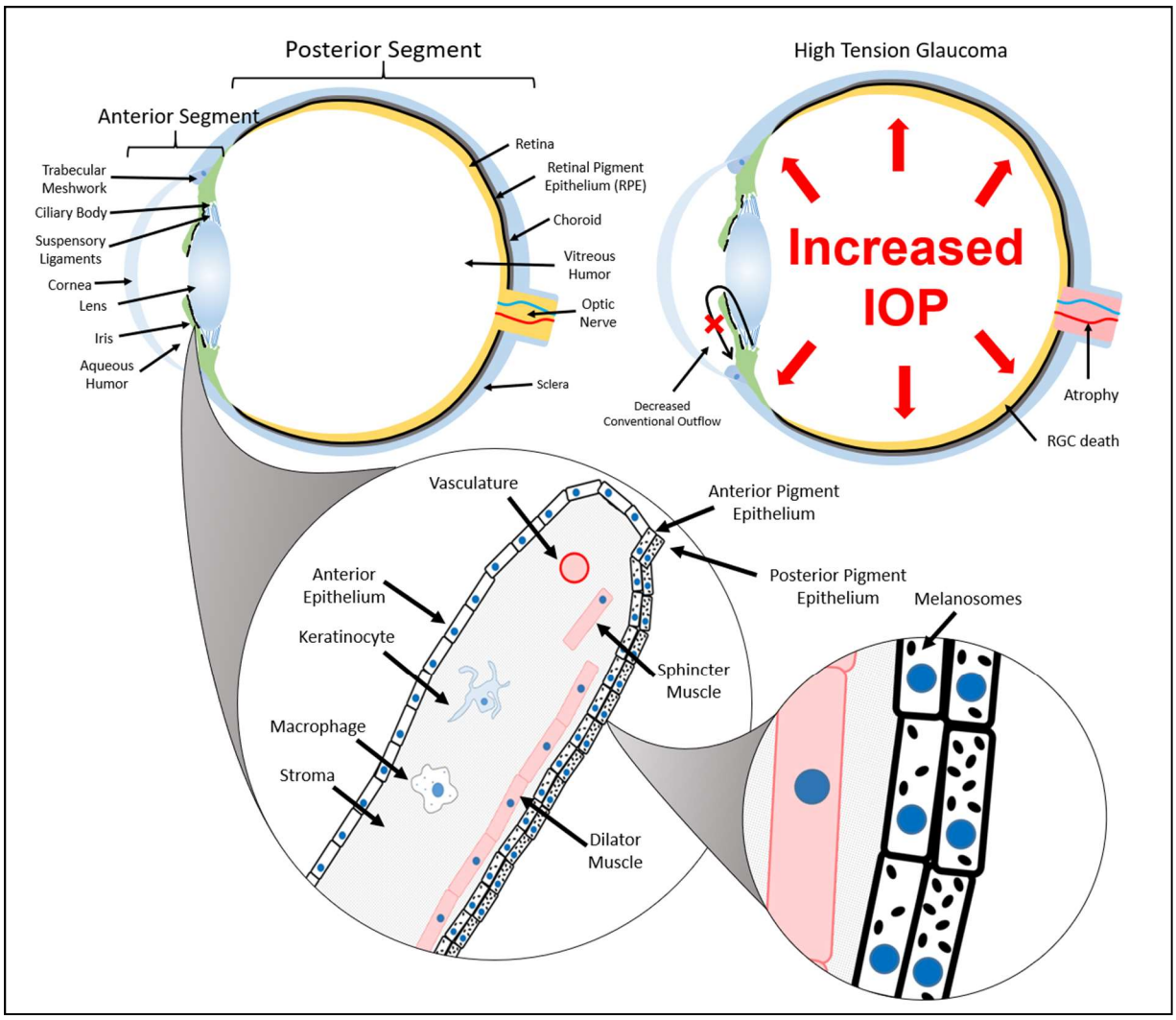

Figure 1. The Eye and Glaucoma The human eye is anatomically separated into the anterior and posterior segments. The posterior segment encompasses the retina and associated structure (right side of the eye outlined above) while the anterior segment encompasses the iris, lens, cornea, and associated structure (left side of eye outlined above). The iris is a complex biological aperture (expanded panel below) composed of the stroma encased within an anterior epithelium and a posterior iris pigment epithelium (IPE) bilayer. Both iris sphincter muscles (located centrally) and iris dilator muscles (which span the iris radially) are nourished by vasculature which innervates the stroma. The stroma is additionally supported by keratinocytes which maintain the extracellular matrix and macrophages which defend the eye against pathogens. The anterior iris pigment epithelium is generally less pigmented than the posterior iris pigment epithelium (see blow out panel bottom right) which may reflect different developmental origins. High tension glaucoma (top right) is glaucomatous optic neuropathy associated with increased intraocular pressure (IOP) often caused by decreased conventional outflow in the anterior segment.

Waste removal is accommodated by outflow of the aqueous humor via either the conventional or uveoscleral route. Conventional outflow is responsible for the majority of outflow and involves removal of aqueous humor through the trabecular meshwork which both facilitates outflow via a series of channels and filters waste products through phagocytosis. Uveoscleral outflow does not have a defined pathway but involves escape of aqueous humor through the intervening spaces between the ciliary body, trabecular meshwork, cornea, and sclera.

Finally, the iris is a complex biological aperture which dynamically controls light access to the retina. It is composed of several layers including a transparent anterior epithelium, a bilayer posterior pigment epithelium, and intervening heterogenous stroma. The stroma contains vasculature that nourishes the iris dilator and sphincter muscles which function together with innervating nerves to control contraction or dilation of the pupil. Iris sphincter muscles are key to rapid contraction of the iris in response to intense light due to their unique photosensitive properties, acting as non-neural photoreceptors in the human body. The iris pigment epithelium (IPE) is a bilayer composed of an anterior layer of melanocytes derived from neuroectoderm sharing a developmental origin with the RPE and a posterior layer of melanocytes derived from the inner layer of the optic cup and sharing a developmental origin with the neural retina. There is limited information detailing the functional differences between these two layers, but developmentally the iris sphincter and dilator muscles are derived from the posterior IPE or anterior IPE respectively. Additionally, the posterior IPE often appears more highly pigmented and may contribute more to the light blocking function of the iris. Melanocytes contain specialized membrane bound pigmented organelles called melanosomes which synthesize and contain melanin, a pigment which absorbs both visible and damaging UV spectrum light.

Combined, the IPE and muscles of the iris allow strict control over the amount of light entering the retina.

The complexity of the eye is mirrored in the myriad of medical conditions which impair vision. Diverse in their pathology, epidemiology, genetics, and patient impact it is important to acknowledge the heterogeneity of conditions vision scientists and medical professionals face. However, by far the most impactful eye disease globally, alongside diabetic retinopathy and age-related macular degeneration, is glaucoma. With a combined world-wide prevalence of 3.54% in individuals 40-80 years of age[1], glaucoma affects more individuals than any other inherited eye disease even without including earlier onset cases. An umbrella term, glaucoma describes a heterogenous set of diseases with unique pathologies phenotypically converging on death of retinal ganglion cells and optic nerve atrophy (together termed glaucomatous optic neuropathy) leading to vision loss. Although commonly associated with elevated intraocular pressure (IOP), both high (IOP>20 mm Hg) and low-tension forms of glaucoma exist[2]. The true diversity of glaucoma subtypes has been challenging to quantify statistically, but high-pressure forms of glaucoma are the most common subtypes with primary open-angle glaucoma (POAG) alone making up an estimated 87.57% of all glaucoma cases[1]. 'Primary' refers to glaucoma with an unknown biological origin (most cases) as opposed to 'secondary' glaucoma which has a definable cause such as trauma. 'Open angle' refers to subtypes in which the space between the trabecular meshwork and cornea remains open, allowing access to conventional outflow whereas in angle-closure glaucoma this space is restricted physically preventing conventional outflow[2]. Management strategies for high-pressure glaucoma include both surgical and pharmacological interventions, mostly targeted at managing pressure through improved outflow or reduced humor

production. Usually an IOP reduction of 20-50% is enough to prevent the progression of vision loss but depends on the extent of existing damage. Despite progress in the treatment of glaucoma, the pathophysiological diversity between subtypes can make management of certain cases challenging.

1.2 An Introduction to Pigment Dispersion Syndrome and Pigmentary Glaucoma

Pigment Dispersion Syndrome (PDS) is the shedding of pigment from the posterior surface of the iris into the anterior segment following the flow of aqueous humour. This shedding does not independently impair vision in most affected individuals. However, a subset of patients with PDS progress to Pigmentary Glaucoma (PG) with high intraocular pressure (IOP) and glaucomatous optic neuropathy. To date, although several population studies have established a relationship between these two disorders, the underlying pathology remains cryptic[3–6]. A heterogenous and possibly complex genetic component appears to underlie at least a proportion PDS/PG cases[7]. Understanding this genetic component can not only provide insight in the underlying pathology of PDS/PG but also forms the basis for rationally designed therapeutics for this important cause of blindness worldwide.

1.3 Pathophysiology

The defining characteristic of PDS is the bilateral shedding of pigment from the posterior iris pigment epithelium (IPE) and the subsequent deposition of this pigment in the anterior segment, first described in 1899[8]. Pigment lost in this way can be visualized using gonioscopy as iris transillumination defects which describe depigmented zones that abnormally allow light to pass through them[9]. These slit-like depigmented zones tend to be observed radially in the mid-peripheral iris and, according to ultrasound biomicroscopy studies, patients with PDS often have abnormal irido-zonular contacts[10,11]. As described in more detail below, these abnormal contacts have previously been proposed to be responsible for pigment shedding via a mechanical rubbing model[10]. Iris transillumination defects are observed in approximately 86% of patients with PDS[12]. Liberated pigment is transported into the anterior segment via aqueous humour flow. Aqueous humour convection currents driven primarily iris vasculature and blinking[13] then deposit this pigment in a vertical stripe on the cornea known as a Krukenberg spindle[8,14] (Figure 2). This phenotype is observed in around 90% of PDS patients, and does not correlate with differences in corneal thickness or density[15,16]. Possibly the most important clinical sign in the pathophysiology of PDS is the observation of dense trabecular meshwork pigmentation[14]. PDS patients tend to have a diffuse and uniformly dense pigmented trabecular meshwork, unlike patients with the phenotypically-related pseudoexfoliation syndrome where punctate deposits of material in the trabecular meshwork are observed[17].

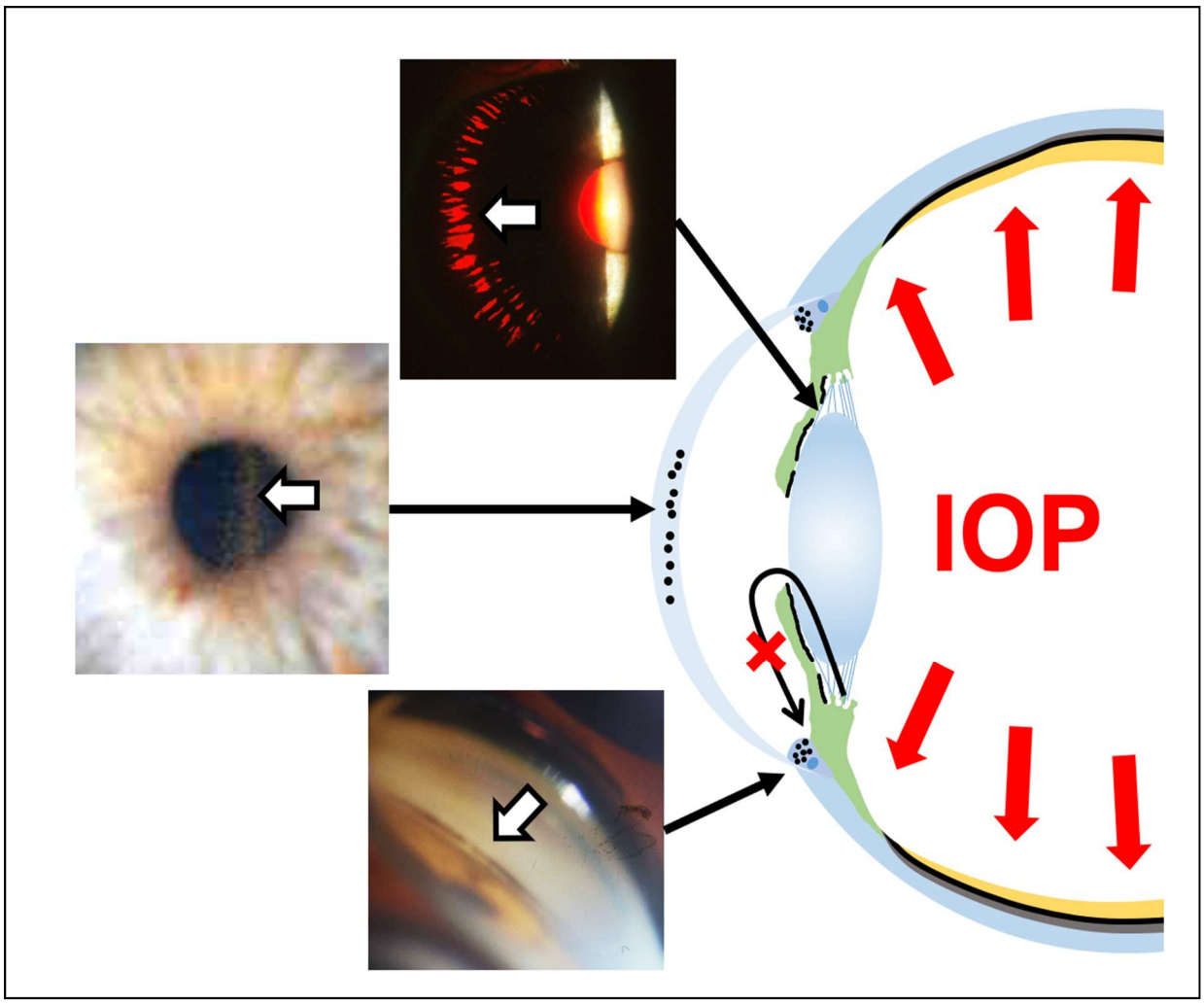

Figure 2 – Phenotype of Pigment Dispersion Syndrome and Pigmentary Glaucoma Loss of pigmented material from the iris pigment epithelium (IPE, pictured in green) results in deposition of pigment in the anterior segment. Available histology suggests this pigment loss is the result of melanocyte death and detachment causing fragments of these cells to follow the flow of aqueous humor into the anterior chamber. This can be visualized as a transillumination defect (top left panel, Edward S. Harkness Eye Institute) wherein the light shone through the pupil reflect off the retina and back through the iris abnormally in a usually slit-like and radially distributed pattern. Pigment phagocytosed by the corneal endothelium presents as a stripe called the Krukenburg spindle (center left panel Edward S. Harkness Eye Institute) whose appearance is a by-product of convection currents in the anterior chamber aqueous humor driven by iris vasculature blinking. Pigment is also phagocytosed by the trabecular meshwork which can be pictured as a dark ring of pigment localized around the edge of the pupil (bottom panel, Courtesy of Dr. Ordan J. Lehmann). Death of cells in the trabecular meshwork leads to decreased conventional outflow, increased intraocular pressure (IOP), and glaucomatous optic neuropathy.

Histologic examination has revealed that pigment granules are phagocytosed by both corneal epithelium cells and trabecular meshwork cells rather than being adsorbed onto their surface[18–21]. Phagocytic stress causes alterations to trabecular meshwork extracellular matrix structure and adhesion[22,23] which could explain the trabecular meshwork dysfunction observed in PDS/PG patients[21]. In PDS/PG patients, trabecular meshwork cells die and exhibit localized necrosis[24]. This necrosis leads to a collapse of channels in meshwork and a concomitant decrease in the essential filtering function of trabecular cells which aids in waste removal. The resultant reduced outflow is likely the primary mechanism in conversion from PDS to PG. as reduced outflow is an established mechanism for IOP increase and glaucomatous optic neuropathy[24,25]. However, the degree of trabecular meshwork pigmentation does not directly correlate with conversion risk, but is however related to the severity of optic neuropathy in PG patients[5,26]. The lens and iris have been suggested to function together in a ball-valve pressure mechanism, called the reverse pupillary block, maintaining one way aqueous humour flow[27]. Elevated anterior segment pressure may bend the iris posteriorly, increasing irido-zonular contact and as a result exacerbate pigment shedding[6,28]. However, the iris bending cannot be solely due to pressure as a study using *ex vivo* iris explants showed that iris bowing is a normal feature of iris dilator muscle activity and position[29]. Hyperplastic iris dilator muscles have been observed in several patients with PDS and this dysfunction may contribute to posterior iris bowing[30–32].

Although currently limited, some evidence has accrued to support the involvement of the retinal pigment epithelium (RPE) in PDS/PG. Patients with PDS have significantly lower Arden ratios than patients with primary open-angle glaucoma (POAG) or ocular hypertension (OHT) which may indicate RPE degeneration[33]. Arden ratios express the result of an electrooculogram which

measures the standing potential between the RPE and choroid. Lower ratios reflect RPE dysfunction as the retina is less capable of adapting to the variable light stimulus in the test. Lattice retinal degeneration occurs in 22-33% of PDS/PG cases which is high, despite the known association between PDS and myopia[34–36]. An estimated 12% of eyes with PDS also experience retinal detachment; occurring in 5.5-6.6% of total PDS cases[6,36,37]. Together these data support a more general involvement of pigmented cells in the pathology of PDS/PG, but further characterization of possible RPE dysfunction associated with PDS/PG is necessary.

1.4 Epidemiology

At a population scale, there are several long-standing questions to answer about PDS and PG. As PDS is the underlying condition, it is important to know how many people are affected as well as details regarding their demographic characteristics. The incidence of PDS has been estimated to be between 1.4 per 100,000 to 4.8 per 100,000[12] in the United States. However, some estimates place prevalence as high as 2.45% in the United States[38]. Screening for PDS however is complicated by its subclinical nature, the fact that pigment dispersion is more easily observed in lightly pigmented eyes, and the phenomenon of symptom abatement known as 'burn-out' where pigment stops being shed[12,26]. People affected by PDS may not seek out eye exams since their vision is not impaired and affected individuals, may be asymptomatic for obvious pigmentary defects due to 'burn-out', together leading to an underestimation of PDS prevalence. Burn-out typically occurs in older individuals and it is possible some patients who present with glaucomatous optic neuropathy, who are then diagnosed with POAG, may be more accurately described as PG cases with burn-out. PDS is known to affect young myopes which may explain some of the structural iris pathologies associated with the disease[14,36,39]. North American studies

have established a higher prevalence of PDS in white patients and a lower than expected incidence of PDS in black patients[39–41], but the aforementioned ability to more readily detect aberrantly located pigment in light coloured eyes might lead to an ascertainment bias.

Conversion from PDS to PG is a highly variable and heterogeneous phenomenon impacted by both genetic and environmental factors. For example, despite the prevalence of PDS being approximately equal in both men and women, more males progress to PG[5,6,13,36] and that conversion occurs about a decade earlier in men than women[3,13,27,36,39]. PDS patients have an increased family history (4-21%) of glaucoma[12,36,42] however that percentage increases greatly in patients with PG (26-48%)[12,39,43,44]. Rigorous exercise has been shown to induce pigment dispersion, enhance posterior iris bending, and increase IOP which all contribute to conversion risk[45–48]. IOP is a major risk factor for PDS to PG conversion, with the increase in risk being proportional to increase in IOP[12,49]. The actual rate of conversion is highly variable between studies and seems to in part depend on the ethnic background of patients. Conversion rates as high as 35-50% have been reported in US populations[3–5]. However in another study which evaluated conversion over time, the conversion rate was estimated at 10% at 5 years and 15% at 15 years[12]. In a Latin American cohort conversion rate was observed to be 37.5% at 50 months which is in good agreement with US studies[49]. However, in a Pakistani cohort the observed conversion rate was only 4% at 15 years which may support ethnicity as a risk factor for conversion[50]. Ultimately the diversity in conversion rates supports the observation of heterogenous genetic and environmental risk factors. In the Western world, PG represents 1-1.5% of total glaucoma cases and, due to its early age of onset, is the most common cause of

non-traumatic glaucoma in young adults[38,51] making it an important cause of debilitating blindness.

1.5 Human Genetics

Current research on the genetic component of PDS/PG supports a genetically heterogeneous and possibly complex inheritance model. Analysis of four 3-generation pedigrees with Irish or mixed western European ancestry affected by PDS/PG supported an autosomal dominant mode of inheritance given the identification of affected individuals in every generation without a sex bias[52]. In 1997 using microsatellite markers, a chromosomal region named *GPDS1* (glaucoma-related pigment dispersion syndrome 1) (OMIM ID 600510) was mapped to human chromosome 7 (7q35-q36; 2-point lod score ZAmax: 5.72 at theta = 0) in a subset of patients affected by PDS. To date this linkage has not been replicated by other mapping studies. Additionally, no candidate genes in this region have been successfully associated with PDS/PG. Of several genes in the region, the most promising candidate is likely human endothelial nitric oxide synthase (*NOS3*) as it is known to play a role in maintaining vascular tone and dysfunction may contribute to structural abnormalities of the iris[53–55]. However, mutations in *NOS3* have not been reported to be associated with PDS/PD to date.

Another region, on chromosome 18, has also been associated with PDS/PG in several studies. Using a single pedigree, significant linkage to the 18q11-q21 region was observed[56] and later analysis of four additional pedigrees not linked to *GPDS1* found significant linkage to the 18q21 region, assuming an autosomal dominant mode of inheritance[57]. Finally, there exists one case study of an Estonian man with PDS harbouring novel deletions on both the nearby 18q22 and

2q22.1[58]. However, as for the *GPDS1* locus, no genes in these regions have been associated with PDS/PG.

Two candidate genes associated more broadly with other subtypes of glaucoma, myocilin (*MYOC*) and lysyl oxidase homolog 1 (*LOXL1*), have shown limited association with PDS/PG. *MYOC* is well known for association with several subtypes of glaucoma including juvenile open-angle glaucoma (JOAG) and primary open-angle glaucoma (POAG)[59–61]. Several cases of potentially damaging mutations in *MYOC* in patients with PDS/PG have been observed[62–64] and *MYOC* is expressed in several ocular tissues including the iris which makes it biologically plausible, despite its still cryptic biological function. However, the very small number of *MYOC* variants found associated with PDS/PG suggest that MYOC is either a very infrequent cause of PDS/PG or that this association is due to chance. Given the phenotypic similarities between pseudoexfoliation syndrome (PXS) and PDS (deposition of material in the anterior segment) several studies have investigated a possible association between *LOXL1*, a gene strongly associated with PXS[65–69], and PDS/PG. To date no causal association of PDS/PG and LOXL1 variants has been observed[70,71] but variants in LOXL1 could act as a modifier of both of disease risk and age of onset[70,72]. Interestingly, a patient with coexisting[73] PXS and PDS has been described, supporting again the idea that these related disorders are separate clinical and genetic entities.

There may be also some overlap between PDS and the rare recessive disease Knobloch syndrome (OMIM # 267750) caused by mutations in *COL18A1*[74,75]. Knobloch syndrome is a developmental disorder with ocular abnormalities and severe skull formation defects. Recently it

has been reported that PDS and PG are a hallmark sign of Knobloch syndrome and that understanding PDS/PG is important for management of Knobloch syndrome[76]. However, given the severity of the other diagnostic symptoms of Knobloch syndrome, variants in *COL18A1* are unlikely to cause a large proportion of PDS/PG cases. Two case reports have associated Marfan syndrome (OMIM # 154700) with PDS/PG and suggested that *FBN1* variants, while not causative for PDS, may contribute to conversion to glaucoma[77,78]. Although glaucoma generally has been associated with Marfan syndrome[79] there currently exists insufficient evidence to associate PDS/PG directly with Marfan syndrome or variants in *FBN1*.

1.6 Animal Studies

Whereas human studies have failed to elucidate any gene associated with PDS/PG, animal research has successfully identified several genes associated with similar phenotypes. Undoubtedly the most significant progress has been made using the DBA/2J mouse glaucoma model which has proven invaluable to both PDS/PG research and understanding of glaucomatous optic neuropathy as a whole[80–84]. DBA/2J mice were observed to sporadically develop iris atrophy, pigment dispersion, increased IOP, and glaucoma-like retinal ganglion cell death[84]. Later the genes responsible for these sporadic phenotypes were mapped to two main genes; *Tryp1* and *Gpnmb* which accounted for the iris atrophy and pigment dispersion respectively[80]. Iris pigment dispersion and associated atrophy have also been observed in several other mouse models and causative genes together implicate melanosome genes as playing a central role in iris pigment dispersion pathogenesis[80,85–87].

Melanin synthesis is a tightly regulated process whereby potentially cytotoxic intermediates[88] polymerize onto structural protein fibrils in melanosomes, the specialized pigmented organelle in melanocytes. Several genes involved in melanin synthesis have been implicated in iris pigment dispersion and atrophy in mice studies. *Tyrp1* encodes *tyrosinase-related protein 1*, an important melanosome membrane-bound structural component of the tyrosinase complex that oxidizes 5,6-dihydroxyindole-2-carboxylic acid (DHICA), has catalase activity, and modulates tyrosinase (*Tyr*) function[89–91]. In a screen of coat color variants, the $Tyrp1^{b\text{-}lt}$ (*light* coat) allele (which contains a single missense *Tyrp1* mutation) was associated with iris pigment dispersion in the LT/SvEiJ inbred mouse[85,92]. The $Tyrp1^{b}$ (*brown* coat) allele has two missense mutations and has been shown to cause iris atrophy in both the DBA/2J and YBR/EiJ inbred mouse strains[80,87,93]. Mutation of essential cysteine residues in both $Tryp1^{b\text{-}lt}$ and $Tyrp1^{b}$ alleles causes release of cytotoxic melanin synthesis intermediates from melanosomes leading ultimately to melanocyte cell death[90,92]. A spontaneous coat colour variant *nm2798* is caused by the *dopachrome tautomerase* (*Dct*) allele $Dct^{slt\text{-}lt3J}$, and is associated with iris pigment dispersion[85]. Dct is another protein in the Tyrosinase complex and also participates in melanin synthesis by converting dopachrome to DHICA[94]. Mutations of *Dct* are likely to cause melanosomal dysfunction and melanocyte toxicity via escape or accumulation of cytotoxic melanin synthesis intermediates[88,89,94,95]. A large scale genetic analysis of genetic modifiers of the iris transillumination defect in the DBA/2J mouse model identified the *oculocutaneous albinism type 2* (*Oca2*) gene, an important regulator of melanin synthesis through melanosomal pH control[96,97]. The human homologue *OCA2* also has a direct tie to iris pigmentation, being the causative loci for both it's namesake disease, oculocutaneous albinism Type 2 (OMIM# 203200) and iris color[97–101].

Several genes important to melanosome function, but not involved in melanin synthesis, have also been implicated in iris pigment dispersion phenotypes. A C-terminally truncated allele of *glycoprotein nonmetastatic melanoma protein b* (*Gpnmb*) allele, *Gpnmb*^{r150x}, was mapped as causing iris pigment dispersion in the DBA/2J strain[80]. Although not directly involved in melanin synthesis, *Gpnmb* is important to melanosome structural integrity and containing the cytotoxic melanin synthesis intermediates[80]. *Gpnmb* has additional neuronal and immune cell adhesion functions that are important to the pathology of glaucoma in DBA/2J mice[102–104]. Understanding the immune component of *Gpnmb*^{r150x} mediated iris pigment dispersion may be important to elucidating the known involvement of the immune system in PDS[30,105]. Similarly, *Lyst* encodes the lysosomal trafficking regulator protein which is important for trafficking components to the early stage 1 melanosomes, and variants can cause Chediak-Higashi syndrome (# 214500)[106]. The *Lyst*$^{bg\text{-}j}$ allele causes *beige* coat color in the C57BL/6J background. Beige mice exhibit pronounced pigment dispersion and increased melanosome volume with similarities to both PDS and PXS[85,86]. The underlying molecular mechanism for this phenotype is not yet understood but could be related again to cytotoxic melanin synthesis intermediates. Intriguingly C-terminal truncation of its homologue *Pmel* (*Si* allele) in mice causes melanosome dysfunction and melanocyte cell death leading to body wide pigmentary abnormalities but not iris pigment dispersion [107–109]. However, most variants identified in this study are in the RPT domain of *PMEL* which is lost in *GPNMB* possibly explaining this difference.

The same large-scale genetic analysis which identified *Oca2* also identified several genes not directly involved in melanin synthesis. The motor protein *Myosin Va* (*Myo5a*) gene, signalling

protein *protein kinase C ζ* (*Pkcζ*), and transcription factor *zinc finger and BTB domain-containing protein 20* (*Zbtb20*) were identified as key modifiers of the iris transillumination defect[96]. Both *Myo5a* and *Pkcζ* have a direct tie to pigmentation either through intercellular trafficking of melanosomes[110–112] or through melanocyte dendrite formation[113] (a structure important to intercellular trafficking) respectively. It is not clear how *Zbtb20* may influence this phenotype as the gene remains an understudied transcription factor with ties to the nervous, detoxification, immune system function thus far, the latter having been already implicated in the DBA/2J mouse model previously[114–116]. Finally, in the *vitiligo* substrain of C57BL/6J mice, a variant in the master pigmented cell transcription factor *Mitf* (*Microphthalmia-associated transcription factor*)[117] caused relatively late onset pigment dispersion and increased eye size, possibly due to increased IOP[85]. The $Mitf^{mi\text{-}vit}$ allele likely disrupts the regulation of *Tyrp1*, *Dct*, *Gpnmb*, *Lyst, Myo5a*, and even *PKCζ* given *Mitf*'s essential role in regulating melanocyte identity and function[118–120].

One additional animal model exists with some relevance to PDS/PG. Canine ocular melanosis (OM) shares some phenotypic similarities with PDS/PG in that pigment is lost from the posterior of the iris leading to transillumination defects, pigment accumulates aberrantly in the TM, and increased IOP with glaucoma develops in affected canines. However, OM is characterized by a host of other pigmentary anomalies and pathogenic phenotypes including but not limited to iris root thickening, uveal melanocytic neoplasms, large scleral/episcleral pigment plaques, fundus pigmentation, corneal edema, and anterior uveitis[121,122]. Together these dramatic anomalies are more reminiscent of cancer than PDS/PG making the applicability of this model to human

disease limited. A genetic screen in Cairn terriers assuming an autosomal dominant mode of inheritance ruled out genes implicated in the DBA/2J model as being causative for OM[123].

Together the body of animal research strongly supports a central role for dysregulation of melanin synthesis, melanosome integrity, and melanocyte health in the pathogenesis of PDS. Although biased by the reverse genetic nature of screening coat color (and thus pigmentation) affecting variants for iris pigment dispersion, it is striking that so many different genes acting in similar processes have been associated with this phenotype in mice. In some sense the animal literature on iris pigment dispersion is in marked contrast with human clinical research that has focused on the structural features of PDS as opposed to the cellular ones. None of the genes implicated in mouse models have yet been associated with PDS/PG in humans. Interestingly a recent large genetic analysis has revealed that the iris transillumination defect is independent of the increased IOP observed the DBA/2J model[124]. Instead this glaucoma-like phenotype seems to be regulated primarily by other genes such as the calcium voltage-gated channel auxiliary subunit alpha2delta1 (Cacna2d1) which have broader relevance for POAG[125]. Although glaucoma develops in both the DBA/2J and YBR/EiJ mouse strains, it is important to note that strong evidence suggests glaucomatous optic neuropathy may be linked to underlying neurodegeneration independent of *Tyrp1* alleles[87,126]. This gap between the iris pigment dispersion phenotype and the glaucomatous phenotypes observed in these mouse models limits their applicability to PG but remains an interesting contrast to the research in humans.

1.6 Melanosomes and Premelanosome Protein Biology

Melanocytes are the specialized pigmented cells which reside in our skin, eyes, and ears. Pigmentation serves primarily to protect cells from UV damage but in some animals has a secondary role to generate colorful patterns or absorb light for heat generation (like the polar bear)[127]. Developmentally, melanocytes arise from neural crest cells with some key genes controlling their development being *PAX3*, *SOX10*, and *MITF*[117,128–130]. In the eye there are several distinct melanocyte populations including in the RPE, choroid, and iris which together protect the eye from UV damage and ensure the optical properties of the eye are conducive to vision by focusing light and preventing internal light scattering. Melanosomes are a lysosome derived organelle which contains the required machinery for the production and storage of melanin[131]. Melanosome biogenesis is a complex process which involves coordination of the trafficking and post-translational processing of many proteins which induce the melanosomal fating of a lysosome away from an endosome. Two distinct classes of melanosomes exist, those which produce eumelanin (black) and pheomelanin (red)[132]. Although they share many features, both beginning melanin synthesis with tyrosine, pheomelanosomes diverge after dopaquinone synthesis and lack a melanosomal matrix[133]. Melanosomes importantly compartmentalize melanin synthesis which generates several highly cytotoxic intermediates that induce oxidative stress in the cytosol[88]. Important to the function of melanosomes in vertebrates is the matrix forming protein PMEL. Not only does PMEL induce the characteristic ellipsoidal shape of melanosomes it is also important to their biological function[134]. Heavily modified fragments of PMEL trafficked to the lumen form proteinaceous fibrils which facilitate melanin synthesis and transfer[135]. Amyloids act as a scaffold for melanin polymerization making greatly increasing synthesis efficiency[136]. In human's melanosomes are transferred from melanocytes to

keratinocytes coloring both the hair and skin[137]. PMEL fibers uniquely represent an example of a functional amyloid in physiological conditions and understanding their biology may have broad implications for amyloid pathologies such as Alzheimer's and prion disease.[138–141]

Several functional domains within PMEL contribute to processing, trafficking, and the proteins final function (Figure 3). Beginning from the N-terminus the protein contains a small signal domain which is removed during translation. This is proceeded by a large N-terminal region (NTR) which coordinates protein folding, trafficking, and processing in part due to three highly conserved N-linked glycosylation sites[142]. Three short domains follow the NTR which together form the final fibril structure including the Core Amyloid Fragment (CAF); a small fragment which was recently identified[143]. The polycystic kidney disease domain (PKD) adopts a β-pleated sheet structure and is essential to proper fibril formation[144]. Controversial in this process is the heavily O-linked glycosylated Repeat Domain (RPT) named for 13 imperfect 10 amino acid repeats which compose it[135,145]. Although *in vitro* experiments using RPT fragments synthesized by bacteria form fibrils at acidic pH (like stage 2 melanosomes), these fibrils were unstable at the neutral pH excepted in mature melanosomes challenging their role in the final fibrils[139,146,147]. These results should be interpreted with caution since bacterial experiments use RPT domain fragments which lack O-linked glycosylation which has been shown to be necessary for fibril formation *in vivo*[145]. One hypothesis is that the RPT domain shields developing fibrils from lysosomal proteases which are abundant in the early melanosome[148]. Finally come the Kringle-like domain (KLD) which aids proper folding, the transmembrane domain which anchors the protein in the membrane, and a small cytoplasmic domain which is removed by γ-secretase but has no known signalling function[149,150].

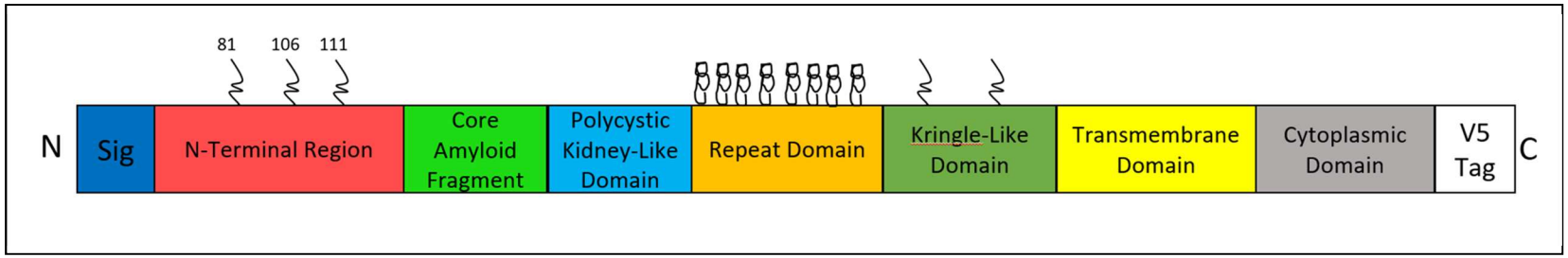

Figure 3. PMEL Structure Curled lines indicate N-linked glycosylation. Stacked circles indicate O-linked glycosylation. Colored blocks indicate protein domains. Sig-Signal domain; NTR-N-Terminal Region; CAF-Core Amyloid Fragment; PKD-Polycystic-Kidney Disease Domain; RPT-Repeat Domain; Kringle-Kringle-Like Domain; TM-Transmembrane Domain; Cyt-Cytoplasmic Domain; V5-V5 Tag.

PMEL is initially synthesized in the Endoplasmic Reticulum (ER) as an integral type 1 transmembrane glycoprotein. During initial synthesis the short N-terminal signal domain is removed, some initial N-glycosylation occurs, and di-sulfide bonds between the NTR and KLD form to prevent non-fibrillar miss aggregation[149]. This intermediate (called P1) is trafficked to the Golgi via a COPII dependent mechanism where O-glycosylation (generating a short-lived P2 form) and proteolytic cleavage by proprotein convertase occurs[135,145,151,152]. This cleavage separates PMEL into a membrane anchored C-terminal Mβ fragment (KLD, TM, and Cyt) and the lumenal N-terminal Mα fragment (NTR, CAF, PKD, and RPT)[152–154]. These fragments importantly remain connected via di-sulfide bonds between the KLD and RPT domains facilitating intact trafficking to the Premelanosome (this intermediate is called Mα-s-s-Mβ)[154]. Although some of this cleaved form goes directly to the Premelanosome from the trans Golgi network the majority of immature PMEL goes to the plasma membrane where it is internalized via AP-2 before it reaches the Premelanosome[152,155]. PMEL remains anchored onto the limiting membrane of the Premelanosome leaving Mα exposed to both the lumen and the protease BACE2 which cleaves PMEL between the KLD and TM domains releasing the N-terminal portion[156]. This cleavage is necessary to expose Mα and the KLD to ADAM17 and other yet unidentified lumenal proteases which separate the required fibrillogenic fragments (PKD, CAF, and RPT) and initiate fibrillogenesis[157].

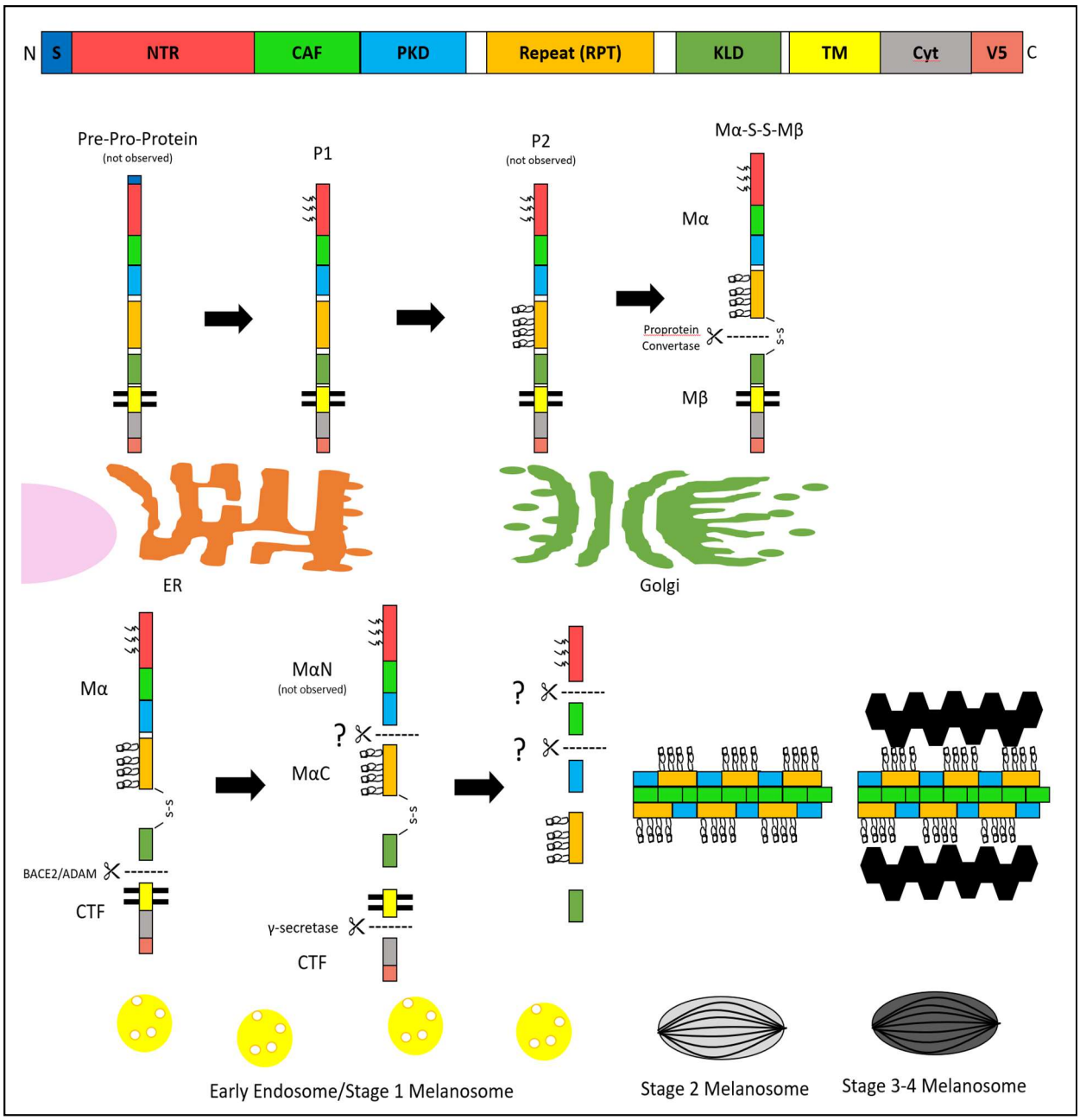

Figure 4. PMEL Processing and Fibril Formation Schematic representation of PMEL protein and functional domain is at the top of the figure, not to scale (see figure 3 for more detail). Basic processing steps in the PMEL processing pathway are outlined below. PMEL is initially synthesized as a Pre-Pro-Protein in the Endoplasmic Reticulum (ER) where some initial N-linked glycosylation occurs generating the P1 intermediate. This form is then trafficked to the Golgi apparatus where extensive glycosylation (Both N and O-linked) as well as additional proteolytic cleavage. The P2 form is rapidly proteolytically processed and thus is not detected by standard protein detection techniques. Following cleavage by proprotein convertase PMEL exits the Golgi and either cycles to the plasma membrane or is directly trafficked early endosomes/stage 1 melanosomes. Here, PMEL is exposed to ADAM17 and other unknown proteases which complete processing and initiate fibrillogenesis with the liberated CAF, PKD, and RPT fragments.

Accompanying this proteolytic cleavage, lumenal fragments are sorted onto developing ILVs and the small CTF is removed via the endosomal sorting complexes required for transport (ESCRT) machinery reflecting the lysosomal origin of melanosomes[158]. Loading onto ILVs is essential to fibril formation and is mediated by important amyloid related proteins APOE and CD63[158,159]. Depletion of either of these genes causes lumenal fragments to be removed by the ESCRT machinery suggesting amyloid genesis is actively encouraged and expression of these genes is one of the factors separating the melanosomal and endosomal organelle fates. ILVs serve as nucleation points for fibril formation and as amyloid fibrils expand into sheets ILVs disappear from the lumen[160]. Most broadly, amyloids can be described as a class of aggregating proteins with a cross-β pleated sheet quaternary structure[161]. They share chemical properties such as specific binding to dyes like Congo Red and insolubility in non-ionic detergents[138,162]. However, these chemical properties do not reflect the key physiological differences between pathological amyloids, such as APP, and physiologically tolerated amyloids such as PMEL. Although this difference is not well understood research into PMEL suggests that physiological amyloids tend to remain compartmentalized and reaction kinetics favor rapid aggregation[138]. Initially amyloid proteins form as soluble oligomers which aggregate and become insoluble over time. Current theoretical models suggest the toxic effect of pathological amyloids is mediated by the soluble oligomer state and both compartmentalization and rapid aggregation limit cellular exposure[140]. As a result, variants which disrupt trafficking or processing can have broad implications for the conversion from physiological to pathological amyloids.

Owing to its important role in coat pigmentation several animal models of *PMEL* variants have been easily identified visually. Knockouts of PMEL result in mild hypopigmentation due to

reduced melanin synthesis efficiency and slightly impaired melanocyte viability. However, mutations which preserve PMEL expression but perturb its ability to traffic or form fibrils show more severe phenotypes. A classical example of a severe PMEL mutation is the Dominant White chicken mutation which has a 3aa insertion in the TM domain which severely slows fibrillogenesis by reducing proper association with both the limiting and ILV membranes resulting in pathological aggregation instead of proper fibril formation[163,164]. The *Silver* mouse which has a frameshift in the Cyt removing important signals for ER export and lysosomal targeting resulting in severe ER stress and altered fibril formation[152,165]. Both these mutations result in severely impacted melanocyte viability and thus a strong overall reduction in pigmentation. The toxic effect of these mutations is thought to be mediated by release of cytotoxic melanin synthesis intermediates and soluble unaggregated PMEL oligomers[166]. Of interest to this investigation is another class of animal model which have severe ocular abnormalities in addition to other pigmentary phenotypes associated with PMEL mutations. Silver dapple Horses[167], Merle dogs, and the Fading Vision Zebrafish all have ocular anomalies resulting from melanocyte dysfunction during development[165,168,169]. In all these animal's histology reveals that melanosomes appear rounded and there is a lower than expected abundance of melanosomes in melanocytes of affected tissues. This may reflect decreased melanosome viability, increased melanosome turnover, increased need for endosomal machinery resulting from cell stress, or a combination of all these pathways.

To decipher the genetic basis of PDS/PG in human we decided to leverage advances in genetic sequencing to investigate two pedigrees affected with the disease. We hypothesized that although the inheritance may not be monogenic, based on the population scale evidence that PDS/PG have

a complex inheritance pattern, we would be able to identify variants with large effect sizes in pedigrees with many affected. In this way the inheritance of the disease in those families may be more similar but not identical to a medallion pattern. Using whole exome sequencing we determined a panel of candidate genes based on inheritance pattern, gene ontology, predicted pathogenicity of variants, and expression pattern. We then expanded the study to sequence high priority candidates in a large singleton panel to identify additional variants and investigate their prevalence in a test population. Thanks to a collaboration with Dr. Janey Wiggs and Dr. Jamie Craig, one additional pedigree and two singleton case panels were added to the analysis. Two pedigrees with different heterozygous non-synonymous variants PMEL which segregated with the disease phenotype were observed. Screening the panels revealed seven additional non-synonymous PMEL variants, heterozygous in all cases, which together with the pedigrees and the known biological function made it a high priority candidate for molecular characterization. Animal models of PMEL mutations indicated that damaging variants often impair trafficking, processing, fibril forming, or all these processes. We hypothesized that PDS/PG associated PMEL variants impaired PMEL function in a manner consistent with a dominant negative pathology.

Chapter Two:

Materials and Methods

Portions of this chapter were written in "*Non-Synonymous variants in Premelanosome Protein (PMEL) are associated with ocular pigment dispersion and pigmentary glaucoma*." Adrian A. Lahola-Chomiak et al. (In Prep)

This Chapter Includes Experiments Designed by Tim Footz. M.Sc.
(Whole Exome Sequencing and High-Throughput Sequencing)

2.1 Whole Exome Sequencing

Prior to me joining the lab, Tim Footz in collaboration with Dr. Ordan J. Lehmann and Dr. Michael A. Walter undertook a genetic study of two families affected by PDS/PG using Whole Exome Sequencing (WES). Genomic DNA from Family 1 and 2 was submitted to the Beijing Genome Institute for WES with the Ion Proton AmpliSeq Exome RDY kit, followed by standard bioinformatics analysis to provide lists of annotated variants (BGI Americas, Cambridge, MA). PDS/PG-associated exonic variants were filtered for base-calling and alignment quality to yield a set of 11 candidate genes for Family 1 and a non-overlapping set of five candidate genes for Family 2 (Table 1)

2.2 High-Throughput Sanger Sequencing

To rapidly and economically genotype the CA/UK cohort a high-throughput targeted next generation sequencing approach was designed by Tim Footz. I contributed to this project by completing a large portion of the primary PCR reactions whereas secondary PCR and subsequent steps were handled by Tim Footz. PCR primers were designed using Primer3 34 and SNPCheck3 (https://secure.ngrl.org.uk/SNPCheck/snpcheck.htm) to amplify all coding exons of PMEL, avoiding or minimizing the number of polymorphic base-pairing sites (Table 3). Primary PCR products were amplified in 20ul reactions using 0.2uM of each forward and reverse primer, 1x FailSafe Premix J (Epicentre Biotechnologies), 40ng genomic DNA, and 1U Taq polymerase (New England Biolabs), using a standard touchdown cycling protocol as follows: denaturation at 95°C for 3min followed by five cycles of 95°C for 30s, 64-56°C for 30s (2°C decrease per cycle), 68°C for 30s and then 24-33 cycles (optimized per primer-pair to produce all bands of

similar intensity) of 95°C for 30s, 54°C for 30s and 68°C for 30s, with a final extension at 68°C for 5min. After confirmation of successful amplification using agarose gels, PCR products were pooled for each individual, purified enzymatically (ExoSAP-IT, Affymetrix USB), and subjected to secondary "barcoding" PCR with unique pairs of Nextera XT v2 index primers (Illumina) as follows: denaturation at 95°C for 3min followed by eight cycles of 95°C for 30s, 55°C for 30s, 68°C for 30s, with a final extension at 68°C for 5min. Samples were then bead-purified (Agencourt AMPure XP), with confirmation on a QIAxcel (QIAGEN Inc.). Samples were then pooled and the library was quantified with a Qubit 2.0 fluorometer (ThermoFisher Scientific) and sized with a Bioanalyzer 2100 (Agilent Technologies) before being analyzed on a MiSeq desktop sequencer (Illumina) at The Applied Genomic Core at the University of Alberta. 360Mb of sequence was generated with 90% of the 1.4 million reads (2x250bp) at a Phred quality score of >Q30. The FASTQ files were aligned to the human genome (GRCh38) with the Burrows-Wheeler Aligner v0.6.1-r104 29 and indexed with SAMtools v1.3.1.30 Variants were called with VarScan v2.4.2 35 using a minimum variant allele frequency threshold of 0.35, and annotated with Ensembl's Variant Effect Predictor.36 The identified variants were confirmed by conventional Sanger sequencing.

2.3 Cloning PMEL variants

A cDNA encoding wild-type PMEL17-i, the most abundant protein isoform (NP_008859.1)37 was purchased from the DNASU Plasmid Repository and subcloned into pGEM-T plasmid (Promega) with an in-frame C-terminal V5 epitope (GKPIPNPLLGLDST). Site-directed mutagenesis was performed (QuikChange Lightning Site-Directed Mutagenesis Kit, Agilent Technologies) to generate plasmids for each patient variant. All plasmid inserts were then

subcloned into the pCI mammalian expression vector (Promega) and the full insert sequences were confirmed by sanger sequencing.

2.4 Cell Culture

HeLa cells were grown in high-glucose Dulbecco's modified Eagle's medium supplemented with 10% fetal bovine serum and 1× antibiotic-antimycotic solution (ThermoFisher Scientific). Cells were transfected with the plasmid constructs using Lipofectamine 2000 (ThermoFisher Scientific), per the manufacturer's protocol.

2.5 Immunoblotting Soluble and Insoluble Fractions

HeLa cell lysates were harvested 48 hours post-transfection using lysis buffer (0.1% SDS, 0.5% sodium deoxycholate, 1% IGEPAL CA-630, in PBS) for analysis by denaturing SDS-PAGE. Insoluble fractions were suspended using inclusion body solubilisation buffer (8M Urea, 100mM β-ME, 100mM Tris/HCl). PMEL proteins were detected by immunoblotting using anti-V5 antibody (Sigma-Aldrich) or HMB45 (Novus Biologicals, Oakville, ON) and visualized by chemiluminescence (SuperSignal West Femto Maximum Sensitivity Substrate, ThermoFisher Scientific).

2.6 Immunofluorescence Colocalization

HeLa cells, grown and transfected on glass coverslips, were fixed with 2% paraformaldehyde 48 hours post-transfection, then incubated with the indicated cell localization markers for 1hr: endoplasmic reticulum (anti-Calreticulin, a generous gift from Dr. Marek Michalak), Golgi (anti-GM130, product #AF8199, Novus Biologicals), and endosomes (anti-LAMP1, product

#GR314073, Abcam). Fluorescent secondary antibodies (Jackson ImmunoResearch Laboratories, Inc.) were incubated at 1:5000 dilution for 1hr. Nuclei were visualized by staining with 4′, 6-diamidine-2-phenylindole (DAPI) dye (10ug/ml). Slides were imaged using a confocal microscope (Olympus IX-81 microscope, Yokagawa CSU 10 spinning disk confocal, Lumen Dynamics X-Cite 120, Hamamatsu EMCCD (C9100-13), acquisition using Perkin Elmer's Volocity).

2.8 Electron Microscopy

Cells were cultured and transfected as outlined in section 2.5 then fixed in 2.0% glutaraldehyde for 1hour at room temperature before resin embedding. This was completed by me supervised by Woo Jung Cho an experienced technician in the cell imaging center. Ultra-thin sections with a thickness of 60 nm were generated using a Leica UC7 ultramicrotome (Leica Microsystems, Inc.) and contrasted with 2% uranyl acetate and Reinold's lead citrate. Sections were imaged using a Hitachi H-7650 transmission electron microscope (Hitachi-High Technologies) at 60 kV and a 16-mega pixel TEM camera (XR111, Advanced Microscopy Techniques). Images were qualitatively assessed by scoring each observed pseudomelanosomes for three morphological features using WT PMEL and p.RPTdel as known normal or aberrant examples respectively. 1) Fibril Appearance, WT fibrils appear straight and uniform 2) Fibril Organization, WT fibrils have regular spacing and only one cluster of fibrils per pseudomelanosomes 3) Organelle Shape, WT organelles appear ellipsoid. If pseudomelanosome features were ambiguous, they were assumed to be normal.

2.9 Statistical Methods

Statistical analysis was used to compare the quantification of immunoblotting data. Images were quantified using ImageJ and then values for three biological replicates were compared using a Student's T-test (two tailed, $p<0.05$). For quantifying V5 images the proportion of total intensity made up by Mβ was compared between WT and all variants to express the efficiency of processing. For quantifying HMB45 immunoblots the proportion of total intensity made up by each MαC processing form (1, 2, or 3) was compared to WT to express the efficiency of processing. Images gathered by TEM were qualitatively assessed by scoring all gathered images for examples of pseudomelanosomes then rating each pseudomelanosomes as normal or abnormal for three features outlined in 2.8 Electron Microscopy. A Z-stat test (two tailed, $p<0.05$) was used to compare PDS/PG-associated PMEL variants to WT using the percent of pseudomelanosomes observed to be abnormal for those features.

Chapter Three:

Results

Portions of this chapter were written for "*Non-Synonymous variants in Premelanosome Protein (PMEL) are associated with ocular pigment dispersion and pigmentary glaucoma."* Adrian A. Lahola-Chomiak et al. (In Prep)

This Chapter Includes Data from Experiments Conducted by Tim Footz. M.Sc. (Whole Exome Sequencing and High-Throughput Sequencing)

3.1 Sequencing

Genomic DNA from the two Family 1 affected cousins, as well as four samples from a second Mennonite family segregating PDS and PG (Figure 4) was sent for whole exome sequencing. For the Family 1 samples, 92% of targeted exons were sequenced with an average of 203x coverage, with 80% of bases at a quality score of Q20 or higher (Quality score for each (Qx; Q20 is defined as a 99% confidence based on experimentally determined probability of an incorrect base call). For the Family 2 samples, 93% of targeted exons were sequenced with an average of 148x coverage, with 89% of bases at Q20 or higher. The PDS/PG exomes were compared (separately for each family) against an unaffected ethnically matched control individual.

Prior to my joining the lab, PDS/PG-associated exonic variants were filtered for base-calling and alignment quality to yield a set of 11 candidate genes for Family 1 and a non-overlapping set of five candidate genes for Family 2 (Table 1). None of the candidate genes are in the reported PDS linkage regions. Of the 16 candidate genes, *PMEL* (premelanosome protein; Family 1) has a reported gene ontology association with pigmentation and thus was selected for further validation. PG in Family 1 is associated with a rare non-synonymous PMEL variant (p.Ala340Val) in a heterozygous state (Table 1). Pathogenicity prediction software (PolyPhen-2, SIFT, MutationTaster-2) for p.Ala340Val did not predict pathogenic effects. This is expected since the variant does not alter amino acid charge (neutral [Alanine] → neutral [valine]) and is in the highly variable (between species) RPT domain both of which are the basis of pathogenicity prediction.

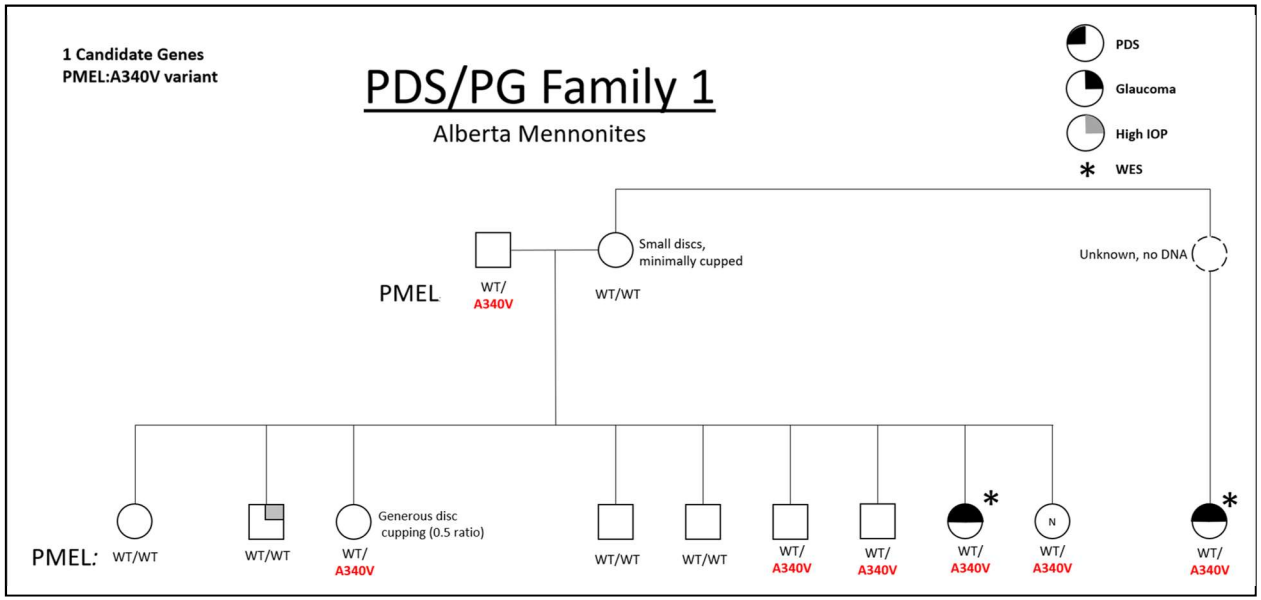

Figure 5. Pigment Dispersion Syndrome and Pigmentary Glaucoma Family 1 Pedigree A Mennonite Family from Alberta affected by PDS/was analyzed in this study. The individuals marked with an asterisk (*) were analyzed by whole exome sequencing and other individuals were genetically analyzed during high-throughput sequencing. Genotypes are indicated below the individuals.

Table 1. Family 1 Filtered Whole Exome Sequencing Variants

Gene	HGVS cDNA	HGVS Protein	dbSNP ID	gnomAD Allele Freq.	Gene Ontology - Biological Process
ANKHD1	NM_017747.2:c.3980C>T	NP_060217.1:p.Thr1327Met	n/a	0.00001219	innate immune response
ARHGEF40	NM_018071.4:c.937G>A	NP_060541.3:p.Gly313Arg	rs374664276	0.0001215	regulation of Rho protein signal transduction
GSTA5	NM_153699.1:c.282G>A	NP_714543.1:p.Met94Ile	rs775966246	0.00001834	glutathione metabolic process
HCK	NM_002110.3:c.1049delG	NP_002101.2:p.Gly350AlafsTer98	n/a	n/a	cell adhesion; cell differentiation; cytokine-mediated signaling pathway; Fc-gamma receptor signaling pathway involved in phagocytosis; inflammatory response; innate immune response-activating signal transduction; integrin-mediated signaling pathway; interferon-gamma-mediated signaling pathway; leukocyte degranulation; leukocyte migration involved in immune response; lipopolysaccharide-mediated signaling pathway; mesoderm development; negative regulation of apoptotic process; peptidyl-tyrosine autophosphorylation; peptidyl-tyrosine phosphorylation; positive regulation of actin cytoskeleton reorganization; positive regulation of actin filament polymerization; positive regulation of cell proliferation; protein autophosphorylation; protein phosphorylation; regulation of cell shape; regulation of defense response to virus by virus; regulation of inflammatory response; regulation of phagocytosis; regulation of podosome assembly; regulation of sequence-specific DNA binding transcription factor activity; respiratory burst after phagocytosis; transmembrane receptor protein tyrosine kinase signaling pathway; viral process
KCNH6	NM_030779.3:c.263G>T	NP_110406.1:p.Gly88Val	n/a	n/a	regulation of membrane potential
OR4M1	NM_001005500.1:c.300G>C	NP_001005500.1:p.Gln100His	n/a	0.000004061	detection of chemical stimulus involved in sensory perception; G-protein coupled receptor signaling pathway
PMEL	NM_001200054.1:c.1019C>T	NP_001186983.1:p.Ala340Val	rs756974126	0.00005796	developmental pigmentation; melanin biosynthetic process; melanosome organization
POLR3E	NM_001258033.1:c.200C>G	NP_001244962.1:p.Pro67Arg	rs368180184	0.000004063	defense response to virus; innate immune response; positive regulation of type I interferon production; transcription from RNA polymerase III promoter
SLITRK5	NM_015567.1:c.1616A>G	NP_056382.1:p.His539Arg	n/a	n/a	adult behavior; axonogenesis; cardiovascular system development; chemical synaptic transmission; dendrite morphogenesis; grooming behavior; positive regulation of synapse assembly; response to xenobiotic stimulus; skin development; striatum development
SNPH	NM_014723.3:c.803T>C	NP_055538.2:p.Val268Ala	n/a	n/a	brain development; neuron differentiation; neurotransmitter secretion; synaptic vesicle docking
TESK2	NM_007170.2:c.1475G>A	NP_009101.2:p.Arg492Lys	rs373927435	0.00004072	actin cytoskeleton organization; focal adhesion assembly; intracellular signal transduction; protein phosphorylation; spermatogenesis

The cDNA and protein notations shown conform to the Human Genome Variation Society (HGVS) recommendations.

Sequenced individuals in Family 2 do not possess any disease-associated variants in *PMEL*. Variants in two genes, *ZFHX2* and *PCDH15*, were chosen for further analysis based on gene ontology, expression, and pathogenicity prediction (Figure 6). We identified the p.Val1039Ile rare variant in *ZFHX2* which is a poorly characterized predicted transcription factor with broad low expression pattern that shows mild enrichment in brain tissue and gonads (GTEx Analysis Release V7). Also, in Family 2 we observed the rare *PCDH15* variant p.Pro838Leu segregating with PG. PCDH15 is a cell adhesion molecule which has an important role in maintaining cell-cell adhesion both in the retina and cochlea.

To rapidly and economically genotype 113 additional cases of PDS with or without PG, all the coding exons of *PMEL*, *ZFHX2*, and *PCDH15* were PCR amplified using primers modified to be compatible with next generation sequencing on an Illumina flow cell. In this CA/UK cohort of 113 additional cases of PDS/PG one additional variant, p.E370D, and one novel variant, p.N111S, were detected in two separate cases (Table 2). Additionally, the rare variant, p.L389P was detected in two cases.

Owing to a collaboration with Dr. Janey Wiggs (Massachusetts Eye and Ear Infirmary, Harvard) and Dr. Jamie Craig (Department of Ophthalmology, Flinders University), our genetic study expanded to include one additional family, called Family 3, and two additional panels of singleton patients (146 US PDS/PG cases and 135 AU PDS/PG cases). To identify the causative gene variant in this family, WES was completed for five affected members (Figure 7). Variants were filtered to retain those with presumed functional effects (nonsense, missense or splice site mutations) that were common to all five patients. Further filtering to select variants with minor

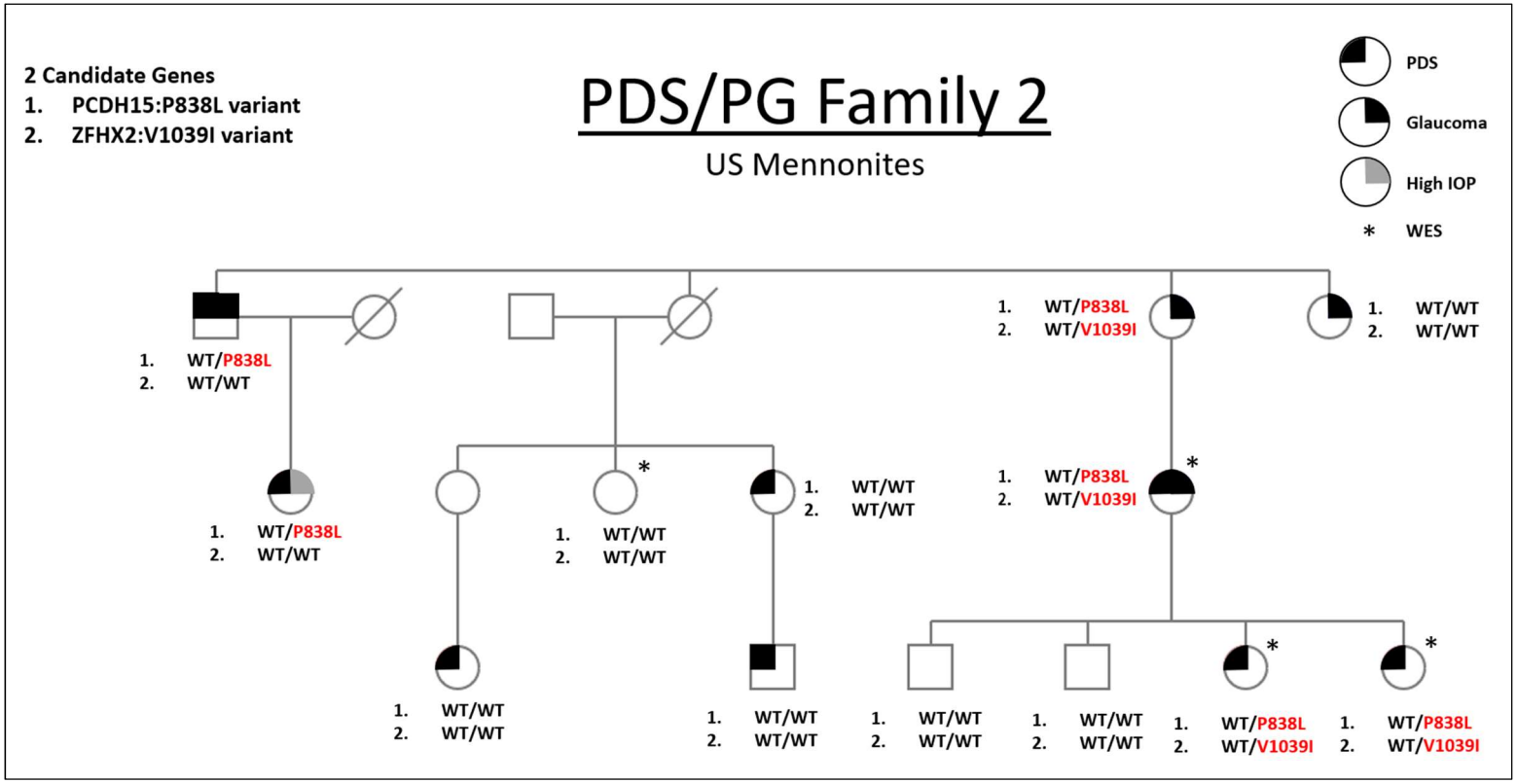

Figure 6. Pigment Dispersion Syndrome and Pigmentary Glaucoma Family 2 Pedigree A Mennonite Family from the United States affected by PDS/was analyzed in this study. The individuals marked with an asterisk (*) were analyzed by whole exome sequencing and other individuals were genetically analyzed during high-throughput sequencing. Genotypes are indicated below the individuals.

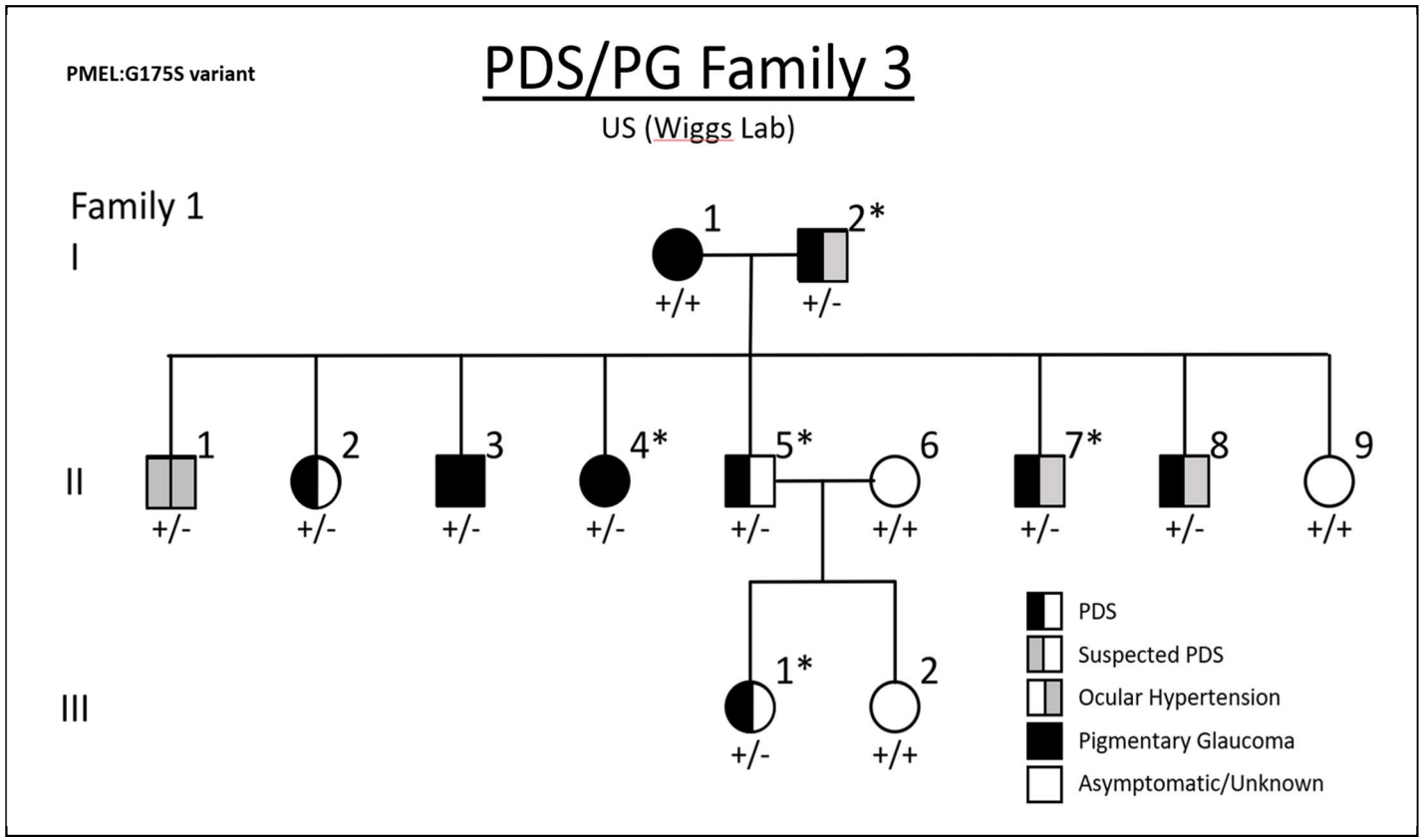

Figure 7. Pigment Dispersion Syndrome and Pigmentary Glaucoma Family 3 Pedigree A Family from the United States affected by PDS/was analyzed in this study. The individuals marked with an asterisk (*) were analyzed by whole exome sequencing and other individuals were genetically analyzed during high-throughput sequencing. Genotypes are indicated below the individuals. This family was seen and analyzed by the lab of Dr. Janey Wiggs

Table 2. Clinical features of affected individuals

Ind	Mutation	Age Dx	K-spindle	Angle Pigm.	IOP> 21	VF defects	Refraction	Surgical tx and other conditions
Family 3								
I-1	--	51		Y	Y	Y		
I-2	p.G175S	60		Y	Y		NA	
II-1	p.G175S	45	NA	NA	Y		NA	
II-2	p.G175S	41	Y	Y			-6.75 OU	Laser tx
II-3	p.G175S	40	Y	Y	Y	Y	-7.00 OU	Multiple surgeries
II-4	p.G175S	45	NA	NA	NA	NA	Y	
II-5	p.G175S	37	Y	Y			Y	
II-7	p.G175S	37	Y	Y	Y		-2.00 OU	
II-8	p.G175S	35	Y	Y	Y		-7.00/-7.25	Laser tx
III-1	p.G175S	19		Y			NA	
Family 1								
II-1	p.A340V	40	Y	Y	Y	Y	NA	Laser tx
II-2	p.A340V	47	Y	Y	Y	Y	NA	Laser tx
Singleton Patients from Panels								
CA/UK	p.N111S	NA	Y	Y			NA	
US	p.G325V	40	Y	Y	Y	Y	-7.00/-7.00	Laser tx OU
AU	p.V332I	NA	Y	Y	NA	NA	NA	
CA/UK	p.E370D	NA	Y	Y	Y		NA	
AU	p.E370D	NA	Y	Y	NA	NA	NA	
AU	p.E370D	NA	Y	Y	NA	NA	NA	
AU	p.S371T	NA	Y	Y	NA	NA	NA	
CA/UK	p.L389P	NA	Y	Y			NA	
CA/UK	p.L389P	NA	Y	Y			NA	
US	p.L389P	18	Y	Y			-1.00/-2.00	Laser tx OS
US	p.Ser641_S642del	42	Y	Y	Y	Y	-4.75/-4.25	

Table 2. Clinical Features of Affected Individuals with PMEL Variants Abbreviations: Age Dx, age at diagnosis; K-spindle, presence of Krukenberg spindle, yes (Y) or no (blank); Angle Pigm., amount of pigment visible in the trabecular meshwork located in the ocular angle, yes (Y) or no (blank); IOP >21; Intraocular pressure greater than 21 mmHg, yes (Y) or no (blank); VF defects, Visual field defects, yes (Y) or no (blank); Refraction, spherical equivalent refractive error, right eye/left eye, + values indicate hyperopia, - values indicated myopia; Not available (NA.); Surgical tx and other conditions, surgical procedures (if any) and other ocular or systemic conditions. Clinical Features of Patients from Family 2 were not available.

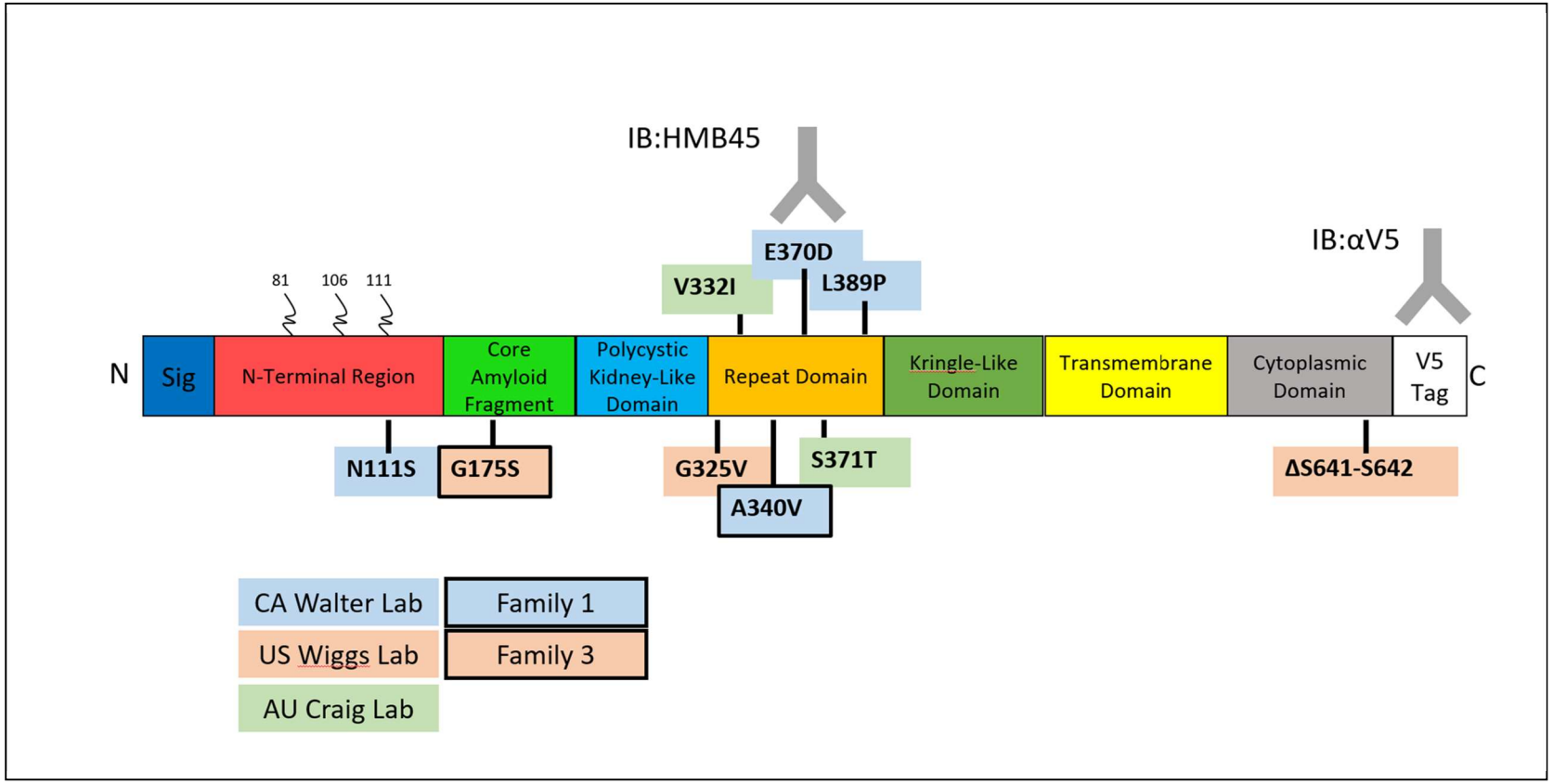

Figure 8. PMEL Structure and PDS/PG Associated Variants Curled lines indicate N-linked glycosylation. Colored blocks indicate protein domains. Sig-Signal domain; NTR-N-Terminal Region; CAF-Core Amyloid Fragment; PKD-Polycystic-Kidney Disease Domain; RPT-Repeat Domain; Kringle-Kringle-Like Domain; TM-Transmembrane Domain; Cyt-Cytoplasmic Domain; V5-V5 Tag. IB:αHMB45 antibody binds in the repeat domain and is specific to mature sialylated PMEL while IB:αV5 binds a C-terminal tag. IB:HMB45 binds PMEL somewhere in the RPT domain and is specific to mature sialylated protein. PMEL protein was C-terminally tagged with a V5 epitope and the binding site of the antibody is indicated above. Nine missense mutations in PMEL were discovered in individuals affected with PDS: one in the NTR, one in the CAF, six in the RPT, and one in the Cyt. PDS/PG associated variants are indicated in boxes. Color coding indicates where the variant was identified, blue for Walter lab, orange for Wiggs lab, green for Craig lab, with variants initially identified in a pedigree outlined in black. A cluster of variants was identified in the RPT domain.

allele frequencies <1% in the Exome Aggregate Consortium database (ExAC), and predicted pathogenicity identified the novel missense allele p.G175S in the gene *PMEL*. Using Sanger sequencing, we evaluated *PMEL* in the rest of Family 1 to find that the p.G175S heterozygous variant segregated with all affected individuals in generations 2 and 3.

In the US cohort of 146 total PDS/PG cases sanger sequencing targeting all exons of *PMEL* identified three rare non-synonymous variants. p.G325V and p.S641_S642del were identified in two separate cases and p.L389P was observed again in one case. In the Australian cohort of 135 PDS/PG cases, the rare variants p.V332I and p.S371T were found in two separate cases. The p.E370D variant was observed again in two additional cases in this cohort.

Overall, nine different non-synonymous PDS/PG-associated *PMEL* variants were identified in a total of 13 patients, with six different variants located in the essential structural domain called "RPT", and three located in other functional domains. Notably, p.N111S is situated at a confirmed N-linked glycosylation site.[170] These variants are summarized in Table 3. All variants were found in a heterozygous state in the individual patients supporting a dominant mode of inheritance. Allele frequencies of all PDS/PG-associated *PMEL* variants are shown in Table 3.

Table 3. Non-synonymous PMEL Variants in PDS/PG Cases						
				Allele Frequency		
Protein NP_001186983.1	Variant	cDNA NM_001200054.1	dbSNP ID	gnomAD MAF§	Current Study (# alleles / 792)	PMEL Domain*
p.Asn111Ser	N111S	c.332A>G	n/a	n/a	0.0013 (1)	NTR
p.Gly175Ser	G175S	c.523G>A	n/a	n/a	0.0013 (1)	CAF
p.Gly325Val	G325V	c.974G>T	rs148258956	0.003320	0.0013 (1)	RPT
p.Val332Ile	V332I	c.994G>A	rs748713829	0.00005610	0.0013 (1)	RPT
p.Ala340Val	A340V	c.1019C>T	rs756974126	0.00006353	0.0013 (1)	RPT
p.Glu370Asp	E370D	c.1110G>C	rs17118154	0.002478	0.0038 (3)	RPT
p.Ser371Thr	S371T	c.1112G>C	rs770516374	0.000008952	0.0013 (1)	RPT
p.Leu389Pro	L389P	c.1166T>C	rs142410496	0.000735	0.0038 (3)	RPT
p.Ser641_Ser642del	ΔS641-S642	c.1926T>C	rs765828110	0.00005377	0.0013 (1)	Cyt

Table 3. Non-synonymous PMEL variants in PDS/PG cases. Targeted resequencing of PMEL confirmed the p.G175S and p.A340V variants found in Families 1 and 2, and identified seven other variants in 11 isolated PDS/PG cases. The cDNA and protein notations shown conform to the Human Genome Variation Society (HGVS) recommendations. gnomAD, Genome Aggregation Database; MAF, minor allele frequency; PDS, pigmentary dispersion syndrome; PG, pigmentary glaucoma. §European (Non-Finnish). *See Figure 2 for PMEL protein domain structure. Abbreviations refer to PMEL protein domains. N-Terminal Region (NTR) Core Amyloid Fragment (CAF) Repeat Domain (RPT) and Cytoplasmic domain (Cyt).

3.2 Immunoblotting Results

To investigate whether the PMEL variants identified above alter protein processing, PMEL-expressing plasmids (with a C-terminal V5 epitope tag) were transiently transfected into HeLa cells. Despite not being melanocytic in origin HeLa cells have been extensively used to study the post-translational processing of recombinant PMEL protein as its extensive modifications and essential intracellular trafficking steps are largely conserved. PMEL is extensively modified both proteolytically and by glycosylation (N- and O-linked) and as such immunoblots with certain antibodies show multiple bands representing different processing intermediates. Immunoblot analysis of cell lysates with IB:αV5 antibody directed against the C-terminal tag revealed the two-expected immature PMEL peptide intermediates P1 and Mβ in WT (Figure 8). P1, an intact form of PMEL modified with initial N-linked glycosylation was observed for WT PMEL and all variants (Figure 4). P1 converted to the short-lived P2 intermediate and then rapidly proteolytically processed by proprotein convertase in the Golgi to generate two products, Mα (N-terminal) and Mβ (C-terminal). The mature Mβ form was observed for WT PMEL and all variants, however only weakly for p.N111S. Signal intensity of the Mβ band expressed as a percentage of total PMEL intensity in each lane to express the efficiency of processing.

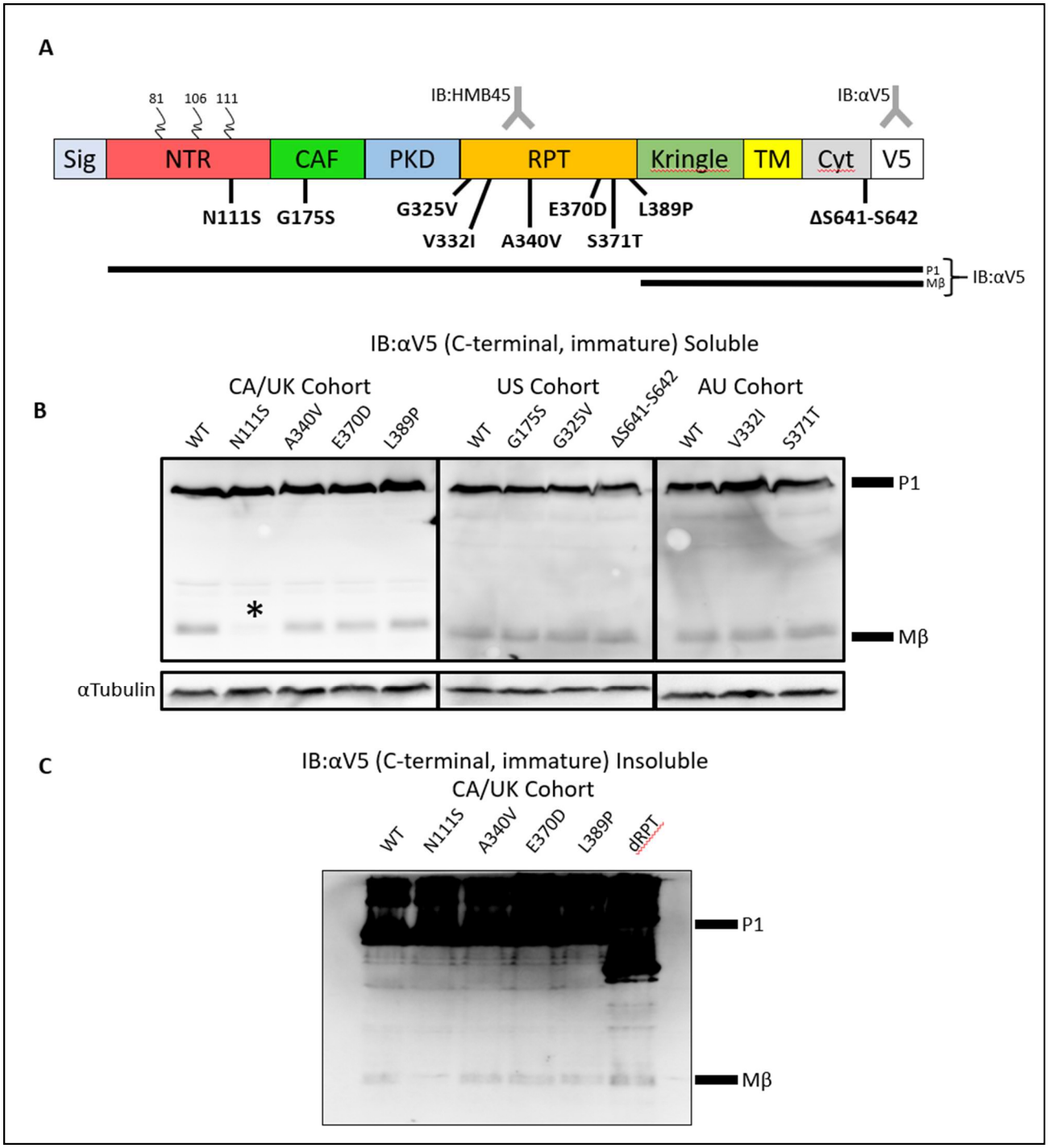
A
81
106
111
IB:HMB45
IB:αV5
Sig
NTR
CAF
PKD
RPT
Kringle
TM
Cyt
V5
N111S
G175S
G325V
V332I
A340V
E370D
S371T
L389P
ΔS641-S642
P1
Mβ
IB:αV5
B
IB:αV5 (C-terminal, immature) Soluble
CA/UK Cohort
US Cohort
AU Cohort
WT
N111S
A340V
E370D
L389P
WT
G175S
G325V
ΔS641-S642
WT
V332I
S371T
P1
Mβ
αTubulin
C
IB:αV5 (C-terminal, immature) Insoluble
CA/UK Cohort
WT
N111S
A340V
E370D
L389P
dRPT
P1
Mβ

Figure 9. Western blotting using IB:αV5 processing defects in variant PMEL. (A) Schematic representation of PMEL showing processing intermediates detected by the C-terminal IB:αV5 and internal sialylation specific IB:HMB45 antibodies. Curled lines indicate N-linked glycosylation. Colored blocks indicate protein domains. Sig-Signal domain; NTR-N-Terminal Region; CAF-Core Amyloid Fragment; PKD-Polycystic-Kidney Disease Domain; RPT-Repeat Domain; Kringle-Kringle-Like Domain; TM-Transmembrane Domain; Cyt-Cytoplasmic Domain; V5-V5 Tag. Black lines underneath represent intermediate processing forms detected by either antibody. IB:αHMB45 antibody binds in the repeat domain and is specific to mature sialylated PMEL while IB:αV5 binds a C-terminal tag. Nine missense mutations in PMEL were discovered in individuals affected with PDS: one in the NTR, one in the CAF, six in the RPT, and one in the Cyt. **(B)** Probing transfected Hela cell lysates with IB:αV5 shows that the Mβ band for the p.N111S sample has significantly lower relative intensity compared to WT (student's 2-tailed T-test [$p<0.05$]) suggesting processing defects. **(C)** Probing transfected Hela cell insoluble lysates from the CA panel of variants generated using an inclusion body solubilisation buffer with IB: αV5 revealed no differential detection of PMEL fragments using this method.

The p.N111S variant was the only significantly different variant ($p<0.0001$, n=3 biological replicates, with Mβ accounting for only ~3% of total intensity (compared to 28% for WT PMEL) (Figure 10). No accumulation of the short-lived protein intermediate P2 was observed suggesting that this is not due to inefficient proprotein convertase cleavage but instead that p.N111S prevents efficient ER protein folding and reduces export from the ER. I treated the insoluble fraction of the cell lysates with an inclusion body solubilisation buffer to address the possibility that the p.N111S variant alters the physical properties of the Mβ fragment causing it to become insoluble or resistant to SDS denaturing thus preventing detection by IB:αV5. Containing 8M Urea and 2-Mercaptoethanol, the buffer is designed to break apart protein aggregates and tertiary protein structure to solubilise challenging targets[171]. Probing a subset of variant (p.N111S, p.A340V, p.E370D, and p.L389P) lysates treated in this way showed results identical to the results obtained with standard Levin Lysis buffer (Figure 8). This confirmed that the defect appears to be the result of slow processing of the P1 form and not a change in physical properties.

To further characterize PMEL protein processing, cell lysates were also probed with IB:HMB45 antibody which is specific to mature sialylated PMEL processing intermediate Mα and to three smaller proteolytically processed forms, MαC1, MαC2, and MαC3, containing slight variations of the Repeat domain (RPT) (Figure 4). Three of the nine variants (p.L389P, p.G175S, and p.V332I) were detected and processed normally. However, IB:HMB45-reactive bands for p.N111S and p.A340V were not observed, suggesting these variants impair glycosyl group maturation or render the RPT-containing peptides unable to be detected by standard immunoblotting (Figure 2C). In a subset of variants altered ratios of the MαC1, MαC2, and

MαC3 subtypes were observed (Figure 9, 10). Significantly ($P<0.05$, n=3 biological replicates, Student's Two-tailed T-test) less MαC1 relative to Mα was observed for p.E370D, indicating that the variant impairs the production of this product. For p.G325V and p.S371T significantly ($P<0.05$, n=3 biological replicates, Student's Two-tailed T-test) more MαC1 and a concomitant decrease in MαC3 was observed suggesting these variants prevent or reduce the production of MαC3 and lead to an accumulation of MαC1. These data are consistent with PDS/PG-associated PMEL variants affecting protein processing. The same inclusion body solubilisation method detailed previously was applied again to investigate the possibility of solubility changes induced by the subset of variants from the CA cohort. Like prior results with IB:αV5, no differential detection of the missing fragments was observed when probing these immunoblots with IB:HMB45. This confirmed that the failure to detect the p.N111S and p.A340V variants was not caused by solubility or denaturation differences suggesting that the biochemical defects are in post-translational modification, protein stability, or that HMB45 reactive fragments of these variants form non-fibrillar aggregates not sensitive to highly denaturing conditions due to altered amyloid properties.

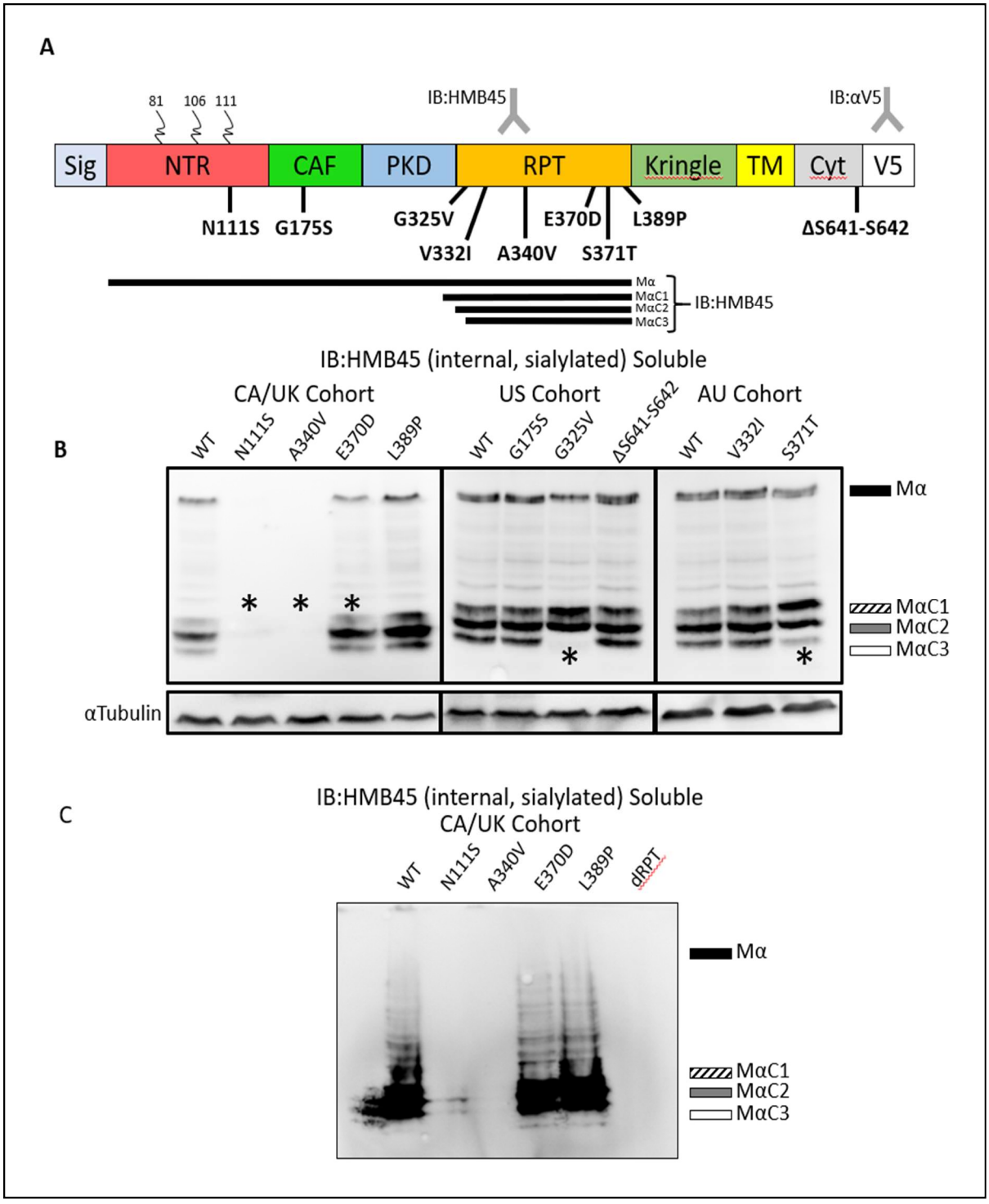
A
81
106
111
IB:HMB45
IB:αV5
Sig
NTR
CAF
PKD
RPT
Kringle
TM
Cyt
V5
N111S
G175S
G325V
V332I
A340V
E370D
S371T
L389P
ΔS641-S642
Mα
MαC1
MαC2
MαC3
IB:HMB45
IB:HMB45 (internal, sialylated) Soluble
CA/UK Cohort
US Cohort
AU Cohort
B
WT
N111S
A340V
E370D
L389P
WT
G175S
G325V
ΔS641-S642
WT
V332I
S371T
Mα
MαC1
MαC2
MαC3
αTubulin
C
IB:HMB45 (internal, sialylated) Soluble
CA/UK Cohort
WT
N111S
A340V
E370D
L389P
dRPT
Mα
MαC1
MαC2
MαC3

Figure 10. Western blotting using IB:HMB45 reveals processing defects in PMEL. (A) Schematic representation of PMEL showing processing intermediates detected by the C-terminal IB:αV5 and internal sialylation specific IB:HMB45 antibodies. Curled lines indicate N-linked glycosylation. Colored blocks indicate protein domains. Sig-Signal domain; NTR-N-Terminal Region; CAF-Core Amyloid Fragment; PKD-Polycystic-Kidney Disease Domain; RPT-Repeat Domain; Kringle-Kringle-Like Domain; TM-Transmembrane Domain; Cyt-Cytoplasmic Domain; V5-V5 Tag. Black lines underneath represent intermediate processing forms detected by either antibody. IB:αHMB45 antibody binds in the repeat domain and is specific to mature sialylated PMEL while IB:αV5 binds a C-terminal tag. Nine missense mutations in PMEL were discovered in individuals affected with PDS: one in the NTR, one in the CAF, six in the RPT, and one in the Cyt. **(B)** Probing transfected Hela cell lysates with IB:HMB45 shows that the Mβ band for the p.N111S sample has significantly lower relative intensity compared to WT (student's 2-tailed T-test [$p<0.05$]) suggesting processing defects. **(C)** Probing transfected Hela cell insoluble lysates from the CA panel of variants generated using an inclusion body solubilisation buffer with IB:HMB45 revealed no differential detection of PMEL fragments using this method.

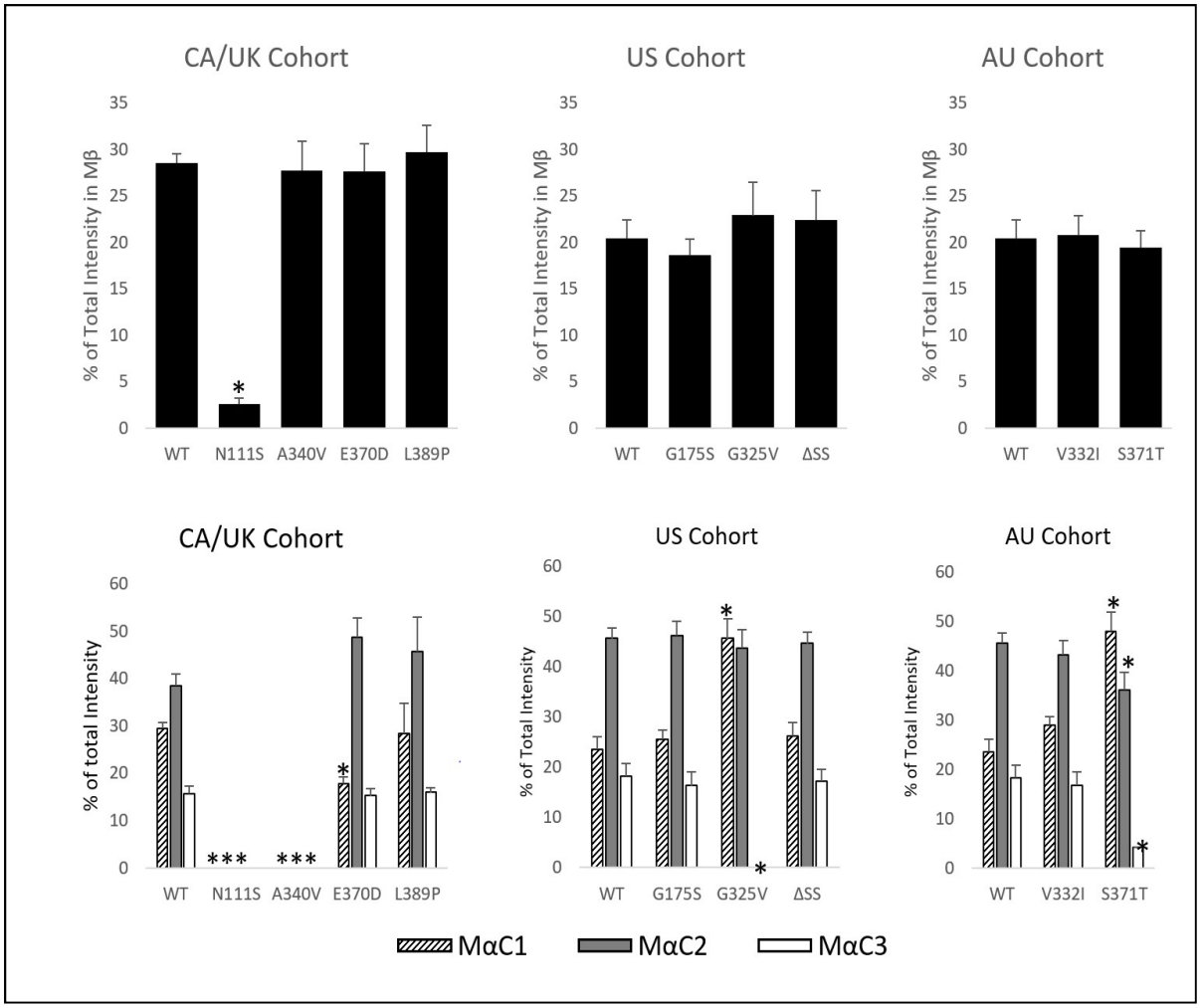

Figure 11. Quantification of Soluble Fractions from Western Blots (A) Quantification of the amount of mature Mβ processing form relative to the immature P1 form in the western blots from Figure 2. Relative amounts were quantified for three biological replicates using ImageJ. Significantly different (student's 2-tailed T-test [$p<0.05$]) relative amount of Mβ was detected only for p.N111S which showed a significant processing deficit. **(B)** Quantification of the relative amounts of MαC1 (hatched bar), MαC2 (solid grey bar), or MαC3 (white bar) relative to the immature Mα form in the western blots from Figure 2C. Relative amounts were quantified for three biological replicates using ImageJ. Significantly different (student's 2-tailed T-test [$p<0.05$]) relative amounts of MαC1, MαC2, or MαC3 were detected for p.E370D, p.G325V, p.S371T.

3.3 Immunofluorescence Colocalization

The immunoblotting results revealed that five of the nine tested variants (PMEL-N111S, -G325V, -A340V, -E370D, and -S371T) are linked with PMEL processing defects. In animal models, several pathological PMEL mutations lead to changes in subcellular localization[107,108]. To determine if PDS/PG associated PMEL variants may cause similar effects we examined protein trafficking using Immunofluorescence microscopy and colocalization of transfected HeLa cells was used to assess the trafficking of PMEL-variants to endosomes. Previous research has shown that while antibodies directed against the C-terminus of PMEL (V5 epitope in this study) mainly detect signals in the ER and Golgi, probing with HMB45 detects puncta which primarily colocalize with endosomes that contain mature PMEL, marking the final step in trafficking to the endosome.[135,167,172] V5 immunostaining revealed cytosolic mesh-like staining for all constructs, consistent with ER staining as expected (Figure 11). Strikingly, punctate HMB45 immunostaining was observed for all constructs (Figure 11), including PMEL-N111S and -A340V, indicating that sialylated RPT-containing peptides are indeed generated by these mutants despite being undetectable via SDS-PAGE immunoblotting. An altered glycosylation pattern may lead to premature degradation of a portion of the recombinant protein pool.[150] Overall the observed staining pattern with two PMEL specific antibodies appeared normal and consistent among all variants indicating trafficking was not disrupted.

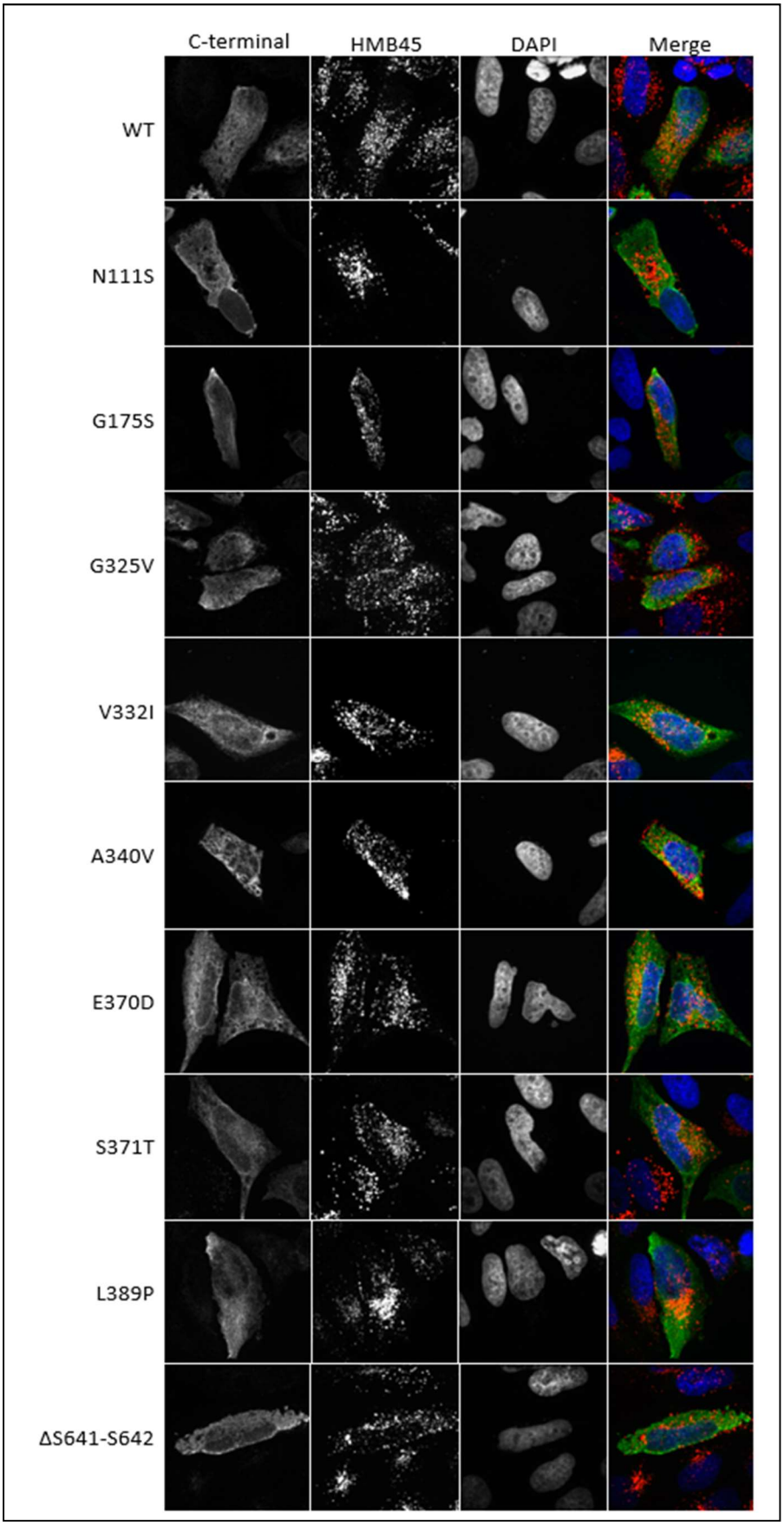
C-terminal
HMB45
DAPI
Merge
WT
N111S
G175S
G325V
V332I
A340V
E370D
S371T
L389P
ΔS641-S642

Figure 12. Immunofluorescence microscopy shows that PMEL variants appear to traffic normally (A) V5-tagged PMEL (green) appears mesh like suggesting ER localization in all variants. No differences between PMEL-WT and any PDS/PG associated variants were observed. HMB45-reactive PMEL (red) appears correctly as cytoplasmic puncta suggesting correct trafficking to a subset of endosomes and no clear retention in the Golgi. The same pattern was observed for all variants suggesting no defects in trafficking. DAPI staining was used to show the nucleus (blue).

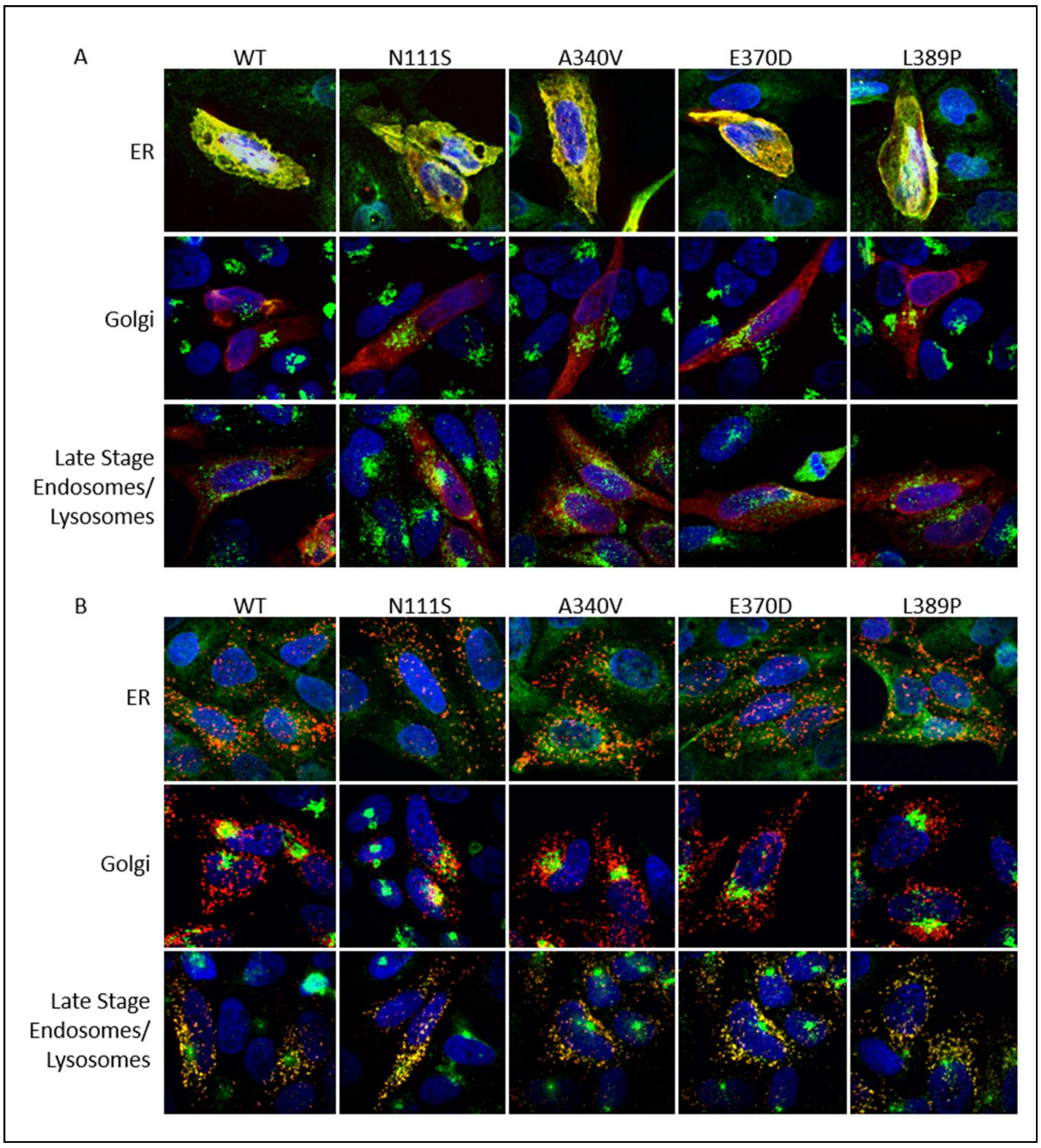

Figure 13. Subcellular colocalization immunofluorescence demonstrates that PMEL variants do not impair trafficking To confirm that variants do not impair trafficking a more thorough subcellular colocalization analysis for a subset of variants was undertaken. **(A)** V5-tagged PMEL (red) colocalizes with ER (green, upper panels) and partially with Golgi (green, middle panels), but not endosomal markers (green, bottom panels). No differences between WT PMEL and PDS/PG associated PMEL variants were detected. **(B)** HMB45-reactive mature sialylated PMEL (red) shows correct trafficking to a subset of endosomes (green, bottom panels), and is not retained within the ER (green, top panels) or Golgi (green, middle panels).

To rule out a subtle subcellular localization defect, a subset of variants (PMEL-WT, -N111S, -A340V, -E370D, and -L389P) were chosen for quantitative immunofluorescence subcellular colocalization analysis with several organelle specific markers. V5 and HMB45 signals were assessed relative to ER, Golgi, and endosome markers (Figure 12). Interestingly, PMEL-N111S is able to be normally trafficked, suggesting instead that there is sufficient mature protein accumulated by 48 hours to mask differences. Together these data indicate that all variants traffic normally and thus the defects in protein processing for PMEL-N111S, -G325V, -A340V, -E370D, and -S371T variants cannot be explained by trafficking defects.

3.4 Transmission Electron Microscopy

The essential function of PMEL is dependent on its ability to form amyloid fibrils in the melanosome. Ultrastructural analysis of transfected HeLa cells through transmission electron microscopy (TEM) has been extensively used to assess PMEL fibrillization potential[157,173]. Exogenous expression of PMEL induces ectopic pseudomelanosomes in endosomes containing processed fibrillar PMEL. PMEL expression constructs containing WT or PDS/PG-associated PMEL variants were transfected into HeLa cells to examine their effects on the ultrastructure of the induced pseudomelanosomes. An artificial deletion variant lacking the RPT domain called ΔRPT, previously shown to lack fibril forming capacity in Hela cells, was used as a comparator. 37 Differences in fibril formation, fibril organization, and organelle shape were qualitatively assessed and scored for all observed pseudomelanosomes in WT or variant PMEL expressing cells (Figure 13). Generally, although a range of structures were observed, WT pseudomelanosomes tended to have one set of straight evenly spaced fibrils in ellipsoid organelles as expected. A significant fraction of pseudomelanosomes with abnormal fibril

structure (jagged and densely packed) and/or multiple sets of fibrils were observed in cells expressing p.N111S, p.G325V, p.V332I, p.E370D, and p.L389P suggesting that melanosomes in cells expressing these variants are different from cells expressing wildtype PMEL (Figure 13). Although p.N111S does not change the primary sequence of the RPT domain, the previous observation that p.N111S is inefficiently processed may have downstream consequences causing disordered fibrils. Intriguingly, these data may indicate that some PDS/PG-associated PMEL variants are gain-of function mutations.

In total, 5/9 PMEL variants displayed defects in protein processing with a separate 5/9 variants having defects in melanosome structure or fibril formation. Together, my results revealed that 7/9 of the variants of PMEL (3/9 with defects on both immunoblotting and TEM assays) found in PDS/PG patients displayed detectable defects.

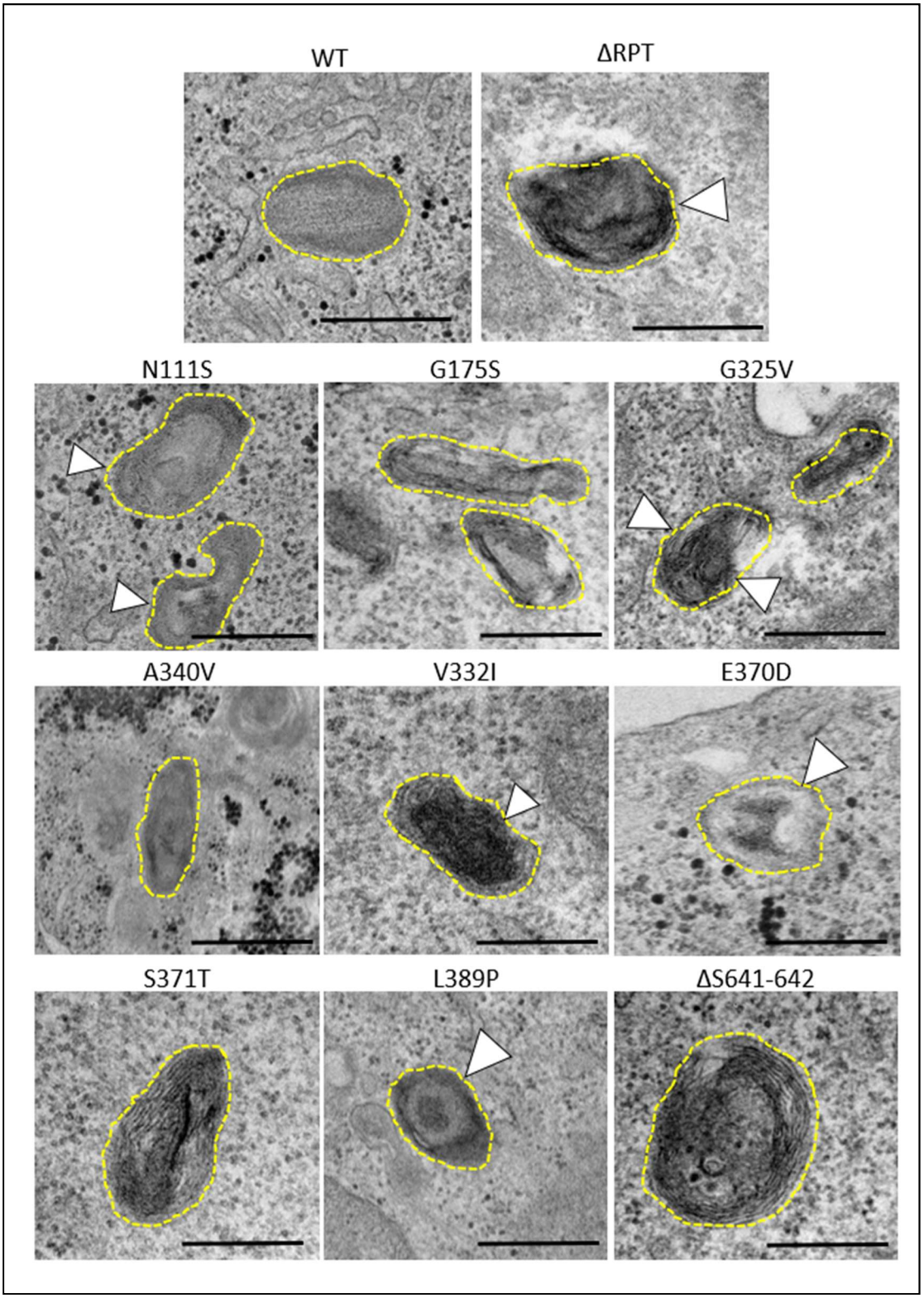
WT
ΔRPT
N111S
G175S
G325V
A340V
V332I
E370D
S371T
L389P
ΔS641-642

Figure 14. Ultrastructural Analysis of PMEL-variants reveals defects in fibril formation and organization PDS/PG associated PMEL variants were transfected into HeLa cells where PMEL expression induces the formation of ectopic pseudomelanosomes in endosomes. These pseudomelanosomes were identified based on appearance and scored for several features including abnormal fibril appearance, organization, and overall organelle shape. Variants were compared to both WT PMEL and p.ΔRPT a synthetic deletion lacking the RPT which has previously been shown to have significant fibrillogenesis defects. Representative images for all PMEL variants are shown. WT pseudomelanosomes mostly appeared to have straight fibrils with regular spacing and an overall ellipsoid shape. Abnormal fibrils or abnormal fibril organization were observed for 5 PDS/PG associated variants (white arrowheads) p.N111S, p.V332I, p.E370D, p.L389P, and p.G325V (Figure 15). Overall fibrillogenesis defects were observed for 5/9 variants analyzed. Scale Bar = 500 nm

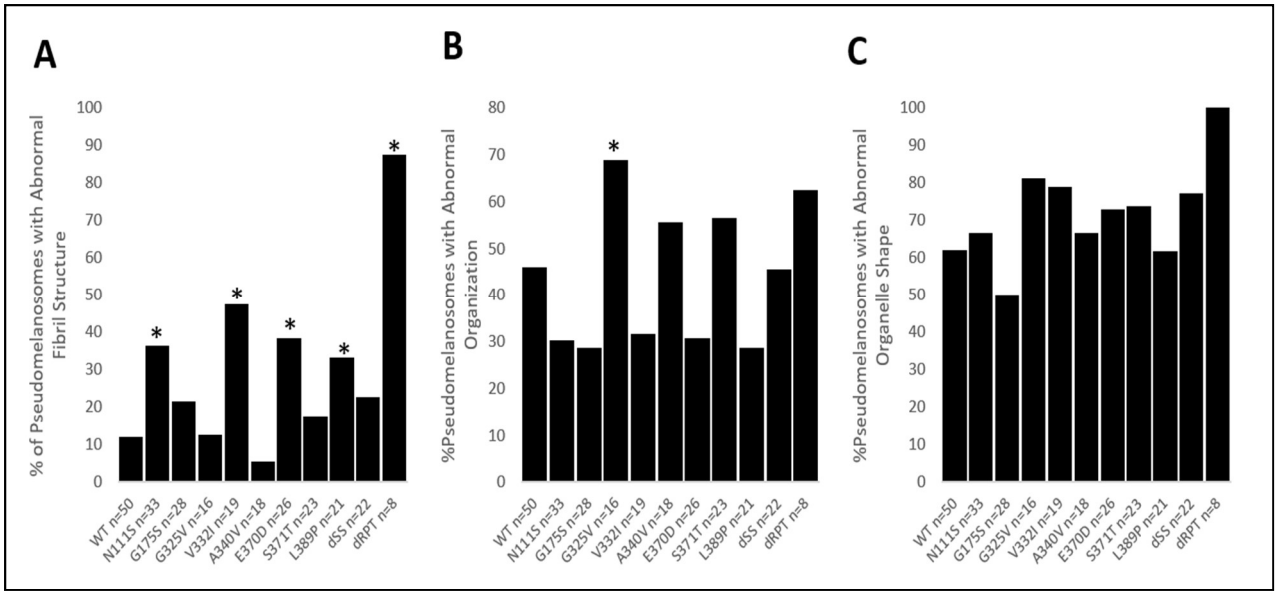

Figure 15. Quantification of ultrastructural defects observed in pseudomelanosomes show four variants with abnormal fibril formation and one variant with abnormal organization.
Pseudomelanosomes were scored for three features (n=# of pseudomelanosomes scored). Proportion of pseudomelanosomes exhibiting a certain defect were compared using a one-tailed Z-statistic proportion test ($p<0.05$). (A) Pseudomelanosomes were scored for the appearance of abnormal fibrils. PMEL-N111S, -V332I, -E370D, and –L389P contained significantly more pseudomelanosomes with abnormal fibrils ($p<0.05$). (B) Pseudomelanosomes were scored for abnormal fibril organization. Significantly more pseudomelanosomes with abnormal fibril organization were observed for PMEL-G325V than WT ($p<0.05$). (C)) Pseudomelanosomes were scored for abnormal organelle shape. No significant difference in the proportion of abnormally shaped pseudomelanosomes between PMEL-WT and PDS/PG associated variants was observed.

Chapter Four:

Discussion

Portions of this chapter were written for "*Non-Synonymous variants in Premelanosome Protein (PMEL) are associated with ocular pigment dispersion and pigmentary glaucoma*." Adrian A. Lahola-Chomiak et al. (*In Prep*)

Portions of this section were previously published in
"*Molecular Genetics of Pigment Dispersion Syndrome and Pigmentary Glaucoma: New Insights into Mechanisms*"
by Adrian A. Lahola-Chomiak and Michael A. Walter
in the *Journal of Ophthalmology* Volume 2018 March 26 2018

4.1 Genetics

This study establishes *PMEL* as a candidate gene for PDS/PG based on the discovery of multiple mutations in patients and the biochemical defects within cells expressing PMEL variants. Interestingly, mutation of *Gpnmb,* a close homologue of *PMEL* with conservation of many functional domains,[174] induces iris pigment dispersion in the DBA/2J murine model of glaucoma[166] with homozygous mutations in the genes for tyrosinase-related protein 1 (*Tyrp1*^{b}) and glycoprotein nonmetastatic melanoma B (*Gpnmb*^{r150x}). In mice, more than 10 genes involved in melanosome biogenesis, melanin synthesis, or melanosome transfer have been implicated in iris pigment dispersion and iris atrophy[80,85–87,96]. Prior association between *TYRP1* and *GPNMB* variants and disease has not been observed in humans [166]. Consistent with our data, mutations of *PMEL* have been shown to be responsible for impaired pigmentation and ocular developmental defects in animals; silver dapple horses with multiple congenital ocular anomalies (MCOA),[175] blue merle dogs with dapple pigmentation and MCOA,[168] silver mice with misshapen melanosomes of the retinal pigment epithelium (RPE) and uveal melanocytes,[176] and the *fading vision* zebrafish with reduced pigmentation in the body and RPE accompanied by disrupted photoreceptor morphology and visual deficits as measured by optokinetic response.[169] Melanin synthesis is a tightly regulated process that can generate cytotoxic melanin synthesis intermediates[88], and melanosomal dysfunction could lead to melanocyte death in the IPE[80,88].

In all three families examined affected individuals were observed in each generation with both males and females affected consistent with an autosomal dominant mode of inheritance. Supporting this model heterozygous non-synonymous *PMEL* variants were associated with PDS/PG in two families (1 and 3) and 9 cases in the singleton panels. *PMEL* was initially

selected as a high priority candidate for biochemical analysis following genetic analysis of Family 1 and the CA 113 singleton case panel. This was based primarily on the biological function and existing knowledge concerning *PMEL* with respect to ocular and pigmentary defects in animal models. *ZFHX2* and *PCDH15*, two additional candidate genes generated from the WES analysis, were chosen for screening in the CA panel but not biochemical analysis for several reasons. Variants in *ZFHX2* and *PCDH15* segregated with PDS/PG in certain branches of Family 2 and at least one additional genetic variant was identified in the PDS/PG panel for both genes. Since no single gene showed segregation throughout Family 2 both *ZFHX2* and *PCDH15* were included in the panel screen. However, neither gene had a promising biological function tying it to the pathology of PDS/PG. *ZFHX2* is an under characterized but seemingly broad functioning transcription factor making an eye disease specific role challenging to hypothesize. Pathological variants in *PCDH15* are tightly associated with Usher syndrome Type 1D/F (OMIM #601067 and #602083) which is characterized primarily by pigmentary retinopathy and not iris dysfunction or glaucoma. Additionally, more non-synonymous *PMEL* variants were identified in the CA singleton case panel than both *ZFHX2* and *PCDH15* combined. The decision to focus on *PMEL* was further supported by a collaborator identifying an additional pedigree where the PDS/PG phenotype segregated perfectly with variants in *PMEL* (excluding one individual who was symptomatic but did not harbor a *PMEL* variant) and identification of four additional non-synonymous variants between the US and AU singleton panels.

A critical look at the collected genetic evidence in this study reveals the challenging nature of studying the heritable component of PDS/PG. Despite the relatively strong evidence for PMEL variants playing a role in the pathology of PDS/PG, both the pedigree and panel results suggest it

is unlikely to be a common monogenic cause. In family 1 the p.A340V PMEL variants was associated with PDS/PG in two affected cousins and not shared by their unaffected mothers (who were related). However, Sanger sequencing of other individuals in the family revealed five individuals who carried the variant but were normal under examination drawing the association into question. This interpretation assumes high fidelity regarding the phenotyping, but given the transient nature of the PDS phenotype and the circumstances of the exams (done with portable equipment in the patient's remote home), it remains possible that some individuals have undiagnosed PDS thus masking the true impact of the variant. Regardless, even in family 2 which had higher fidelity exams, the p.G175S variant is observed in all but one affected individual (I-I). This branch of the family is affected by PDS/PG independent of the p.G175S variant with a likely candidate gene identified by Dr. Janey Wiggs (unpublished). Together the pedigree data demonstrate that these PMEL variants are unlikely to be Mendelian causes of PDS/PG given the observation of unaffected individuals carrying the variants. Instead they are more likely major contributors to the pathology in a complex inheritance model where several genetic and environmental factors contribute to the overall disease risk.

In total the three singleton panels (CA, US, and AU) comprised 394 patients of which 11 cases with variants in *PMEL* were identified. Although the study is limited by the number of patients, the panel results clearly demonstrate that PMEL variants are not a widespread cause of PDS/PG with only a combined 1.39% allele frequency when including all *PMEL* variants. Additionally, there is no enrichment of *PMEL* variants in the singleton cohort relative to a comparator population when considering all missense and LoF alleles in the ExAC database (1.39 vs 5.48%) which contains high quality data for 60,706 exomes. As expected the variants observed more

than once, p.E370D and p.L389P, are the amongst the most common variants in the population being the 1st and 14th most common variants respectively. There is some complexity regarding ethnicity with respect to p.E370D given that it is far more common in African (7.48%) than in European non-Finnish populations (0.27%). Since most of the study participants are of European ancestry a more accurate comparator may be this allele frequency which suggests a slight enrichment of this variant in our population (0.38% in panel vs 0.27% population). Additionally a challenge when using the ExAC database is that the included individuals are only superficially phenotyped and as such we would expect PDS/PG causing variants to be at a population frequency in this data set. One interpretation of the depleted PMEL allele frequency in the singleton panels is that only variants which impair PMEL function in a specific manner cause PDS/PG. This hypothesis is consistent with evidence from animal models where total PMEL LoF alleles such as deletions, are less damaging than gain of function alleles. As the underlying pathology of PDS/PG remains cryptic the properties of variants which contribute to PDS/PG is challenging to predict but may be a function of a switch from physiological to pathological amyloid. Of the 9 variants, 7 are in domains which participate in the final fibril formation supporting this hypothesis. Finally, it is unclear which observed *PMEL* variants are benign polymorphisms given that pathogenicity prediction for poorly conserved genes such as *PMEL* can be challenging. It is possible that a large proportion of the observed variation in the public databases in *PMEL* does not impact protein function and thus is not relevant to PDS/PG.

4.2 Biochemical Experiments

The molecular experiments outlined in this study describe relatively mild biochemical defects caused by seven of the nine PDS/PG associated PMEL variants. This is consistent with the

known pathophysiology of PDS/PG. Patients usually present with PDS around age 12 and do not suffer from systematic pigmentary abnormalities. In contrast, strongly pathological animal *PMEL* mutations cause acute melanocyte cell death leading to severe developmental ocular anomalies and body wide pigmentation defects. Thus, we hypothesized mild defects may which lead to iris melanocyte impairment and eventual death over longer time scales. This model exploits the fact that iris melanocytes uniquely undergo continuous melanogenesis but do not transfer melanosomes, which in PDS/PG patients may be toxic, to keratinocytes as in hair and skin. This difference could explain the iris specific pigmentary abnormalities caused by PMEL variants. Given the known properties impaired by pathological variants I interrogated PMEL trafficking, processing, and fibril forming capacity to identify mild defects.

Using a transiently transfected non-melanocytic (HeLa) *in vitro* cell model we determined PDS/PG associated PMEL variants do not cause major trafficking defects. Mature HMB45 reactive PMEL puncta presumably representing endosome trafficked protein was observed in for all variants. This indicates all PDS/PG associated variant PMEL protein retains the capacity to properly traffic to melanosomes rather than becoming totally ER retained as with the D^{w} (Dominant white) chicken mutation. This analysis takes advantage of the fact that the melanosome trafficking pathway in melanocyte is analogous to the endosomal trafficking pathway in HeLa cells. To confirm this observation a subset of variants (p.N111S, p.A340V, p.E370D, and p.L389P) were chosen for in depth subcellular colocalization analysis. These confirmed that immature PMEL localizes entirely to the ER and part of Golgi apparatus as expected but is excluded from the other parts of the Golgi and endosomes. This coincides with HMB45 reactive detection appearing in the Golgi and persisting in LAMP2 reactive endosomes.

There are two major challenges to interpreting these data. The use of non-melanocytic HeLa cells may mask subtle or melanocyte specific defects but extensive prior work with these cells has established that both Golgi specific and membrane trafficking pathways are retained. This is because the machinery required to traffic PMEL is generic and widely expressed. More important to this analysis may be the time frame on which the cells were examined. These experiments do not address the rate of trafficking PMEL protein only its capacity, leaving open the possibility that PDS/PG associated PMEL variants slow but do not stop PMEL trafficking. 48 hours after transfection when these cells were examined they may appear identical because PMEL, and amyloids in general, are remarkably stable proteins which can accumulate. Physiological amyloid formation is dependent on rapid fibril formation and mutations which impair the speed of trafficking could have broader consequences for proper fibril formation. Mutations such as p.N111S may cause mild misfolding in the ER by eliminating the glycosl group which can be corrected by chaperones but still slows the overall rate of ER export. Current experiments which examine a single late time point do not address this possibility.

Immunoblotting experiments highlighted mild defects with several variants consistent with our pathology hypothesis. Probing against the C-terminal V5 antibody revealed p.N111S caused slow processing of the P1 intermediate to Mβ. Underlying this may be non-fibrillar aggregation caused by misfolding in the ER and subsequently reduced processing by proprotein convertase due to slow export. Proprotein convertase cleavage itself was not affected however because no accumulation of the short-lived intermediate P2 was observed. Inclusion body solubilisation buffer results demonstrate that this reduced detection is not because of altered physical properties as there was no differential detection. Probing with HMB45 provided more varied and

challenging to interpret results. Two variants (p.N111S and p.A340V) were undetected in either the soluble or insoluble fraction, but current experiments do not elucidate the reason. This effect was specific to immunoblotting results as the same antibody was able to specifically detect mature PMEL puncta in immunofluorescence experiments. Slow accumulation of mature PMEL caused by the p.N111S variants may impair proper RPT domain O-glycosylation or sialylation rendering these fragments undetectable in denaturing conditions. Similarly impaired glycosylation could explain this observation with respect to p.A340V but the effect could also be caused by this variant residing in the presumptive binding site. When fixed in its native conformation PMEL fibrils remain detectable explaining immunofluorescence results but dissociating these fibrils into their component fragments (PKD, CAF, RPT) prevents detection by HMB45. Another class of variants (p.E370D, p.G325V and p.S371T) maintained detection of PMEL by HMB45 but altered the ratio or presence of the three mature RPT containing fragment, called MαC1, MαC2, and MαC3. This is a challenging observation to interpret as no differential function is ascribed to these forms in the literature. Differences in the appearance and ratio of these forms has been noted between melanocyte, melanoma, and non-melanocytic origin cell lines but all these retain fibril forming capacity. One hypothesis regarding the function of the RPT domain is that it protects forming fibrils from intralumenal proteases in the developing melanosome. It is possible that increased sensitivity to proteases during melanosome formation causes mild defects which manifest over the melanosome lifetime. Unincorporated toxic soluble amyloid oligomers or protein aggregates which form within the melanosome could impair melanin synthesis and slowly cause the predicted pathology.

There is some evidence that a subset of variants cause defects in either fibril formation or maintenance from EM experiments. Ultrathin section images were analyzed using a qualitative analysis system which scored all observed examples of induced ectopic psuedomelanosomes for three scorable features. Five variants were statistically worse than WT with respect to the proportion of scored psuedomelanosomes displaying pathological features (p.N111S, p.G325V, p.V332I, p.E370D, and p.L389P). An important facet to acknowledge with respect to the hypotheses outlined to explain to immunoblotting results is that these images were taken 48 hours after transfection which means subtle defects which manifest on longer time scales were not assessed. Regardless, the fact that five of nine variants appeared worse than WT at this time suggests that PDS/PG associated PMEL variants may converge on disrupting fibril function as a mechanism of pathology. However, EM analysis is challenging in a transiently transfected model given that only a small number of cells (relative to immunofluorescence) are captured for imaging and interpretation requires subjective input. Although images were analyzed with the input of an experienced EM technician, lacking a specific immunogold detection means that there remains some ambiguity in what can be classified a psuedomelanosome. Additionally, qualitative analysis of these organelles is limited in part by human interpretation. Methods like EM tomography could perhaps more faithfully capture fibril structure. Ultimately these data serve as a foundation for future analysis of fibrils in stably expressing cell lines with more precise analytical approaches to the data. They support the hypothesis that PDS/PG fibrils cause biochemical defects consistent with melanosome dysfunction arising from improper fibril function. Importantly TEM experiments directly queried PMEL function demonstrating a definable defect in a biological process which could be the basis for PDS/PG pathology.

4.3 Models of PDS and PG considering Results

The discordance between structural features being primarily implicated in human PDS and melanocyte death being implicated in animal studies suggests it is essential to revaluate classical models of PDS/PG. Undoubtedly, the most thoroughly investigated model of PDS/PG is the '*structural model'* in which a structural abnormality of the iris is responsible for excessive irido-zonular contact which removes pigmented cells from the IPE via a mechanical rubbing force (Figure 1)[10]. Several lines of evidence support this structural model. Some patients with PDS have demonstrable iris concavity, and most are myopic further supporting some structural component [11,14,36,39]. Abnormal irido-zonular contact can be observed in patients with PDS where mechanical rubbing may occur[10,11] correlating well with the midperipheral and radial distribution of iris transillumination defects[6,9]. Mechanical strain on the eye via rigorous exercise leading to pigment liberation demonstrates the potential mechanical nature of this defect[45–48]. The concept of the reverse-pupillary block acting to maintain this abnormal contact and facilitate mechanical rubbing has relevance for both PDS and pseudophakia[10,28]. However, there are several limitations of this structural model as well. Notable is the lack of evidence supporting laser peripheral iridotomy (LPI) as a beneficial surgical intervention. LPI is designed to flatten the iris and alleviate iris concavity. Given that in a structural paradigm of PDS/PG such an abnormality would be the source of the abnormal irido-zonular contact and thus pigment shedding. However, a Cochrane review of LPI found no clear benefit of LPI in preventing loss of visual field, but rated studies examining the technique as very low quality[177]. LPI appears to be effective at flattening the iris, thus eliminating the structural insult, but this does not prevent progression to PG[178–180]. Additionally, a paucity of evidence exists surrounding the lifespan progression PDS/PG. Structural abnormalities are associated with PDS, but whether they predate the onset of

pigment shedding is unknown. It has previously been proposed that "a gene affecting some aspect of the development of the middle third of the eye early in the third trimester of fetal development may responsible for the structural defect" given the timing of iris development[6]. However, no such gene has been discovered and known anterior segment developmental control genes such as *PAX6*[181], *FOXC1*[182], and *PITX2*[183] are not associated with PDS/PG but are instead causative of other types of glaucoma[184]. It would be highly informative to carefully examine the structure of juvenile eyes, in pedigrees where PDS/PG appears to have a stronger genetic component, to address this shortfall.

An *IPE dysfunction model* of PDS/PG has the possibility to address the shortcomings of the structural model and has several interesting implications. Most notably IPE dysfunction is best supported by the existing animal literature on iris pigment dispersion, iris atrophy, and pigmentary glaucoma. Consistently, mouse models of these phenotypes have been determined to be caused by genes controlling melanin synthesis, melanosome integrity, and melanocyte health[80,85]. Although these models are not perfect analogues to PDS/PG, the theoretical model of IPE dysfunction provides a reasonable causal relationship between a genetic component and the observed clinical features of PDS. IPE dysfunction at the melanocyte level may be mediated by inappropriate release of cytotoxic melanin synthesis intermediates or impaired response to cellular stresses as pigmentation is inherently a stressful process and the iris undergoes continuous melanogenesis[88,95,185]. Melanocytes impaired in this way may die or detach constituting the liberated pigmented material (Figure 1). It is currently unknown if this material is comprised of melanin granules, melanosomes, or whole cellular debris, but resultant melanocyte cell death in the IPE is well established[18,20,30]. A melanocyte focused model has the

added benefit of providing a reasonable theoretical basis for involvement of the RPE in the pathophysiology of PDS/PG given that both structures are pigmented. The differential involvement of the tissues may be a consequence of active melanogenesis in iris melanocytes versus retinal melanocytes which seem to undergo a burst of melanosome biogenesis in development that are then retained for the patient's lifetime[185,186]. Careful consideration thus should be given to pigmentation and/or melanocyte genes in future investigations into the genetic aetiology of PDS/PG.

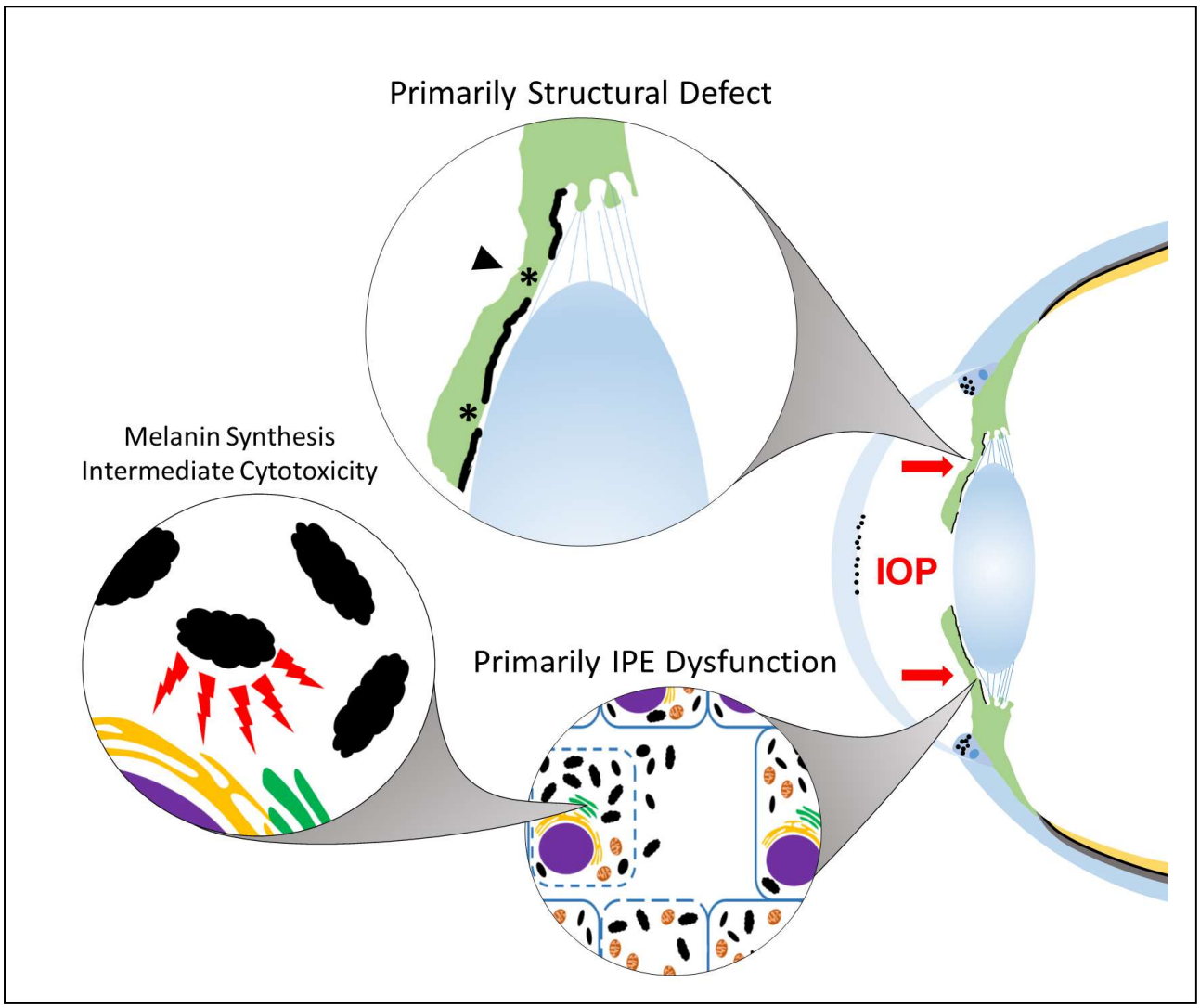

Figure 16. Schematic representation of PDS/PG models. In patients with PDS, Pigment liberated from the posterior surface of the iris (green) circulates into the anterior chamber following the flow of aqueous humor where it deposits into the cornea and trabecular meshwork (black dots). High IOP can maintain iris bowing (red arrows) due to the reverse pupillary block in which the lens and iris act together in a ball-valve pressure system which normally acts to maintain unidirectional aqueous humor flow. There are two models of PDS/PG which differ in respect to the origin of pigment dispersion from the ciliary body to the trabecular meshwork. The *structural model* of PDS/PG proposes that posterior iris bowing creates inappropriate irido-zonular contacts (black arrowhead, top circle) and that mechanical rubbing between the iris, zonules, and lens is responsible for liberating pigment from the IPE (asterisks, top circle). Although these structural features are well established is remains unclear if they predate pigment dispersion as the underlying mechanism. Animal models support IPE dysfunction as the primary driver of this dispersion. In this model, pigmented melanocytes die and/or detach from the IPE (bottom right circle) due to release of cytotoxic melanin synthesis intermediates from dysfunctional melanosomes (bumpy ovals, bottom left circle).

My data are consistent with the hypothesis that the primary cause of pigment release is melanocyte cell death and consequent detachment in accordance with previous observations in mice.[165] Given that human ocular pigment deposition is commonly juvenile onset and progresses gradually over decades, we hypothesize that dysfunctional melanosomes lead to the accumulation of ROS and/or cytotoxic melanin synthesis-intermediates in iris melanocytes. Iris melanocytes represent a unique population that undergo continuous melanosome biogenesis but do not transfer those melanosomes to keratinocytes as in the hair or skin. This may make them particularly susceptible to mutations which affect melanosome function as mildly damaging effects can accumulate over time. Although the structural role of PMEL in melanosomes has been well-established, it has previously been suggested that the primary function of PMEL is to sequester these ROS and cytotoxic melanin-synthesis intermediates to protect the cell.[187] Since the factors regulating pigmentation and ROS response are diverse (several of which have been previously implicated in glaucoma[188–190]), this process could be influenced by many genetic and environmental factors explaining the observed genetic heterogeneity for PDS/PG. As a corollary to this model, we anticipate that genetic variants that dramatically affect these processes could lead to simpler PDS/PG inheritance modes due to a larger pathological contribution, whereas combinations of genetic variants with subtle effects could underlie complex inheritance modes. The *PMEL* variants characterized here cause defects in processing and/or fibrillogenesis that likely impair PMEL's ability to protect melanocytes from ROS generated during melanin synthesis and storage. Simultaneously, *PMEL* variants that cause a transition from functional to pathogenic amyloid may also cause cell death through an alternative pathway due to the toxic effect of soluble amyloid oligomers. This mode of pathology is consistent with the observed altered fibril forming capacity and processing of the variants.

The most likely mechanism by which *PMEL* variants contribute to PDS/PG is melanocyte dysfunction causing an increase in pigment-containing cellular debris in the aqueous humor. Phagocytosis of this material by trabecular meshwork cells causes the accumulation of pigmented material in the TM, which is known to cause TM cell detachment and/or death.[191–195] The resultant loss of aqueous humor homeostasis is then associated with increased IOP-mediated retinal ganglion cell death and high-pressure glaucoma[196]. Considering the important role of melanosomes in protecting the RPE from ROS generated during photoreceptor outer segment turnover, it is intriguing to consider whether PMEL variants also simultaneously alter RPE function thereby contributing to PDS/PG retinal phenotypes as has been suggested previously.[197,198] However, it is important to consider alternate or synergistic pathologies which may contribute to the overall phenotype of PDS/PG.

Given the experimental data suggesting that at least one variant (p.N111S) undergoes non-fibrillar aggregation due to misfolding in the ER, it is important to consider if ER stress mediated pathologies contribute to melanocyte death. Furthermore, this mechanism of pathology is shared amongst neurodegenerative disease such as Huntington's Disease, Alzheimer's Disease, and Parkinson's Disease many of which are in part caused by proteins with amyloid properties[140,199,200]. The Unfolded Protein Response (UPR) is a non-protein specific mechanism which first senses aggregation of unfolded protein and then responds by downregulating protein production machinery and upregulating chaperones and degradation factors. Sensor protein such as Glucose Related Protein 78 (*GRP78*), PKR-like ER-kinase (*PERK*) and activating transcription factor 6 (*ATF6*) induce a transcriptional response culminating in activation of X-

Box bind protein 1 (*XBP-1*) which induces several UPR response genes[201]. Together these genes sequester misfolded protein by increasing retro-translocation of misfolded proteins to the ER, attempt to correct misfolding with chaperones, and massively increase the degradation of ER associated proteins[201]. Importantly this response can also induce programmed cell death via caspase induced apoptosis through several diverse pathways which can function intrinsically (such as mitochondrial mediated Caspase 9 induced cell death) or extrinsically (death receptor caspase 8 induced cell death). Both dominant white chickens and silver dapple horses have *PMEL* variants which cause profound pigmentary and ocular (for horses) defects which are in part mediated by ER stress causing melanocyte death[163,165]. Alongside melanosome dysfunction, ER stress should be a high priority candidate for future study for these reasons.

Limited evidence, primarily from studies with the DBA/2J model of glaucoma, also supports an immune component to PDS/PG. Caused in part by a variant in the PMEL homologue, GPNMB, the DBA/2J is a highly studied glaucoma model and immune dysfunction in the anterior segment has been extensively characterized as a major factor in the development of glaucoma in this model. Aqueous humor from eyes which will become glaucomatous fails to properly suppress T-cell activation leading to increased inflammation which predates iris pigment dispersion in this model. It is unclear if inflammation predating iris pigment dispersion is some indication that melanocyte dysfunction may in part be mediated by an autoimmune reaction or if this basal immune dysfunction predisposes the eye to problems when melanocyte antigens begin to deposit in the anterior segment. This interpretation is somewhat complicated in the DBA/2J mouse model because *GPNMB* has an important immune function in neural tissue which PMEL does not, leaving the possibility that this is a model specific effect[202]. There remains a significant

knowledge gap with respect to an immune component in PDS/PG in humans due to a paucity of clinical studies on the subject. Since the inheritance of PDS/PG is certainly complex, an immune component could in part explain some of this complexity not captured by existing studies. Patients affected by both PDS and PG may be predisposed to a pathological reaction to melanocyte components circulating in the aqueous humor and deposited in the trabecular meshwork contributing not to PDS risk but instead primarily to the risk of conversion between these diseases.

Further study is expected to elucidate how these variants contribute to the pathology of PDS/PG and impact melanocyte health. Significant knowledge gaps exist with respect to the clinical, genetic, and cellular aspects of PDS/PG pathology. Clinically the natural history of PDS/PG is not well understood which has significant implications for understanding the basis of the disease. Families with high numbers of affected individuals such as those outlined in this study provide unique opportunities for both patients and researchers to gain insight into the early stages of disease. As mentioned above an immune insult may proceed PDS and be a major factor for conversion risk. Establishing early events in the development of PDS/PG of young patients may could be useful for pre-symptomatic detection of high risk individuals and open up new non-palliative treatment options which target the underlying pathology and not the symptoms of glaucoma. Pre-symptomatic detection is also dependent on our knowledge of genetic risk factors for PDS/PG. This study established PMEL as the first candidate gene for PDS/PG in humans but broader studies which capture the heterogeneity underlying PDS/PG will be important. It remains highly likely that a pigmentary or melanocyte abnormality underlies the pathology of this disease. Targeted genetic screens in large populations of patients focusing on genes involved

in melanosome biogenesis, melanin synthesis, or melanocyte health could be informative with respect to understanding how defects in these processes underlie the disease. Our interpretation of our *PMEL* results predicts that other genes involved in these processes would act as modifiers of disease risk in the complex inheritance model.

4.4 Future directions

With consideration to PMEL there are several intriguing lines of inquiry to understand how these variants impact PDS/PG pathology. Primarily the focus should be put on experiments which elucidate how PDS/PG associated PMEL variants impact melanocyte health and TM function. As presented, the data in this study provide a strong argument for the genetic association of PMEL variants with PDS/PG and that these variants cause biochemical defects but do not build a strong case for how these variants cause the pathology for PDS/PG. In part this is because of the use of transiently transfected non-melanocytic origin cell lines which complicates the interpretation of these defects. HeLa cells remain excellent candidates for studying the biochemical properties of PMEL but given that transfection is itself a stress and important predicted components of the pathology such as melanin synthesis are absent in these cells using stably expressing PMEL melanocyte cell lines is important to future experiments. These cells could be generated using homology directed repair (HDR) CRISPR (Clustered Regularly Interspaced Short Palindromic Repeats) or a random insertion of a PMEL construct in a non-PMEL expressing melanoma cell line like Mel220. These tools could be used to query the viability and growth rate when expressing PDS/PG associated PMEL variants to determine the impact of variant PMEL protein. Additionally, pigmentation can be pharmacologically induced or repressed to separate possible toxic amyloid oligomer, ER stress, and cytotoxic melanin

synthesis intermediate mediated pathologies. Investigating the activation of programmed cell death pathways can provide additional insight into this complicated issue as specific insults elicit specific caspase mediated cell death pathways. Established and easily adapted methods such immunoblotting, immunofluorescence, and qPCR can be used to investigate what stress responses PDS/PG associated PMEL variants and pigmentation elucidate. Aside from cell viability the pathology of PDS/PG may in part be the result of extracellular matrix (ECM) alterations in both the IPE and TM. A variety of cell stresses can cause ECM alterations which could be the underlying cause of melanocyte detachment from the IPE. Additionally, phagocytic stress can cause identical alterations which is important when considering the large amount of melanocyte derived material found inside TM cells as is evident from the observation of both TM cells and macrophages laden with pigment granules. These granules serve as an easily scorable marker for the phagocytosis of many cellular components which together cause phagocytic stress and contribute to inflammation in the TM. Clinical studies have established TM dysfunction as an important step in the conversion from PDS to PG and underlying this dysfunction is likely ECM alterations in TM cells which cause drainage canal closure and proper meshwork filtering function. Cell adhesion assays which measure cells ability to either attach onto culture dishes from suspension or maintain this connection under stress can be used to investigate if expression or expression variant PMEL, melanocyte fragment uptake, or melanin synthesis impacts both melanocytes and TM cells ability to maintain their ECM. Together these studies will provide significant insight into how these variants may underly the pathology of PDS/PG and form the basis for rationally designed therapeutics.

Finally, more detailed studies elucidating the nature of the biochemical defects caused by PDS/PG associated *PMEL* variants will be important. Given that the kinetics of amyloids are so finely tuned measuring the reaction kinetics of specifically the RPT domain across a range of pH will elucidate if altered fibrillogenesis is a consequence of variants located in this domain. Both the speed of fibril formation and the pH at which this occurs are informative as to the overall fibril forming kinetics of the fibrils. Better description of these fibrils using detailed EM experiments such as TEM tomography which provides a 3D models of fibrils could reveal more subtle defects and provide a quantifiable measurement for future analysis. Additionally, fibril integrity may have implications for melanin synthesis. Measuring the speed and efficiency of melanin synthesis in the presence of variant PMEL fibrils is potentially highly informative as inefficient melanin synthesis may underly ROS pathology. This study implies that at least one variant (p.N111S) is slowly processed but these data do not directly address this possibility. Classically pulse-chase experiment which leverage radioactive isotopes to measure the rate at which a population of tagged atoms are incorporated into a protein and then visualize the time it takes for that protein to be processed could be used to address this. Lastly, there exists a large variety of PMEL specific antibodies not used in this study. A simple way to broadly interrogate the biochemical features altered by these variants is to utilize the plethora of unique antibodies in immunoblotting and immunofluorescence experiments. Each antibody highlights different processing and trafficking aspects some of which have not been targeted in this study. Together these experiments will provide more insight into the nuanced biochemical defects which underly the specific contribution of *PMEL* variants to the pathology of PDS/PG.

Bibliography

1. Tham Y-C, Li X, Wong TY, Quigley HA, Aung T, Cheng C-Y. Global Prevalence of Glaucoma and Projections of Glaucoma Burden through 2040. *Ophthalmology*. 2014;121(11):2081-2090. doi:10.1016/j.ophtha.2014.05.013.
2. Jonas JB, Aung T, Bourne RR, Bron AM, Ritch R, Panda-Jonas S. Glaucoma. *Lancet*. 2017;390(10108):2183-2193. doi:10.1016/S0140-6736(17)31469-1.
3. Richter CU, Richardson TM, Grant WM. Pigmentary Dispersion Syndrome and Pigmentary Glaucoma. *Arch Ophthalmol*. 1986;104(2):211. doi:10.1001/archopht.1986.01050140065021.
4. Farrar SM, Shields MB, Miller KN, Stoup CM. Risk factors for the development and severity of glaucoma in the pigment dispersion syndrome. *Am J Ophthalmol*. 1989;108(3):223-229. doi:10.1016/0002-9394(89)90110-4.
5. Migliazzo C V., Shaffer RN, Nykin R, Magee S. Long-term Analysis of Pigmentary Dispersion Syndrome and Piegmentary Glaucoma. *Ophthalmology*. 1986;93(12):1528-1536. doi:10.1016/S0161-6420(86)33526-7.
6. Ritch R. A unification hypothesis of pigment dispersion syndrome. *Trans Am Ophthalmol Soc*. 1996;94:381-405; discussion 405-9. http://www.ncbi.nlm.nih.gov/pubmed/8981706. Accessed December 5, 2017.
7. Lahola-Chomiak AA, Walter MA. Molecular Genetics of Pigment Dispersion Syndrome and Pigmentary Glaucoma: New Insights into Mechanisms. *J Ophthalmol*. 2018;2018:1-11. doi:10.1155/2018/5926906.
8. Krukenberg F. Beiderseitige angeborene Melanose der Hornhaut. *Klin Monatsbl Augenheilkd*. 1899;37:254-258.

9. SCHEIE HG, FLEISCHHAUER HW. Idiopathic atrophy of the epithelial layers of the iris and ciliary body; a clinical study. *Trans Am Ophthalmol Soc*. 1958;55(2):369-88; discussion 388-91. doi:10.1001/archopht.1958.00940030084007.

10. Campbell DG. Pigmentary Dispersion and Glaucoma. *Arch Ophthalmol*. 1979;97(9):1667. doi:10.1001/archopht.1979.01020020235011.

11. Potash SD, Tello C, Liebmann J, Ritch R. Ultrasound Biomicroscopy in Pigment Dispersion Syndrome. *Ophthalmology*. 1994;101(2):332-339. doi:10.1016/S0161-6420(94)31331-5.

12. Siddiqui Y, Ten Hulzen RD, Cameron JD, Hodge DO, Johnson DH. What is the risk of developing pigmentary glaucoma from pigment dispersion syndrome? *Am J Ophthalmol*. 2003;135(6):794-799. doi:10.1016/S0002-9394(02)02289-4.

13. Sugar HS. Pigmentary glaucoma. A 25-year review. *Am J Ophthalmol*. 1966;62(3):499. doi:10.1016/0002-9394(66)91330-4.

14. SUGAR HS, BARBOUR FA. Pigmentary glaucoma; a rare clinical entity. *Am J Ophthalmol*. 1949;32(1):90-92. doi:10.1016/0002-9394(49)91112-5.

15. Murrell WJ, Shihab Z, Lamberts DW, Avera B. The Corneal Endothelium and Central Corneal Thickness in Pigmentary Dispersion Syndrome. *Arch Ophthalmol*. 1986;104(6):845-846. doi:10.1001/archopht.1986.01050180079034.

16. Lehto I, Ruusuvaara P, Setälä K. Corneal endothelium in pigmentary glaucoma and pigment dispersion syndrome. *Acta Ophthalmol*. 2009;68(6):703-709. doi:10.1111/j.1755-3768.1990.tb01699.x.

17. Prince AM, Ritch R. Clinical Signs of the Pseudoexfoliation Syndrome. *Ophthalmology*. 1986;93(6):803-807. doi:10.1016/S0161-6420(86)33664-9.

18. Gottanka J, Johnson DH, Grehn F, Lutjen-Drecoll E. Histologic findings in pigment dispersion syndrome and pigmentary glaucoma. *J Glaucoma*. 2006;15(2):142-151. doi:10.1097/00061198-200604000-00011.

19. Iwamoto T, Witmer R, Landolt E. Light and Electron Microscopy in Absolute Glaucoma with Pigment Dispersion Phenomena and Contusion Angle Deformity. *Am J Ophthalmol*. 1971;72(2):420-. doi:10.1016/0002-9394(71)91315-8.

20. Kupfer C, Kuwabara T, Kaiser-Kupfer M. The histopathology of pigmentary dispersion syndrome with glaucoma. *Am J Ophthalmol*. 1975;80(5):857-862. http://www.ncbi.nlm.nih.gov/pubmed/1190279. Accessed December 5, 2017.

21. Shimizu T, Hara K, Futa R. Fine structure of trabecular meshwork and iris in pigmentary glaucoma. *Albrecht Von Graefes Arch Klin Exp Ophthalmol*. 1981;215(3):171-180. http://www.ncbi.nlm.nih.gov/pubmed/6908466. Accessed December 5, 2017.

22. Matsumoto Y, Johnson DH. Trabecular Meshwork Phagocytosis in Glaucomatous Eyes. *Ophthalmologica*. 1997;211(3):147-152. doi:10.1159/000310782.

23. Naitoh H, Suganuma Y, Ueda Y, et al. Upregulation of matrix metalloproteinase triggers transdifferentiation of retinal pigmented epithelial cells in *Xenopus laevis* : A Link between inflammatory response and regeneration. *Dev Neurobiol*. 2017;77(9):1086-1100. doi:10.1002/dneu.22497.

24. Alvarado JA, Murphy CG. Outflow Obstruction in Pigmentary and Primary Open Angle Glaucoma. *Arch Ophthalmol*. 1992;110(12):1769. doi:10.1001/archopht.1992.01080240109042.

25. Von Hippel E. Zur pathologischen Anatomie des Glaukom. *Arch Ophthalmol*. 1901;52:498.

26. Niyadurupola N, Broadway DC. Pigment dispersion syndrome and pigmentary glaucoma--a major review. *Clin Experiment Ophthalmol*. 2008;36(9):868-882. doi:10.1111/j.1442-9071.2009.01920.x.

27. Campbell DG, Schertzer RM. Pathophysiology of pigment dispersion syndrome and pigmentary glaucoma. *Curr Opin Ophthalmol*. 1995;6(2):96-101. http://www.ncbi.nlm.nih.gov/pubmed/10150864. Accessed December 5, 2017.

28. Karickhoff JR. Pigmentary dispersion syndrome and pigmentary glaucoma: a new mechanism concept, a new treatment, and a new technique. *Ophthalmic Surg*. 1992;23(4):269-277. http://www.ncbi.nlm.nih.gov/pubmed/1589198. Accessed December 5, 2017.

29. Amini R, Whitcomb JE, Al-Qaisi MK, et al. The posterior location of the dilator muscle induces anterior Iris bowing during dilation, even in the absence of pupillary block. *Investig Ophthalmol Vis Sci*. 2012;53(3):1188-1194. doi:10.1167/iovs.11-8408.

30. S Fine B, Yanoff M, G Scheie H. *Pigmentary "Glaucoma". A Histologic Study.* Vol 78.; 1974.

31. Haynes WL, Alward WLM, Thompson HS. Distortion of the Pupil in Patients with the Pigment Dispersion Syndrome. *J Glaucoma*. 1994;3(4). http://journals.lww.com/glaucomajournal/Fulltext/1994/00340/Distortion_of_the_Pupil_in_Patients_with_the.11.aspx.

32. Haynes WL, Thompson HS, Kardon RH, Alward WLM. Asymmetric pigmentary dispersion syndrome mimicking Horner's syndrome. *Am J Ophthalmol*. 1991;112(4):463-464.

33. Greenstein VC, Z S, JM L, R R, (eds) RN. Retinal Pigment Epithelial Dysfunction in

Patients With Pigment Dispersion Syndrome. *Arch Ophthalmol*. 2001;119(9):1291. doi:10.1001/archopht.119.9.1291.

34. Weseley P, Liebmann J, Walsh JB, Ritch R. Lattice degeneration of the retina and the pigment dispersion syndrome. *Am J Ophthalmol*. 1992;114(5):539-543. doi:10.1016/S0002-9394(14)74480-0.

35. Scuderi G, Papale A, Nucci C, Cerulli L. Retinal involvement in pigment dispersion syndrome. *Int Ophthalmol*. 1995;19(6):375-378. doi:10.1007/BF00130858.

36. Scheie HG, Cameron JD. Pigment dispersion syndrome: a clinical study. *Br J Ophthalmol*. 1981;65(4):264-269. doi:10.1136/bjo.65.4.264.

37. Sampaolesi R. Retinal detachment and pigment dispersion syndrome. *Klin Monbl Augenheilkd*. 1995;206(1):29-32. doi:10.1055/s-2008-1035401.

38. Ritch R, Steinberger D, Liebmann JM. Prevalence of pigment dispersion syndrome in a population undergoing glaucoma screening. *Am J Ophthalmol*. 1993;115(6):707-710. doi:10.1016/S0002-9394(14)73635-9.

39. Farrar SM, Shields MB. *Current Concepts in Pigmentary Glaucoma*. Vol 37. Elsevier; 1993:233-252. doi:10.1016/0039-6257(93)90008-U.

40. Semple HC, Ball SF. Pigmentary glaucoma in the black population. *Am J Ophthalmol*. 1990;109(5):518-522. doi:10.1016/S0002-9394(14)70680-4.

41. Roberts DK, Meetz RE, Chaglasian MA. The inheritance of the pigment dispersion syndrome in blacks. *J Glaucoma*. 1999;8(4):250-256.

42. GILLIES WE. PIGMENTARY GLAUCOMA: A CLINICAL REVIEW OF ANTERIOR SEGMENT PIGMENT DISPERSAL SYNDROME. *Aust N Z J Ophthalmol*. 1985;13(4):325-328. doi:10.1111/j.1442-9071.1985.tb00442.x.

43. Gramer E, Thiele H, Ritch R. Family history of glaucoma and risk factors in pigmentary glaucoma. A new clinical study. *Klin Monatsbl Augenheilkd*. 1998;212(6):454-464. doi:10.1055/s-2008-1034930.

44. Gramer G, Weber BHF, Gramer E. Results of a patient-directed survey on frequency of family history of glaucoma in 2170 patients. *Investig Ophthalmol Vis Sci*. 2014;55(1):259-264. doi:10.1167/iovs.13-13020.

45. Epstein DL, Boger WP, Grant WM. Phenylephrine provocative testing in the pigmentary dispersion syndrome. *Am J Ophthalmol*. 1978;85(1):43-50. doi:10.1016/S0002-9394(14)76663-2.

46. Schenker HI, Luntz MH, Kels B, Podos SM. Exercise-induced increase of intraocular pressure in the pigmentary dispersion syndrome. *Am J Ophthalmol*. 1980;89(4):598-600. doi:10.1016/0002-9394(80)90073-2.

47. Haynes WL, Johnson AT, Alward WLM. Effects of Jogging Exercise on Patients with the Pigmentary Dispersion Syndrome and Pigmentary Glaucoma. *Ophthalmology*. 1992;99(7):1096-1103. doi:10.1016/S0161-6420(92)31845-7.

48. Jensen PK, Nissen O, Kessing SV. Exercise and reversed pupillary block in pigmentary glaucoma. *Am J Ophthalmol*. 1995;120(1):110-112. doi:10.1016/S0002-9394(14)73767-5.

49. Gomez Goyeneche HF, Hernandez-Mendieta DP, Rodriguez DA, Sepulveda AI, Toledo JD. Pigment Dispersion Syndrome Progression to Pigmentary Glaucoma in a Latin American Population. Dada T, Shaarawy T, eds. *J Curr glaucoma Pract*. 2015;9(3):69-72. doi:10.5005/jp-journals-10008-1187.

50. Shah IA, Shah SA, Nagdev PR, Abbasi SA, Abbasi NA, Katpar SA. Determination Of Association Of Pigmentary Glaucoma With Pigment Dispersion Syndrome. *J Ayub Med*

Coll Abbottabad. 29(3):412-414. http://www.ncbi.nlm.nih.gov/pubmed/29076672. Accessed November 15, 2017.

51. Yang JW, Sakiyalak D, Krupin T. Pigmentary glaucoma. *J Glaucoma*. 2001;10(5 Suppl 1):S30-2. http://www.ncbi.nlm.nih.gov/pubmed/11890269.

52. Andersen JS, Pralea AM, DelBono EA, et al. A gene responsible for the pigment dispersion syndrome maps to chromosome 7q35-q36. *Arch Ophthalmol*. 1997;115(3):384-388. doi:10.1001/archopht.1997.01100150386012.

53. Robinson LJ, Weremowicz S, Morton CC, Michel T. Isolation and chromosomal localization of the human endothelial nitric oxide synthase (NOS3) gene. *Genomics*. 1994;19(2):350-357. doi:10.1006/geno.1994.1068.

54. Davidge ST, Baker PN, McLaughlin MK, Roberts JM. Nitric Oxide Produced by Endothelial Cells Increases Production of Eicosanoids Through Activation of Prostaglandin H Synthase. *Circ Res*. 1995;77(2):274-283. doi:10.1161/01.RES.77.2.274.

55. Steudel W, Ichinose F, Huang PL, et al. Pulmonary vasoconstriction and hypertension in mice with targeted disruption of the endothelial nitric oxide synthase (NOS 3) gene. *Circ Res*. 1997;81(1):34-41.

56. Andersen JS, Parrish R, Greenfield D, DelBono EA, Haines JL, Wiggs JL. A second locus for the pigment dispersion syndrome and pigmentary glaucoma maps to 18q11-q21. *Am J Hum Genet*. 1998;63(Suppl):A279.

57. Wagner SH, DelBono E, Greenfield DS, Parrish RK, Haines JL, Wiggs JL. A second locus for pigment dispersion syndrome maps to chromosome 18q21. *Invest Ophthalmol Vis Sci*. 2005;46(13):29.

58. Mikelsaar R, Molder H, Bartsch O, Punab M. Two novel deletions (array CGH findings)

in pigment dispersion syndrome. *Ophthalmic Genet*. 2007;28(4):216-219. doi:10.1080/13816810701635269.

59. Fingert JH, Héon E, Liebmann JM, et al. Analysis of myocilin mutations in 1703 glaucoma patients from five different populations. *Hum Mol Genet*. 1999;8(5):899-905. doi:ddc095 [pii].

60. Stone EM, Fingert JH, Alward WL, et al. Identification of a gene that causes primary open angle glaucoma. *Science (80-)*. 1997;275(January):668-670. doi:10.1126/science.275.5300.668.

61. Sheffield VC, Stone EM, Alward WLM, et al. Genetic linkage of familial open angle glaucoma to chromosome 1q21–q31. *Nat Genet*. 1993;4(1):47-50. doi:10.1038/ng0593-47.

62. Vincent AL, Billingsley G, Buys Y, et al. Digenic inheritance of early-onset glaucoma: CYP1B1, a potential modifier gene. *Am J Hum Genet*. 2002;70(2):448-460. doi:10.1086/338709.

63. Faucher M, Anctil J-L, Rodrigue M-A, et al. Founder TIGR/myocilin mutations for glaucoma in the Québec population. *Hum Mol Genet*. 2002;11(18):2077-2090. http://www.ncbi.nlm.nih.gov/pubmed/12189160. Accessed December 6, 2017.

64. Alward WLM, Kwon YH, Khanna CL, et al. Variations in the myocilin gene in patients with open-angle glaucoma. *Arch Ophthalmol*. 2002;120(9):1189-1197. doi:10.1001/archopht.120.9.1189.

65. Lee KYC, Ho SL, Thalamuthu A, et al. Association of LOXL1 polymorphisms with pseudoexfoliation in the Chinese. *Mol Vis*. 2009;15:1120-1126. http://www.ncbi.nlm.nih.gov/pubmed/19503743. Accessed December 6, 2017.

66. Hewitt AW, Sharma S, Burdon KP, et al. Ancestral LOXL1 variants are associated with pseudoexfoliation in Caucasian Australians but with markedly lower penetrance than in Nordic people. *Hum Mol Genet*. 2008;17(5):710-716. doi:10.1093/hmg/ddm342.

67. Fan B, Pasquale L, Grosskreutz CL, et al. DNA sequence variants in the LOXL1 gene are associated with pseudoexfoliation glaucoma in a U.S. clinic-based population with broad ethnic diversity. *BMC Med Genet*. 2008;9(1):5. doi:10.1186/1471-2350-9-5.

68. Aragon-Martin JA, Ritch R, Liebmann J, et al. Evaluation of LOXL1 gene polymorphisms in exfoliation syndrome and exfoliation glaucoma. *Mol Vis*. 2008;14(December 2007):533-541. http://www.ncbi.nlm.nih.gov/pubmed/18385788. Accessed December 6, 2017.

69. Challa P, Schmidt S. Analysis of LOXL1 polymorphisms in a United States population with pseudoexfoliation glaucoma. *Mol Vis*. 2008;14(14):146-149. doi:10.1167/iovs.07-1449.

70. Wolf C, Gramer E, Muïler-Myhsok B, et al. Lysyl Oxidase-like 1 Gene Polymorphisms in German Patients With Normal Tension Glaucoma, Pigmentary Glaucoma and Exfoliation Glaucoma. *J Glaucoma*. 2010;19(2):136-141. doi:10.1097/IJG.0b013e31819f9330.

71. Rao KN, Ritch R, Dorairaj SK, et al. Exfoliation syndrome and exfoliation glaucoma-associated LOXL1 variations are not involved in pigment dispersion syndrome and pigmentary glaucoma. *Mol Vis*. 2008;14(July):1254-1262. http://www.ncbi.nlm.nih.gov/pubmed/18618003. Accessed December 6, 2017.

72. Giardina E, Oddone F, Lepre T, et al. Common sequence variants in the LOXL1gene in pigment dispersion syndrome and pigmentary glaucoma. *BMC Ophthalmol*. 2014;14(1):52. doi:10.1186/1471-2415-14-52.

73. Pokrovskaya O, O'Brien C. What's in a Gene Pseudoexfoliation Syndrome and Pigment Dispersion Syndrome in the Same Patient. *Case Rep Ophthalmol*. 2016;7(1):54-60. doi:10.1159/000443697.

74. Sertié AL, Sossi V, Camargo AA, Zatz M, Brahe C, Passos-Bueno MR. Collagen XVIII, containing an endogenous inhibitor of angiogenesis and tumor growth, plays a critical role in the maintenance of retinal structure and in neural tube closure (Knobloch syndrome). *Hum Mol Genet*. 2000;9(13):2051-2058. http://www.ncbi.nlm.nih.gov/pubmed/10942434. Accessed December 6, 2017.

75. Joyce S, Tee L, Abid A, Khaliq S, Mehdi SQ, Maher ER. Locus heterogeneity and Knobloch syndrome. *Am J Med Genet Part A*. 2010;152(11):2880-2881. doi:10.1002/ajmg.a.33619.

76. Hull S, Arno G, Ku CA, et al. Molecular and Clinical Findings in Patients With Knobloch Syndrome. *JAMA Ophthalmol*. 2016;134(7):753. doi:10.1001/jamaophthalmol.2016.1073.

77. Kuchtey J, Chang TC, Panagis L, Kuchtey RW. Marfan syndrome caused by a novel FBN1 mutation with associated pigmentary glaucoma. *Am J Med Genet Part A*. 2013;161(4):880-883. doi:10.1002/ajmg.a.35838.

78. Chakravarti T, Spaeth G. An Overlap Syndrome of Pigment Dispersion and Pigmentary Glaucoma accompanied by Marfan Syndrome: Case Report with Literature Review. Dada T, Sherwood M, Singh K, Shaarawy T, eds. *J Curr Glaucoma Pract with DVD*. 2013;7(2):91-95. doi:10.5005/jp-journals-10008-1143.

79. Izquierdo NJ, Traboulsi EI, Enger C, Maumenee IH. Glaucoma in the Marfan syndrome. *Trans Am Ophthalmol Soc*. 1992;90:111-7; discussion 118-22. http://www.ncbi.nlm.nih.gov/pubmed/1494814. Accessed December 6, 2017.

80. Anderson MG, Smith RS, Hawes NL, et al. Mutations in genes encoding melanosomal proteins cause pigmentary glaucoma in DBA/2J mice. *Nat Genet*. 2002;30(1):81-85. doi:10.1038/ng794.

81. Williams PA, Howell GR, Barbay JM, et al. Retinal ganglion cell dendritic atrophy in DBA/2J glaucoma. Chidlow G, ed. *PLoS One*. 2013;8(8):e72282. doi:10.1371/journal.pone.0072282.

82. LIBBY RT, ANDERSON MG, PANG I-H, et al. Inherited glaucoma in DBA/2J mice: Pertinent disease features for studying the neurodegeneration. *Vis Neurosci*. 2005;22(05):637-648. doi:10.1017/S0952523805225130.

83. Howell GR, Libby RT, Jakobs TC, et al. Axons of retinal ganglion cells are insulted in the optic nerve early in DBA/2J glaucoma. *J Cell Biol*. 2007;179(7):1523-1537. doi:10.1083/jcb.200706181.

84. John SW, Smith RS, Savinova O V, et al. Essential iris atrophy, pigment dispersion, and glaucoma in DBA/2J mice. *Invest Ophthalmol Vis Sci*. 1998;39(6):951-962.

85. Anderson MG, Hawes NL, Trantow CM, Chang B, John SWM. Iris phenotypes and pigment dispersion caused by genes influencing pigmentation. *Pigment Cell Melanoma Res*. 2008;21(5):565-578. doi:10.1111/j.1755-148X.2008.00482.x.

86. Trantow CM, Mao M, Petersen GE, et al. Lyst mutation in mice recapitulates iris defects of human exfoliation syndrome. *Investig Opthalmology Vis Sci*. 2009;50(3):1205. doi:10.1167/iovs.08-2791.

87. Nair KS, Cosma M, Raghupathy N, et al. YBR/EiJ mice: a new model of glaucoma caused by genes on chromosomes 4 and 17. 2016;9(8). doi:10.1242/dmm.024307.

88. Urabe K, Aroca P, Tsukamoto K, et al. The inherent cytotoxicity of melanin precursors: A

revision. *BBA - Mol Cell Res*. 1994;1221(3):272-278. doi:10.1016/0167-4889(94)90250-X.

89. Olivares C, Jiménez-Cervantes C, Lozano JA, Solano F, García-Borrón JC. The 5,6-dihydroxyindole-2-carboxylic acid (DHICA) oxidase activity of human tyrosinase. *Biochem J*. 2001;354(Pt 1):131-139. doi:10.1042/0264-6021:3540131.

90. Kobayashi T, Imokawa G, Bennett DC, Hearing VJ. Tyrosinase stabilization by Tyrp1 (the brown locus protein). *J Biol Chem*. 1999;273(48):31801-31805. doi:10.1074/jbc.273.48.31801.

91. Halaban R, Moellmann G. Murine and human b locus pigmentation genes encode a glycoprotein (gp75) with catalase activity. *Proc Natl Acad Sci U S A*. 1990;87(12):4809-4813. doi:10.1073/pnas.87.12.4809.

92. Johnson R, Jackson IJ. Light is a dominant mouse mutation resulting in premature cell death. *Nat Genet*. 1992;1(3):226-229. doi:10.1038/ng0692-226.

93. Zdarsky E, Favor J, Jackson IJ. The molecular basis of brown, an old mouse mutation, and of an induced revertant to wild type. *Genetics*. 1990;126(2):443-449. doi:10.1136/bjsports-2011-090257.

94. Hirobe T, Abe H. Changes of melanosome morphology associated with the differentiation of epidermal melanocytes in slaty mice. *Anat Rec Adv Integr Anat Evol Biol*. 2007;290(8):981-993. doi:10.1002/ar.20547.

95. Costin G-E, Valencia JC, Wakamatsu K, et al. Mutations in dopachrome tautomerase (Dct) affect eumelanin/pheomelanin synthesis, but do not affect intracellular trafficking of the mutant protein. *Biochem J*. 2005;391(2):249-259. doi:10.1042/BJ20042070.

96. Swaminathan S, Lu H, Williams RW, Lu L, Jablonski MM. Genetic modulation of the iris

transillumination defect: A systems genetics analysis using the expanded family of BXD glaucoma strains. *Pigment Cell Melanoma Res*. 2013;26(4):487-498. doi:10.1111/pcmr.12106.

97. Yuasa I, Umetsu K, Harihara S, et al. OCA2*481Thr, a hypofunctional allele in pigmentation, is characteristic of northeastern Asian populations. *J Hum Genet*. 2007;52(8):690-693. doi:10.1007/s10038-007-0167-9.

98. Ramsay M, Colman MA, Stevens G, et al. The tyrosinase-positive oculocutaneous albinism locus maps to chromosome 15q11.2-q12. *Am J Hum Genet*. 1992;51(4):879-884. http://www.ncbi.nlm.nih.gov/pubmed/1415228. Accessed February 14, 2018.

99. Sturm RA, Frudakis TN. Eye colour: portals into pigmentation genes and ancestry. *Trends Genet*. 2004;20(8):327-332. doi:10.1016/j.tig.2004.06.010.

100. Duffy DL, Montgomery GW, Chen W, et al. A Three–Single-Nucleotide Polymorphism Haplotype in Intron 1 of OCA2 Explains Most Human Eye-Color Variation. *Am J Hum Genet*. 2007;80(2):241-252. doi:10.1086/510885.

101. Sulem P, Gudbjartsson DF, Stacey SN, et al. Genetic determinants of hair, eye and skin pigmentation in Europeans. *Nat Genet*. 2007;39(12):1443-1452. doi:10.1038/ng.2007.13.

102. Anderson MG, Nair KS, Amonoo LA, et al. GpnmbR150X allele must be present in bone marrow derived cells to mediate DBA/2J glaucoma. *BMC Genet*. 2008;9(1):30. doi:10.1186/1471-2156-9-30.

103. Huang JJ, Ma WJ, Yokoyama S. Expression and immunolocalization of Gpnmb, a glioma-associated glycoprotein, in normal and inflamed central nervous systems of adult rats. *Brain Behav*. 2012;2(2):85-96. doi:10.1002/brb3.39.

104. Nair K, Barbay J, Smith RS, Masli S, John SW. Determining immune components

necessary for progression of pigment dispersing disease to glaucoma in DBA/2J mice. *BMC Genet*. 2014;15(1):42. doi:10.1186/1471-2156-15-42.

105. Mo J-S, Anderson MG, Gregory M, et al. By altering ocular immune privilege, bone marrow-derived cells pathogenically contribute to DBA/2J pigmentary glaucoma. *J Exp Med*. 2003;197(10):1335-1344. doi:10.1084/jem.20022041.

106. Shiflett SL, Kaplan J, Ward DM. Chediak–Higashi Syndrome: A Rare Disorder of Lysosomes and Lysosome Related Organelles. *Pigment Cell Res*. 2002;15(4):251-257. doi:10.1034/j.1600-0749.2002.02038.x.

107. Watt B, Tenza D, Lemmon MA, et al. Mutations in or near the transmembrane domain alter PMEL amyloid formation from functional to pathogenic. Jackson IJ, ed. *PLoS Genet*. 2011;7(9):e1002286. doi:10.1371/journal.pgen.1002286.

108. Theos AC, Berson JF, Theos SC, et al. Dual Loss of ER Export and Endocytic Signals with Altered Melanosome Morphology in the silver Mutation of Pmel17. Linstedt A, ed. *Mol Biol Cell*. 2006;17(August):3598-3612. doi:10.1091/mbc.E06.

109. Kwon BS, Halaban R, Ponnazhagan S, et al. Mouse silver. Mutation is caused by a single base insertion in the putative cytoplasmic domain of Pmel 17. *Nucleic Acids Res*. 1995;23(1):154-158. doi:10.1093/nar/23.1.154.

110. O'Sullivan TN, Wu XS, Rachel RA, et al. dsu functions in a MYO5A-independent pathway to suppress the coat color of dilute mice. *Proc Natl Acad Sci U S A*. 2004;101(48):16831-16836. doi:10.1073/pnas.0407339101.

111. Wu X, Bowers B, Rao K, Wei Q, Hammer JA JA, III. Visualization of melanosome dynamics within wild-type and dilute melanocytes suggests a paradigm for myosin V function In vivo. *J Cell Biol*. 1998;143(7):1899-1918.

http://www.ncbi.nlm.nih.gov/pubmed/9864363. Accessed February 14, 2018.

112. Wu X, Bowers B, Wei Q, Kocher B, Hammer JA. Myosin V associates with melanosomes in mouse melanocytes: evidence that myosin V is an organelle motor. *J Cell Sci*. 1997;110 (Pt 7:847-859. http://www.ncbi.nlm.nih.gov/pubmed/9133672. Accessed February 14, 2018.

113. Scott GA, Arioka M, Jacobs SE. Lysophosphatidylcholine Mediates Melanocyte Dendricity through PKCζ Activation. *J Invest Dermatol*. 2007;127(3):668-675. doi:10.1038/SJ.JID.5700567.

114. Mattioli F, Piton A, Gérard B, Superti-Furga A, Mandel J-L, Unger S. Novel de novo mutations in *ZBTB20* in Primrose syndrome with congenital hypothyroidism. *Am J Med Genet Part A*. 2016;170(6):1626-1629. doi:10.1002/ajmg.a.37645.

115. Xie Z, Zhang H, Tsai W, et al. Zinc finger protein ZBTB20 is a key repressor of alpha-fetoprotein gene transcription in liver. *Proc Natl Acad Sci*. 2008;105(31):10859-10864. doi:10.1073/pnas.0800647105.

116. Zhang W, Mi J, Li N, et al. Identification and Characterization of DPZF, a Novel Human BTB/POZ Zinc Finger Protein Sharing Homology to BCL-6. *Biochem Biophys Res Commun*. 2001;282(4):1067-1073. http://www.ncbi.nlm.nih.gov/pubmed/11352661. Accessed February 14, 2018.

117. Levy C, Khaled M, Fisher DE. *MITF: Master Regulator of Melanocyte Development and Melanoma Oncogene*. Vol 12.; 2006:406-414. doi:10.1016/j.molmed.2006.07.008.

118. Anderson MG, Libby RT, Mao M, et al. Genetic context determines susceptibility to intraocular pressure elevation in a mouse pigmentary glaucoma. *BMC Biol*. 2006;4(1):20. doi:10.1186/1741-7007-4-20.

119. Turque N, Denhez F, Martin P, et al. Characterization of a new melanocyte-specific gene (QNR-71) expressed in v-myc-transformed quail neuroretina. *Embo J*. 1996;15(13):3338-3350. http://www.ncbi.nlm.nih.gov/pubmed/8670835. Accessed December 7, 2017.

120. Aksan I, Goding CR. Targeting the Microphthalmia Basic Helix-Loop-Helix–Leucine Zipper Transcription Factor to a Subset of E-Box Elements In Vitro and In Vivo. *Mol Cell Biol*. 1998;18(12):6930-6938. doi:10.1128/MCB.18.12.6930.

121. Petersen-Jones SM, Forcier J, Mentzer AL. Ocular melanosis in the Cairn Terrier: Clinical description and investigation of mode of inheritance. *Vet Ophthalmol*. 2007;10(SUPPL. 1):63-69. doi:10.1111/j.1463-5224.2007.00558.x.

122. Van De Sandt RROM, Boevé MH, Stades FC, Kik MJL. Abnormal ocular pigment deposition and glaucoma in the dog. *Vet Ophthalmol*. 2003;6(4):273-278. doi:10.1111/j.1463-5224.2003.00306.x.

123. Winkler PA, Bartoe JT, Quinones CR, Venta PJ, Petersen-Jones SM. Exclusion of eleven candidate genes for ocular melanosis in cairn terriers. *J Negat Results Biomed*. 2013;12:1. doi:10.1186/1477-5751-12-6.

124. Lu H, Lu L, Williams RW, Jablonski MM. Iris transillumination defect and its gene modulators do not correlate with intraocular pressure in the BXD family of mice. *Mol Vis*. 2016;22:224-233. http://www.ncbi.nlm.nih.gov/pubmed/27011731. Accessed February 13, 2018.

125. Chintalapudi SR, Maria D, Di Wang X, et al. Systems genetics identifies a role for Cacna2d1 regulation in elevated intraocular pressure and glaucoma susceptibility. *Nat Commun*. 2017;8(1):1755. doi:10.1038/s41467-017-00837-5.

126. Turner AJ, Vander Wall R, Gupta V, Klistorner A, Graham SL. DBA/2J mouse model for

experimental glaucoma: Pitfalls and problems. *Clinical and Experimental Ophthalmology*. http://www.ncbi.nlm.nih.gov/pubmed/28516453. Published June 13, 2017. Accessed December 7, 2017.

127. Lin JY, Fisher DE. Melanocyte biology and skin pigmentation. *Nature*. 2007;445(7130):843-850. doi:10.1038/nature05660.

128. Le Douarin NM, Creuzet S, Couly G, Dupin E. Neural crest cell plasticity and its limits. *Development*. 2004;131(19):4637-4650. doi:10.1242/dev.01350.

129. Shin MK, Levorse JM, Ingram RS, Tilghman SM. The temporal requirement for endothelin receptor-B signalling during neural crest development. *Nature*. 1999;402(6761):496-501. doi:10.1038/990040.

130. Larue L, Delmas V. The WNT/Beta-catenin pathway in melanoma. *Front Biosci*. 2006;11:733-742. http://www.ncbi.nlm.nih.gov/pubmed/16146765. Accessed August 1, 2018.

131. Kushimoto T, Basrur V, Valencia J, et al. A model for melanosome biogenesis based on the purification and analysis of early melanosomes. *Proc Natl Acad Sci*. 2001;98(19):10698-10703. doi:10.1073/pnas.191184798.

132. Slominski A, Tobin DJ, Shibahara S, Wortsman J. Melanin Pigmentation in Mammalian Skin and Its Hormonal Regulation. *Physiol Rev*. 2004;84(4):1155-1228. doi:10.1152/physrev.00044.2003.

133. Land EJ, Riley PA. Spontaneous redox reactions of dopaquinone and the balance between the eumelanic and phaeomelanic pathways. *Pigment cell Res*. 2000;13(4):273-277. http://www.ncbi.nlm.nih.gov/pubmed/10952395. Accessed August 1, 2018.

134. Simon JD, Peles D, Wakamatsu K, Ito S. Current challenges in understanding

melanogenesis: bridging chemistry, biological control, morphology, and function. *Pigment Cell Melanoma Res*. 2009;22(5):563-579. doi:10.1111/j.1755-148X.2009.00610.x.

135. Harper DC, Theos AC, Herman KE, Tenza D, Raposo G, Marks MS. Premelanosome Amyloid-like Fibrils Are Composed of Only Golgi-processed Forms of Pmel17 That Have Been Proteolytically Processed in Endosomes*. *J Biol Chem*. 2008;283(4):2307-2322. doi:10.1074/jbc.M708007200.

136. Li H, Handsaker B, Wysoker A, et al. The Sequence Alignment/Map format and SAMtools. *Bioinformatics*. 2009;25(16):2078-2079. doi:10.1093/bioinformatics/btp352.

137. Van Den Bossche K, Naeyaert JM, Lambert J. The quest for the mechanism of melanin transfer. *Traffic*. 2006;7(7):769-778. doi:10.1111/j.1600-0854.2006.00425.x.

138. Watt B, van Niel G, Fowler DM, et al. N-terminal Domains Elicit Formation of Functional Pmel17 Amyloid Fibrils. *J Biol Chem*. 2009;284(51):35543-35555. doi:10.1074/jbc.M109.047449.

139. McGlinchey RP, Shewmaker F, Hu K -n., McPhie P, Tycko R, Wickner RB. Repeat Domains of Melanosome Matrix Protein Pmel17 Orthologs Form Amyloid Fibrils at the Acidic Melanosomal pH. *J Biol Chem*. 2011;286(10):8385-8393. doi:10.1074/jbc.M110.197152.

140. Fowler DM, Koulov A V, Alory-Jost C, Marks MS, Balch WE, Kelly JW. Functional Amyloid Formation within Mammalian Tissue. Weissman J, ed. *PLoS Biol*. 2005;4(1):e6. doi:10.1371/journal.pbio.0040006.

141. Hoashi T, Muller J, Vieira WD, et al. The Repeat Domain of the Melanosomal Matrix Protein PMEL17/GP100 Is Required for the Formation of Organellar Fibers. *J Biol Chem*. 2006;281(30):21198-21208. doi:10.1074/jbc.M601643200.

142. Theos AC, Truschel ST, Raposo G, Marks MS. The Silver locus product Pmel17/gp100/Silv/ME20: controversial in name and in function Alexander. *Pigment Cell Res*. 2005;18(5):322-336. doi:10.1111/j.1600-0749.2005.00269.x.The.

143. Hee JS, Mitchell SM, Liu X, Leonhardt RM. Melanosomal formation of PMEL core amyloid is driven by aromatic residues. *Sci Rep*. 2017;7:44064. doi:10.1038/srep44064.

144. Bycroft M, Bateman A, Clarke J, et al. The structure of a PKD domain from polycystin-1: implications for polycystic kidney disease. *EMBO J*. 1999;18(2):297-305. doi:10.1093/emboj/18.2.297.

145. Valencia JC, Rouzaud F, Julien S, et al. Sialylated core 1 O-glycans influence the sorting of Pmel17/gp100 and determine its capacity to form fibrils. *J Biol Chem*. 2007;282(15):11266-11280. doi:10.1074/jbc.M608449200.

146. McGlinchey RP, Shewmaker F, McPhie P, Monterroso B, Thurber K, Wickner RB. The repeat domain of the melanosome fibril protein Pmel17 forms the amyloid core promoting melanin synthesis. *Proc Natl Acad Sci U S A*. 2009;106(33):13731-13736. doi:10.1073/pnas.0906509106.

147. Pfefferkorn CM, McGlinchey RP, Lee JC. Effects of pH on aggregation kinetics of the repeat domain of a functional amyloid, Pmel17. *Proc Natl Acad Sci*. 2010;107(50):21447-21452. doi:10.1073/pnas.1006424107.

148. Watt B, van Niel G, Raposo G, Marks MS. PMEL: a pigment cell-specific model for functional amyloid formation. *Pigment Cell Melanoma Res*. 2013;26(3):300-315. doi:10.1111/pcmr.12067.

149. Ho T, Watt B, Spruce LA, Seeholzer SH, Marks MS. The Kringle-like Domain Facilitates Post-endoplasmic Reticulum Changes to Premelanosome Protein (PMEL)

Oligomerization and Disulfide Bond Configuration and Promotes Amyloid Formation. *J Biol Chem*. 2016;291(7):3595-3612. doi:10.1074/jbc.M115.692442.

150. Hoashi T, Tamaki K, Hearing VJ. The secreted form of a melanocyte membrane-bound glycoprotein (Pmel17/gp100) is released by ectodomain shedding. *FASEB J*. 2010;24(3):916-930. doi:10.1096/fj.09-140921.

151. Nufer O, Guldbrandsen S, Degen M, et al. Role of cytoplasmic C-terminal amino acids of membrane proteins in ER export. *J Cell Sci*. 2002;115(Pt 3):619-628. http://www.ncbi.nlm.nih.gov/pubmed/11861768. Accessed August 1, 2018.

152. Theos AC, Berson JF, Theos SC, et al. Dual Loss of ER Export and Endocytic Signals with Altered Melanosome Morphology in the silver Mutation of Pmel17. *Mol Biol Cell*. 2006. doi:10.1091/mbc.E06.

153. Berson JF, Theos AC, Harper DC, Tenza D, Raposo G, Marks MS. Proprotein convertase cleavage liberates a fibrillogenic fragment of a resident glycoprotein to initiate melanosome biogenesis. *J Cell Biol*. 2003;161(3):521-533. doi:10.1083/jcb.200302072.

154. Berson JF, Harper DC, Tenza D, Raposo G, Marks MS. Pmel17 initiates premelanosome morphogenesis within multivesicular bodies. *Mol Biol Cell*. 2001;12(11):3451-3464. http://www.ncbi.nlm.nih.gov/pubmed/11694580. Accessed June 9, 2017.

155. Raposo G, Tenza D, Murphy DM, Berson JF, Marks MS. Distinct protein sorting and localization to premelanosomes, melanosomes, and lysosomes in pigmented melanocytic cells. *J Cell Biol*. 2001;152(4):809-824. http://www.ncbi.nlm.nih.gov/pubmed/11266471. Accessed August 1, 2018.

156. Rochin L, Hurbain I, Serneels L, et al. BACE2 processes PMEL to form the melanosome amyloid matrix in pigment cells. *Proc Natl Acad Sci U S A*. 2013;110(26):10658-10663.

doi:10.1073/pnas.1220748110.

157. Kawaguchi M, Hozumi Y, Suzuki T. ADAM protease inhibitors reduce melanogenesis by regulating PMEL17 processing in human melanocytes. *J Dermatol Sci*. 2015;78(2):133-142. doi:10.1016/j.jdermsci.2015.02.020.

158. van Niel G, Charrin S, Simoes S, et al. The Tetraspanin CD63 Regulates ESCRT-Independent and -Dependent Endosomal Sorting during Melanogenesis. *Dev Cell*. 2011;21(4):708-721. doi:10.1016/j.devcel.2011.08.019.

159. van Niel G, Bergam P, Di Cicco A, et al. Apolipoprotein E Regulates Amyloid Formation within Endosomes of Pigment Cells. *Cell Rep*. 2015;13(1):43-51. doi:10.1016/j.celrep.2015.08.057.

160. Hurbain I, Geerts WJC, Boudier T, et al. Electron tomography of early melanosomes: Implications for melanogenesis and the generation of fibrillar amyloid sheets. *Proc Natl Acad Sci*. 2008;105(50):19726-19731. doi:10.1073/pnas.0803488105.

161. Liu P, Reed MN, Kotilinek LA, et al. Quaternary Structure Defines a Large Class of Amyloid-β Oligomers Neutralized by Sequestration. *Cell Rep*. 2015;11(11):1760-1771. doi:10.1016/j.celrep.2015.05.021.

162. Fowler DM, Koulov A V, Alory-Jost C, Marks MS, Balch WE, Kelly JW. Functional Amyloid Formation within Mammalian Tissue. Weissman J, ed. *PLoS Biol*. 2005;4(1):e6. doi:10.1371/journal.pbio.0040006.

163. Kerje S, Sharma P, Gunnarsson U, et al. The Dominant white, Dun and Smoky Color Variants in Chicken Are Associated With Insertion/Deletion Polymorphisms in the PMEL17 Gene. *Genetics*. 2004;168(3):1507-1518. doi:10.1534/genetics.104.027995.

164. Keeling L, Andersson L, Schütz KE, et al. Chicken genomics: Feather-pecking and victim

pigmentation. *Nature*. 2004;431(7009):645-646. doi:10.1038/431645a.

165. Brunberg E, Andersson L, Cothran G, Sandberg K, Mikko S, Lindgren G. A missense mutation in PMEL17 is associated with the Silver coat color in the horse. *BMC Genet*. 2006;7:46. doi:10.1186/1471-2156-7-46.

166. Anderson MG, Smith RS, Hawes NL, et al. Mutations in genes encoding melanosomal proteins cause pigmentary glaucoma in DBA/2J mice. *Nat Genet*. 2002;30(1):81-85. doi:10.1038/ng794.

167. Leonhardt RM, Vigneron N, Rahner C, Cresswell P. Proprotein Convertases Process Pmel17 during Secretion. *J Biol Chem*. 2011;286(11):9321-9337. doi:10.1074/jbc.M110.168088.

168. Clark LA, Wahl JM, Rees CA, Murphy KE. From The Cover: Retrotransposon insertion in SILV is responsible for merle patterning of the domestic dog. *Proc Natl Acad Sci*. 2006;103(5):1376-1381. doi:10.1073/pnas.0506940103.

169. Schonthaler HB, Lampert JM, von Lintig J, Schwarz H, Geisler R, Neuhauss SCF. A mutation in the silver gene leads to defects in melanosome biogenesis and alterations in the visual system in the zebrafish mutant fading vision. *Dev Biol*. 2005;284(2):421-436. doi:10.1016/j.ydbio.2005.06.001.

170. Yasumoto K -i. KI, Watabe H, Valencia JC, et al. Epitope mapping of the melanosomal matrix protein gp100 (PMEL17). Rapid processing in the endoplasmic reticulum and glycosylation in the early Golgi compartment. *J Biol Chem*. 2004;279(27):28330-28338. doi:10.1074/jbc.M401269200.

171. Palmer I, Wingfield PT. Preparation and extraction of insoluble (inclusion-body) proteins from Escherichia coli. *Curr Protoc protein Sci*. 2004;Chapter 6:Unit 6.3.

doi:10.1002/0471140864.ps0603s38.

172. Leonhardt RM, Vigneron N, Hee JS, Graham M, Cresswell P. Critical residues in the PMEL/Pmel17 N-terminus direct the hierarchical assembly of melanosomal fibrils. *Mol Biol Cell*. 2013;24(7):964-981. doi:10.1091/mbc.E12-10-0742.

173. Hoashi T, Muller J, Vieira WD, et al. The Repeat Domain of the Melanosomal Matrix Protein PMEL17/GP100 Is Required for the Formation of Organellar Fibers. *J Biol Chem*. 2006;281(30):21198-21208. doi:10.1074/jbc.M601643200.

174. Theos AC, Watt B, Harper DC, et al. The PKD domain distinguishes the trafficking and amyloidogenic properties of the pigment cell protein PMEL and its homologue GPNMB. *Pigment Cell Melanoma Res*. 2013;26(4):470-486. doi:10.1111/pcmr.12084.

175. Andersson LS, Wilbe M, Viluma A, et al. Equine Multiple Congenital Ocular Anomalies and Silver Coat Colour Result from the Pleiotropic Effects of Mutant PMEL. *PLoS One*. 2013;8(9):4-11. doi:10.1371/journal.pone.0075639.

176. Hellström AR, Watt B, Fard SS, et al. Inactivation of Pmel Alters Melanosome Shape But Has Only a Subtle Effect on Visible Pigmentation. Jackson IJ, ed. *PLoS Genet*. 2011;7(9):e1002285. doi:10.1371/journal.pgen.1002285.

177. Michelessi M, Lindsley K. Peripheral iridotomy for pigmentary glaucoma. Michelessi M, ed. *Cochrane Database Syst Rev*. 2016;2016(2). doi:10.1002/14651858.CD005655.pub2.

178. Costa VP, Gandham S, Smith M, Spaeth GL. The effects of peripheral iridectomy on pigmentary glaucoma. *Arq Bras Oftalmol*. 1994;57:4.

179. Costa VP, Gandham S, Spaeth GL, et al. THE EFFECT OF ND-YAG LASER IRIDOTOMY ON PIGMENTARY GLAUCOMA PATIENTS-A PROSPECTIVE-STUDY. In: *Investigative Ophthalmology & Visual Science*. Vol 35. LIPPINCOTT-

RAVEN PUBL 227 EAST WASHINGTON SQ, PHILADELPHIA, PA 19106; 1994:1852.

180. Georgopoulos GT, Papaconstantinou DS, Patsea LE, et al. Laser iridotomy versus low dose pilocarpine treatment in patients with pigmentary glaucoma. In: *Investigative Ophthalmology & Visual Science*. Vol 42. ASSOC RESEARCH VISION OPHTHALMOLOGY INC 9650 ROCKVILLE PIKE, BETHESDA, MD 20814-3998 USA; 2001:S817-S817.

181. Baulmann DC, Ohlmann A, Flügel-Koch C, Goswami S, Cvekl A, Tamm ER. Pax6 heterozygous eyes show defects in chamber angle differentiation that are associated with a wide spectrum of other anterior eye segment abnormalities. *Mech Dev*. 2002;118(1-2):3-17. doi:10.1016/S0925-4773(02)00260-5.

182. Berry FB, Lines MA, Oas JM, et al. Functional interactions between FOXC1 and PITX2 underlie the sensitivity to FOXC1 gene dose in Axenfeld-Rieger syndrome and anterior segment dysgenesis. *Hum Mol Genet*. 2006;15(6):905-919. doi:10.1093/hmg/ddl008.

183. Seifi M, Footz T, Taylor SAM, Elhady GM, Abdalla EM, Walter MA. Novel PITX2 gene mutations in patients with Axenfeld-Rieger syndrome. *Acta Ophthalmol*. 2016:n/a-n/a. doi:10.1111/aos.13030.

184. Gould DB, Smith RS, John SWM. Anterior segment development relevant to glaucoma. *Int J Dev Biol*. 2004;48(8-9):1015-1029. doi:10.1387/ijdb.041865dg.

185. Lindquist NG, Larsson BS, Stjernschantz J, Sjöquist B. Age-related melanogenesis in the eye of mice, studied by microautoradiography of 3H-methimazole, a specific marker of melanin synthesis. *Exp Eye Res*. 1998;67(3):259-264. doi:10.1006/exer.1998.0513.

186. Lopes VS, Wasmeier C, Seabra MC, Futter CE. Melanosome maturation defect in Rab38-

deficient retinal pigment epithelium results in instability of immature melanosomes during transient melanogenesis. *Mol Biol Cell*. 2007;18(10):3914-3927. doi:10.1091/mbc.E07-03-0268.

187. Simon JD, Peles D, Wakamatsu K, Ito S. Current challenges in understanding melanogenesis: bridging chemistry, biological control, morphology, and function. *Pigment Cell Melanoma Res*. 2009;22(5):563-579. doi:10.1111/j.1755-148X.2009.00610.x.

188. Izzotti A, Bagnis A, Saccà SC. The role of oxidative stress in glaucoma. *Mutat Res Mutat Res*. 2006;612(2):105-114. doi:10.1016/j.mrrev.2005.11.001.

189. Saccà SC, Izzotti A. Oxidative stress and glaucoma: injury in the anterior segment of the eye. In: ; 2008:385-407. doi:10.1016/S0079-6123(08)01127-8.

190. Ito YA, Walter MA. Genetics and Environmental Stress Factor Contributions to Anterior Segment Malformations and Glaucoma. In: *Glaucoma - Basic and Clinical Aspects*. InTech; 2013. doi:10.5772/54653.

191. Porter KM, Epstein DL, Liton PB, Godeau G, Pellat B. Up-Regulated Expression of Extracellular Matrix Remodeling Genes in Phagocytically Challenged Trabecular Meshwork Cells. Di Cunto F, ed. *PLoS One*. 2012;7(4):e34792. doi:10.1371/journal.pone.0034792.

192. Sherwood ME, Richardson TM. Phagocytosis by trabecular meshwork cells: sequence of events in cats and monkeys. *Exp Eye Res*. 1988;46(6):881-895. http://www.ncbi.nlm.nih.gov/pubmed/3197758. Accessed July 24, 2017.

193. Buller C, Johnson DH, Tschumper RC. Human trabecular meshwork phagocytosis. Observations in an organ culture system. *Invest Ophthalmol Vis Sci*. 1990;31(10):2156-2163. http://www.ncbi.nlm.nih.gov/pubmed/2211012. Accessed July 24, 2017.

194. Johnson DH, Richardson TM, Epstein DL. Trabecular meshwork recovery after phagocytic challenge. *Curr Eye Res*. 1989;8(11):1121-1130. http://www.ncbi.nlm.nih.gov/pubmed/2612200. Accessed July 24, 2017.

195. Shirato S, Murphy CG, Bloom E, et al. Kinetics of phagocytosis in trabecular meshwork cells. Flow cytometry and morphometry. *Invest Ophthalmol Vis Sci*. 1989;30(12):2499-2511. http://www.ncbi.nlm.nih.gov/pubmed/2592162. Accessed July 24, 2017.

196. Mantravadi A V., Vadhar N. Glaucoma. *Prim Care Clin Off Pract*. 2015;42(3):437-449. doi:10.1016/j.pop.2015.05.008.

197. Weseley P, Liebmann J, Walsh JB, Ritch R. Lattice degeneration of the retina and the pigment dispersion syndrome. *Am J Ophthalmol*. 1992;114(5):539-543. http://www.ncbi.nlm.nih.gov/pubmed/1443014. Accessed June 13, 2017.

198. Greenstein VC, Z S, JM L, R R, (eds) RN. Retinal Pigment Epithelial Dysfunction in Patients With Pigment Dispersion Syndrome. *Arch Ophthalmol*. 2001;119(9):1291. doi:10.1001/archopht.119.9.1291.

199. Kaiser DM, Acharya M, Leighton PLA, et al. Amyloid Beta Precursor Protein and Prion Protein Have a Conserved Interaction Affecting Cell Adhesion and CNS Development. Xie Z, ed. *PLoS One*. 2012;7(12):e51305. doi:10.1371/journal.pone.0051305.

200. King C-Y, Tittmann P, Gross H, Gebert R, Aebi M, Wuthrich K. Prion-inducing domain 2-114 of yeast Sup35 protein transforms in vitro into amyloid-like filaments. *Proc Natl Acad Sci*. 1997;94(13):6618-6622. doi:10.1073/pnas.94.13.6618.

201. Rao R V, Bredesen DE. Misfolded proteins, endoplasmic reticulum stress and neurodegeneration. *Curr Opin Cell Biol*. 2004;16(6):653-662. doi:10.1016/j.ceb.2004.09.012.

202. Anderson MG, Hawes NL, Trantow CM, Chang B, John SWM. Iris phenotypes and pigment dispersion caused by genes influencing pigmentation. *Pigment Cell Melanoma Res*. 2008;21(5):565-578. doi:10.1111/j.1755-148X.2008.00482.x.